

Constructing Efficient Flame-Retardant Thermoplastic Polyurethane Coatings with Smoke-Suppression to Enhance the Performance of Glass Fiber Cloth

Yongqian Shi ^{a,*}, Songqiong Jiang ^a, Jinke Wu ^a, Zhendong Chen ^a, Cancan Zhang ^b, Yun Zhang ^{c,*}, Pingan Song ^d, and Yan Zhang ^{e,*}

^a College of Environment and Safety Engineering, Fuzhou University, 2 Xueyuan Road, Fuzhou 350116, China.

^b Jiangsu Xinchanya New Material Co., Ltd, Liuhe Road North Side and Hexiang Road West Side, Baoying Economic Development Zone, Yangzhou 225800, China.

^c Yangzhou Tengfei Electric Cable and Appliance Materials Co., Ltd, 8 Qixin Road, Anyi Industrial Zone, Yangzhou 225800, China.

^d School of Agriculture and Environmental Science, University of Southern Queensland, Springfield, QLD 4300, Australia.

^e Laboratory of Polymer Materials and Engineering, NingboTech University, Ningbo 315100, China.

* Corresponding authors: Prof. Yongqian Shi, Mr Yun Zhang and Prof. Yan Zhang

E-mail addresses: shiyq1986@fzu.edu.cn (Y. Shi), Yangzhoutengfei@126.com (Y. Zhang),

hnpdszy@163.com (Y. Zhang)

Abstract

In order to meet the application requirements for cables in different environments, it is imperative to develop cable tapes with insulation, flame retardancy, and high strength. In this work, a new type of halogen-free flame-retardant and high-strength coating was prepared by synthesizing a new phosphoramidate flame retardant phenyl P-methyl-N-(8-(methylamino)octyl) phosphonamidate (PPNPP) compounded with silicon wrapped ammonium polyphosphate (SiAPP) and molybdenum trioxide (MoO_3) added into thermoplastic polyurethane (TPU), and TPU/glass fiber cloth (TPU/G) composites were obtained by double-sided coating on the surface of glass fiber cloth (GFC) and heat curing. Compared with those of the pure TPU-coated sample, the peak of heat release rate (PHRR) and total heat release (THR) results of the TPU/G composite containing 20 wt% SiAPP-PPNPP- MoO_3 (TPU/G-SPM-1) decreased by 57.7% and 36.8%, respectively. In addition, the TPU/G-SPM-1 sample showed an excellent toxic gases suppression effect, i.e. the peak of carbon monoxide production rate (PCOPR) and total carbon monoxide yield (COTY) decreased by 91.4% and 98.9%, respectively, compared with the pure sample. The coating also imparted excellent mechanical properties to the GFC, which overcame the original defects of glass fiber such as poor abrasion resistance and brittleness, and the tensile strength of TPU/G-SPM-1 was increased by 101% compared with that of pure GFC. This work presents a new method for the preparation of flame-retardant and mechanically strong TPU/G composites used as cable tapes.

Keywords: Thermoplastic polyurethane; Interface engineering; Flame-retardancy; High-strength; Smoke suppression; Glass fiber cloth.

1. Introduction

In recent years, the installation scale of urban cables has been increasing, and cables, as a kind of wire product that transmits signals, conveys electricity or facilitates electromagnetic transformation, are the fundamental assurance for the stable operation of society. However, due to overloading, short circuit, aging and other reasons, cable fire will inevitably occur [1]. Once a cable fire occurs, the consequences are often severe owing to the imperceptibility, rapid spread and the toxicity of the smoke of cable combustion [2, 3]. Therefore, preventing cable fires or effectively controlling their spread is an urgent problem that needs to be addressed.

Cable core tape plays a crucial role in cables. The flame-retardant modification of cable core tapes is an effective measure to prevent cable fires. The common cable core wrapping tape on the market is mainly made of organic materials, for example polyvinyl chloride (PVC), thermoplastic polyurethane (TPU), polypropylene (PP) and polytetrafluoroethylene (PTFE), as the main matrix, and adding flame retardant and adhesive which has the advantages of simple preparation process, low cost and convenient processing. However, due to the single insulation or flame retardant performance, its applicability is limited. In recent years, some organic-inorganic composite products have gradually appeared both domestically and internationally, such products not only inherit the advantages of organic materials, but also integrate the characteristics of inorganic materials, such as excellent mechanical strength, insulation, corrosion resistance and high temperature resistance.

Glass fiber cloth (GFC), an inorganic material known for its excellent insulation, heat resistance, and corrosion resistance, is highly suitable for cable core winding tape. However, its inherent poor abrasion resistance and brittleness limit its service life. To meet the demands of industrial applications, there is an urgent need to improve flame-retardant and mechanical properties of GFC. Various methods

have been developed for modifying fibers, including solution dipping and spraying [4, 5], layer-by-layer assembly (LBL) [6-8], plasma treatment [9, 10], chemical surface grafting [11, 12], and sol-gel reaction [13, 14], etc. Among these, applying appropriate flame retardant coatings is considered as a straightforward and effective approach. Flame retardant coatings can significantly inhibit or slow the spread of flames and the release of toxic smoke. When the flame-retardant materials are concentrated on the surface, they maximize flame retardant efficiency without compromising the mechanical properties of the fabric [15]. Consequently, developing a suitable coating is the current problem that needs to be solved.

TPU is an excellent candidate for coatings due to its remarkable wear resistance, hardness, elasticity and easy processing, etc. Recently, researchers have increasingly applied TPU coatings to improve the hydrophobicity, flame retardancy, mechanical properties, and corrosion resistance of various materials [16-19]. However, the inherent flammability of TPU and heavy smoke release upon burning, significantly limit its applications [11, 20]. Hence, it is critical for finding a suitable way to reduce the fire risk of TPU.

The introduction of flame retardants is the primary method for enhancing the flame retardant properties of TPU. Traditional halogen-containing flame retardants are being phased out due to the release of corrosive gases and fumes during thermal decomposition. In recent years, phosphorous-nitrogen flame retardants have emerged as a preferred alternative, having the advantages of halogen-free, easy to obtain, low toxicity and cost effectiveness. Among all the phosphorous-nitrogen flame retardants, phosphoramidate flame retardants have garnered significant attention from researchers due to their high flame retardancy, low smoke production, as well as the strong interfacial adhesive with the polymeric matrix [21-23]. For example, Xue et al. synthesized an oligomeric phosphoramidate (PPP),

using a one-pot method, and found that PPP was well distributed in polylactic acid (PLA). Besides, the addition of 3 wt% PPP endowed the PLA sample with UL-94 V-0 rating, and the limiting oxygen index (LOI) increased from 20.5% to 32.5% [24]. Liu et al. developed a novel phosphoramidate flame retardant, $\text{Ti}_3\text{C}_2\text{Tx-PPPA}$, followed by incorporating it into TPU. At a 1.0 wt% addition, the total heat release (THR) and total smoke release (TSR) of the TPU composites were reduced by 32.6% and 54.4%, respectively, demonstrating effective flame retardancy and smoke suppression [25]. However, phosphoramidate flame retardants often fail to meet the demands of practical applications when used alone. In order to utilize the advantages of phosphoramidate-based compounds, researchers have considered combining them with other flame retardants to improve flame retardant efficiency. Ammonium polyphosphate (APP) is a halogen-free flame retardant rich in phosphorus and nitrogen, with excellent flame retardant properties due to its ability of release inert gases during combustion and excellent catalytic carbonation properties [26]. As an effective flame retardant, APP can be used alone or in combination with other flame retardants. Some studies have reported that the compounding of APP and phosphoramidate flame retardants could achieve outstanding flame-retardant effects [27]. For instance, Wei et al. synthesized a novel phosphonamide (PSA) through solution polycondensation and incorporated it with APP into epoxy resin (EP). The results indicated that the addition of 12.5 wt% PSA could endow the EP sample with a LOI value of 32%. Besides, the peak of heat release rate (PHRR) and THR of the EP/PSA decreased by 71.9% and 67.8%, respectively [28]. Ye et al. reported a hyperbranched flame retardant (HBPPDA) through polymerization, which significantly improved the flame-retardant performance of APP when 6.25 wt% of HBPPDA was added. The LOI value of the PP composites reached 30.6% with the content of 25 wt% flame retardant. Additionally, the PHRR and THR of the PP composite were reduced by 76.2% and 41.5%, respectively, compared to those of pure

PP [29]. Although several studies have confirmed that the addition of APP-modified phosphoramidites to polymers can achieve significant synergistic flame retardant effects. Unfortunately, there are still few reports on the application of such flame retardants to TPU.

In cable fire accidents, more than 2/3 of the deaths were caused by toxic and harmful smoke, therefore it is very important to inhibit the emission of smoke during cable combustion. Various studies have shown that the incorporation of small amounts of nanofillers (<5 wt%) into polymers can provides excellent flame retardancy and smoke suppression [30-32], which can be attributed to the advantages of small size, large surface area and good thermal conductivity of nanofillers. In addition, there is a synergistic effect between nanofillers and phosphorous-nitrogen flame retardants, due to the fact that the nanofillers with high thermal oxidative resistance can effectively enhance the char quality of the polymer during combustion, leading to an improvement in flame retardancy [15]. Molybdenum trioxide (MoO_3), as a traditional smoke suppression agent, exhibits excellent flame retardant and smoke suppressant effects by promoting the generation of carbon layer on top of polymers during combustion, and has been widely used for smoke suppression of various polymers. For example, Xu et al. prepared different forms of MoO_3 by high-temperature calcination and hydrothermal method, respectively, and added them into polyurethane elastomer (PUE) to study the flame retardant and smoke suppression properties of PUE composites. When the amount of 1 wt% was added, the PHRR of the PUE composite was reduced by 61.0%. As for smoke suppression, at 5 wt% addition, the smoke density of the PUE composites was reduced by 41.3% compared to that of pure PUE sample [33]. Yao et al. prepared $\text{Ti}_3\text{C}_2\text{T}_x\text{-MoO}_3$ flame retardant through electrostatic interactions, and added it into TPU by melt blending, and found that the PHRR and peak of smoke production rate (PSPR) of the TPU composite decreased by 26.2% and 42.9% respectively when the addition amount was 2 wt% [34].

Zeng et al. added three flame retardants, i.e. APP, PEPA and MoO₃, into vinyl ester resins (VERs), and found that the LOI value of VERs composites reached 31% at the addition levels of 10% APP, 10% PEPA and 5% MoO₃, respectively, besides the UL-94 V-0 rating, which showed excellent synergistic flame retardant properties [35].

In this study, a novel phosphoramidate flame retardant phenyl P-methyl-N-(8-(methylamino)octyl) phosphonamidate (PPNPP) was firstly synthesized via the esterification, and subsequently the flame retardant silicon wrapped ammonium polyphosphate (SiAPP)-PPNPP-MoO₃ (SPM) was prepared by solution mixing and incorporated into liquid TPU to create a flame retardant and high-strength TPU coating. This coating was then applied onto the surface of the GFC by brushing and heat curing processes to form the TPU/glass fiber cloth (TPU/G) composites. The synthesized flame retardants were characterised, and the morphological information, the flame retardant and mechanical properties of the TPU/G composites were investigated. In addition, the enhancement mechanism of the coating for flame retardancy and mechanical properties were discussed. This study proposes a novel idea for the development of new flame-retardant cable wrapping tape, which further broadens the application scope of TPU composites.

2. Experimental section

2.1. Materials

TPU (65E85) was produced by Bangtai Chemical Industry Co., Ltd. (Baoding, China). SiAPP (203) was purchased from Shenfeng Changfeng Chemical Co., Ltd. (Shenfeng, China). 1,8-octanediamine (98%), triethylamine (TEA, AR), acetonitrile (AR), phenyl dichlorophosphate (PDCP, 98%), ammonium molybdate tetrahydrate ((NH₄)₆Mo₇O₂₄•4H₂O, 99.9%), nitric acid (HNO₃, 66.5%), and N, N-Dimethylformamide (DMF, AR) were obtained from Aladdin Reagent Co., Ltd. (Shanghai,

China). GFC ($125 \pm 2 \text{ g/m}^2$) was purchased from Hebei Fuhua new building Materials Co., Ltd. (Langfang, China).

2.2. Synthesis of PPNPP

Typically, 8.64 g 1,8-octanediamine, 80 mL acetonitrile, and 18.40 g TEA were poured into the 500 mL three-neck flask equipped with a mechanical stirrer, condenser, and thermometer. Subsequently, 13.86 g PDCP and 40 mL acetonitrile were slowly added into the above solution with mechanical stirring for 1.5 h under ice bath. After that, the mixture was stirred at 60 °C for 3 h, and then heated to 80 °C and kept stirring for 3 h. Finally, the organic phase was separated and washed three times with deionized water and petroleum ether, and dried for 24 h in a vacuum oven.

2.3. Preparation of MoO₃

20.00 g $(\text{NH}_4)_6\text{Mo}_7\text{O}_{24}\cdot 4\text{H}_2\text{O}$ was dissolved in 200 mL deionized water with mechanical stirring for 30 min under room temperature, and then 6.55 mL HNO_3 was added into the above solution. After that, the mixture was transferred into a reaction kettle at 180 °C for 24 h. Finally, the precipitate was separated by filtration, washed with ethanol and deionized water after being cooled down to room temperature, and the product was dried at 60 °C in a vacuum oven for 24 h.

2.4. Fabrication of TPU/G composites

To prepare the fire-retardant coating (TPU/SPM-1.0), 20.00 g TPU was mixed with 60 mL DMF at 80 °C until TPU completely dissolved to liquid. Subsequently, 2.50 g SiAPP and 1.25 g PPNPP were dissolved in 20 mL DMF and thereby added to the TPU solution with mechanical stirring for 10 min. Then, 1.25 g MoO₃ was added into the mixture with ultrasonic mixing for 20 min. Finally, the coating was applied to the surface of GFC by double-sided coating and heat curing processes to prepare TPU/G-SPM-1.0. For the designation of the TPU/G composites, GFC coated with pure TPU is defined

as TPU/G and the composites with added flame retardants are defined as TPU/G-X, the X stands for different ratios of flame retardants. The schematic diagram for preparation of TPU/G-X is shown in Fig. 1, and Table 1 summarizes the formulations of the TPU/G composites.

2.5. Characterization

Fourier transform infrared spectra (FTIR) of the samples were estimated on a Nicolet IS50 spectrometer (Nicolet Instrument Company, USA) with a wavenumber range of 4000 to 400 cm^{-1} . ^1H NMR and ^{13}C NMR were measured on a fully digitalized nuclear magnetic resonance spectrometer (NMR, AVANCE NEO 600, Switzerland) at 600 MHz using DMSO- d_6 as a solvent. X-ray diffraction (XRD) results of samples were obtained using a DY1602/Empyrean x-ray diffractometer ($\lambda = 1.54178$ Å). Scanning electron microscope (SEM, Verios G4, USA) was used to observe the surface morphologies of the GFC and TPU/G composites. The surface elemental distribution of TPU/G-X microstructure and char residues were observed by energy dispersive spectrometer (EDS). Thermal conductivity data were obtained by a thermal conductivity tester (DRP-II, Xiangtan Xiangyi Instrument Co., Ltd.). The combustion behavior of the TPU/G composites was estimated by TTech-GBT16172-2 cone calorimeter (CCT) (TESTech, Suzhou, China) according to the ISO 5660 standard under a heat flux of 35 kW/m^2 . Each sample with a size of 100 mm \times 100 mm \times 0.2 mm and stacked in 10 layers (2 mm). Thermogravimetric analysis (TGA) of the TPU/G composites was performed by thermal analyzer (TA Q5000, USA) from room temperature to 800 $^{\circ}\text{C}$ with 20 $^{\circ}\text{C}/\text{min}$ heating rate under Ar and air conditions. Smoke density data of the samples were obtained by plastic smoke density tester (JSC-2), according to GB/T 8323-2008. Each sample with dimensions of 75 mm \times 75 mm \times 0.2 mm and exposed horizontally to an external heat flux of 25 kW/m^2 with the application of no pilot flame. Mechanical properties of the GFC and TPU/G samples were tested by an electronic universal

testing machine (JPL-1000N) with a tensile rate of 20 mm/min according to GB/T12914-2018. LOI values of the samples were tested by the LOI analyzer (HC-2, Nanjing, China) according to GB/T5454-1997 with specimen dimensions of 150 mm × 58 mm × 0.2 mm. The vertical burning test was carried out by vertical combustion tester (CZF-II, Jiangning Analytical Instruments Co., Ltd.) according to GB/T5455-2014, and each sample with dimensions of 300 mm × 89 mm × 0.2 mm. Raman spectroscopy was provided by a Renishaw Invia Raman Microscope (Invia Reflex, Britain) with a 532 nm argon ion laser.

3. Results and discussion

3.1. Characterization of flame retardants

Fig. 2a shows the preparation route of PPNPP, which was synthesized via the esterification of 1,8-octanediamine and PDCP. Fig. 2b shows the FTIR spectra of PPNPP and its raw materials. The absorption peaks at 3200-3500 cm^{-1} are ascribed to the stretching vibration of primary amine in the 1,8-octanediamine [25]. For PDCP, the peaks at 564 cm^{-1} and 1210 cm^{-1} typically are associated with the stretching vibrations of the P-Cl and P=O bonds, respectively [36]. In contrast to the FTIR spectra of raw materials, the disappearance of P-Cl and primary amine bonds, and the formation of a new peak of secondary amine at 3390 cm^{-1} indicate the complete reaction between 1,8-octanediamine and PDCP [37]. Besides, the new peaks generated at 1100 and 1030 cm^{-1} are ascribed to P-N-C and P-N, respectively [29], which further confirms the successful synthesis of PPNPP.

To further verify the structure of PPNPP, the products were characterized by ^1H and ^{13}C NMR tests. Fig. 2c is the ^1H NMR spectrum of PPNPP, showing that the resonance signals in the range of 7.05-7.22 ppm are attributed to the aromatic protons on the benzene ring (labeled a, b, c), and the signal around 1.17 ppm corresponds to the imine structure on the main chain of PPNPP (labeled d, k) [28].

In addition, the weak signals in the range of 2.98-3.06 ppm and 3.40-3.44 ppm are attributed to the methylene structure on the carbon chain (labeled e-j) [22]. Fig. 2d presents the ^{13}C NMR spectrum. The signal at 150.5 ppm supports the aromatic carbon structure at the junction of the benzene ring and the main chain of PPNPP (labeled a), while the signals in the range of 120.0-130.0 ppm are ascribed to the remaining aromatic structures on the benzene ring (labeled b, c, d). In addition, the signals at 41.0 ppm, 46.2 ppm, and the range of 25.0-32.5 ppm are attributed to the methylene structures on the main carbon chain (labeled e-k). The results above confirm the successful synthesis of PPNPP.

The XRD patterns of MoO_3 nanorods are plotted in Fig. 2e. It can be seen from the XRD patterns that the reflection peaks located at $2\theta = 9.7^\circ$, 19.4° , 25.8° , and 45.5° correspond to the (100), (200), (210), and (410) crystal planes of MoO_3 nanorods, which are consistent with the standard card (JCPDS: 83-1176) [33], proving the successful synthesis of MoO_3 nanorods.

3.2. Surface morphology and element composition

The micromorphology of flame-retardant coating on the GFC was studied by SEM. As shown in Fig. 3a₁-a₃, the pristine GFC has a smooth and flat surface, and a complete fiber structure can be observed. After the introduction of the TPU coating, the surface of the GFC becomes more consistent and rougher (Fig. 3b₁-b₃). It is noted that a thin film is attached onto the surface of the GFC. In comparison to TPU/G, a large number of micro/nano-scale hierarchical structures are obtained on the surface of TPU/G-SPM-1 (Fig. 3c₁-c₃), which can be attributed to the deposition of SPM flame retardant. In addition, the element distribution mapping images for the surface of TPU/G-SPM-1 are shown in Fig. 3d, revealing the homogeneous distributions of C, N, O, Si, P and Mo elements in the flame retardant coating. Meanwhile, these distributions of different elements exhibit a clear fiber shape similar to the GFC, further indicating that the TPU/SPM flame retardant coating have been

successfully applied to the surface of the GFC.

3.3. Thermal stability

The thermal degradation behavior of the TPU/G composites with different coatings was studied through TGA technique. The degradation curves of the TPU/G composites under Ar (a) and air (b) atmosphere are plotted in Fig. 4 (since the test temperature did not reach the degradation temperature of the GFC, this discussion focuses solely on the thermal degradation performance of the TPU flame-retardant coating), and the related thermal data are shown in Table 2. As displayed in Fig. 4a, the thermal degradation of all samples under the Ar atmosphere presents two typical weight loss stages. The first stage involves the degradation of the hard segments of the TPU main chain to diols and diisocyanates, while the second stage is attributed to the further breakdown of isocyanates and polyols in the soft segments of TPU chains [38]. However, the thermal oxidative degradation processes of TPU/G-X under the air atmosphere occur in three different stages (Fig. 4c). In addition to the two thermal degradation stages mentioned above, the final stage can be lied to the further thermal oxidative degradation of the char residues produced in the first stage [39]. As observed from Table 2, the initial decomposition temperature ($T_{5\%}$) of TPU/G-X decreases significantly, compared to that of TPU/G. This may be due to SPM flame retardant can catalyze the decomposition of polyurethane bonds into isocyanates, alcohols, and carbon dioxide at lower temperatures, which can delay heat transfer and decrease the fire hazard of TPU/G-X [40, 41]. After the thermal degradation stages, the char yields of TPU/G under the air and Ar atmospheres are 69.20% and 70.82%, respectively. Notably, the char residues of TPU/G-X at 800 °C are significantly higher than TPU/G, indicating that SPM flame retardant effectively enhances the thermal stability of the TPU coating. Furthermore, by comparing the char yield of different samples, it is noted that under the same loading conditions, TPU/G-SM-1

exhibits the highest char yield at 800 °C in both air and Ar atmospheres, indicating that SiAPP actually performs better char formation ability than PPNPP. This phenomenon can be attributed to SiAPP acting as a suitable acid source and demonstrating superior flame retardant performance in the condensed phase.

Additionally, from the differential thermal gravity (DTG) curves in Fig. 4b, d, it can be seen that the main thermal degradation peaks of TPU/G-X are significantly lower than TPU/G, and the corresponding maximum decomposition rate temperature (T_{\max}) is also lower than the control one. This is primarily related to the increase in char yield, as SPM flame retardant effectively improves the stability of the char layer formed during combustion, physically hindering heat transfer and enhancing the fire resistance of the composites.

3.4. Thermal conductivity

The thermal conductivity serves as an important index to evaluate the heat transfer performance of materials, which can be tested by thermal conductivity tester (Fig. 5a). As shown in Fig. 5b, GFC exhibits high thermal conductivity ($49.9 \text{ mW m}^{-1} \text{ K}^{-1}$), while TPU/G has a thermal conductivity of $32.0 \text{ mW m}^{-1} \text{ K}^{-1}$. In contrast, the thermal conductivity of TPU/G-X samples is reduced to varying degrees. The comparison of different samples reveals that the thermal conductivity of the TPU/G-SPM composites tends to increase as the amount of SPM flame retardant decreases, indicating that the incorporation of SPM flame retardant effectively enhances the thermal insulation properties of the coating, potentially reducing the rate of heat transfer during combustion, and thereby improving fire safety. It is evident that TPU/G-SM-1 has the lowest thermal conductivity ($16.7 \text{ mW m}^{-1} \text{ K}^{-1}$). This phenomenon can be attributed to the reason that introduction of SiAPP alters the arrangement of TPU molecules, resulting in a denser structure that hinders the establishment of an efficient heat channel

[42]. In addition, this leads to the thermal conductivity of TPU/G-PM-1 higher than that of TPU/G-SM-1.

3.5. Flame retardant performance

To evaluate the flame retardant performance of the materials, the LOI and vertical burning test are usually employed to assess flammability of polymeric materials. The relevant flammability data are presented in Table 3. The LOI value of the pristine TPU/G sample is 23.3%, indicating a high fire risk. In contrast, the LOI value of TPU/G-SPM-3 reaches 27%. This means that the TPU coating transforms from a flammable material into a highly flame-retardant one at a low load of SPM. Meanwhile, the LOI value of the TPU composites increases with increasing content of SPM, which indicate a significant improvement in the flame retardant properties of the coating. Moreover, as shown in the digital photographs in Fig. 6, TPU/G is ignited rapidly after encountering fire, which eventually burns all the TPU coating on the sample within 20 s. In contrast, TPU/G-SPM-1 passes the vertical burning test, and self-extinguishes immediately after 6 s of ignition with the char residues morphology remaining intact with a small damaged length (120 ± 2 mm). In summary, these results indicate that the TPU coating added with SPM improves flame retardancy of the TPU/G composites.

The CCT is an instrument for evaluating the combustion behavior of materials, which collects the combustion parameters of composites by simulating the fire scenario to comprehensively evaluate the flame retardancy and smoke suppression properties of materials [43]. As shown in Fig. 7 and Table 4, the time to ignition (TTI) of TPU/G is 47s. In contrast, the TTI of composites incorporating only two types of flame retardants exhibits varying trends (TPU/G-SP-1, TPU/G-SM-1 increasing and TPU/G-PM-1 decreasing) compared to the control one. After comparing different samples, it can be found that the TTI of the composites gradually increases with the increase of SiAPP flame retardant. This

phenomenon can be attributed to the higher thermal stability of SiAPP than PPNPP, which is well consistent with the trends observed in thermal conductivity tests. Furthermore, the TTI values of the TPU composites containing SPM flame retardant are all less than 47 s, and gradually decrease with the increase of SPM addition, indicating that SPM flame retardant can catalyze the early decomposition of the TPU coating.

The PHRR is an important parameter for assessing the fire hazard of composites after combustion [44]. The HRR and THR curves are shown in Fig. 7a, b. Due to the high flammability of TPU, TPU/G exhibits high PHRR of 260 kW/m² and THR of 16.7 MJ/m². In contrast, the incorporation of the SPM flame retardant significantly reduces the PHRR and THR of the composites. Particularly, the PHRR and THR of TPU/G-SPM-1 are 110 kW/m² and 10.6 MJ/m², respectively, which are 57.7% and 36.8% lower than those of TPU/G. Notably, TPU/G-SM-1 shows the lowest THR of 6.3 MJ/m², which can be attributed to the high flame retardant efficiency of SiAPP, significantly shortening the combustion time of the composites. Combined with the CCT data, it is concluded that SPM significantly reduces the fire hazard of the TPU coating, which is in good agreement with the results of the TGA and LOI tests.

The impact of cable combustion is often severe due to its imperceptible, rapidly spreading and the emission of large quantities of toxic and harmful smoke. Therefore, it is extremely important to improve the smoke suppression performance of cable materials. The SPR and TSR data of different samples are presented in Fig. 7c, d. TPU/G shows high PSPR (0.1222 m²/s) and TSR (664.5 m²/m²). In comparison, the PSPR and TSR values of TPU/G-SPM-1 are 0.0658 m²/s and 404.2 m²/m², respectively, which are 46.2% and 39.2% lower than those of TPU/G. However, the PSPR (0.1169 m²/s) and TSR (633.6 m²/m²) of TPU/G-SP-1 respectively decrease by only 4.3% and 4.7%, compared to those of the control one, indicating that the incorporation of a small amount of MoO₃ can effectively

enhance the smoke suppression performance of the TPU coating. This can be due to the explanation that MoO_3 , as an inorganic nanofiller, has been shown to synergize with phosphorous-nitrogen flame retardants in polymers (such as VERs and rigid polyurethane foam) to promote the formation of carbon layer, which enables the composites to exhibit excellent smoke suppression [35, 45-47].

The toxic and harmful gases suppression curves of the TPU composites are shown in Fig. 7e-h. The peak of the carbon dioxide production rate (PCO_2PR) and total carbon dioxide yield (CO_2TY) of TPU/G-X are significantly lower than those of TPU/G. Notably, TPU/G-SPM-1 demonstrates the lowest PCO_2PR (0.0560 g/s), which is 53.6% lower than that of the control sample. However, TPU/G-SM-1 exhibits a lower CO_2TY (2.94 kg/kg). Additionally, carbon monoxide (CO) is one of the deadliest gases in a fire hazard. When CO level in the air reaches 1%, it can cause loss of consciousness [48]. The pristine TPU/G shows high peak of carbon monoxide production rate (PCOPR) (0.00245 g/s) and total carbon monoxide yield (COTY) (0.1377 kg/kg). In contrast, TPU/G-X with varying proportions of SPM (12 wt%, 16 wt%, and 20 wt%) show a reduction of over 90% in COTY compared to TPU/G. Specially, TPU/G-SPM-1 shows significant reductions in PCOPR (0.00021 g/s) and COTY (0.0014 kg/kg) by 91.43% and 99.0%, respectively, compared with the control one. This excellent toxic and harmful smoke suppression performance can be attributed to the synergistic effect of SPM in both the condensed and gas phases. Other studies on CO suppression of TPU composites are listed in Fig. 7i, further demonstrating the superiority of this work in terms of toxic gas inhibition performance [11, 20, 49-57].

The mass loss after combustion is an important factor affecting the flame retardant and smoke suppression performance of the composites, as shown in Fig. 7j, the residual mass of TPU/G only 63.89%, and with the addition of SPM flame retardant, the mass loss of TPU/G-X showed a significant

reduction trend. Among them, TPU/G/SM-1 exhibits the highest residual mass (77.26%), which can be attributed to the excellent performance of SiAPP in the condensed phase, which is consistent with the previous analysis. The addition of flame retardant can well catalyse the TPU matrix to generate a dense and stable carbon layer in combustion, which can well reduce the heat conduction and smoke emission in combustion, and reduce the fire hazard of composites.

3.6. Smoke density test

Smoke density testing simulates the smoke density and concentration released by burning materials under fire conditions, which is crucial for ensuring people's health and safety [58, 59]. The smoke density curves of the TPU/G composites are portrayed in Fig. 7k and Table 5. The $D_{s,10}$ and $D_{s,max}$ are defined as smoke density at 10 min and the maximum smoke density, respectively. For TPU/G, $D_{s,10}$ and $D_{s,max}$ are 74.8 and 75.1, indicating that the pure TPU coating emits large amounts of smoke during combustion. In contrast, with the increase of SPM flame retardant addition, the $D_{s,max}$ values of TPU/G-SPM-3, TPU/G-SPM-2 and TPU/G-SPM-1 are 53.5, 37.6 and 30.4, respectively, which are 28.8%, 49.9% and 59.5% less than that of the control sample, demonstrating that SPM flame retardant effectively reduces the concentration of smoke. Notably, the $D_{s,10}$ and $D_{s,max}$ of TPU/G-X show a similar decreasing pattern when the flame retardants are added in equal amounts, suggesting that either SiAPP or PPNPP in combination with MoO_3 can effectively reduce the smoke density of the TPU coatings during combustion. This phenomenon may be attributed to the quenching effects generated during combustion by the phosphorus-nitrogen flame retardant and MoO_3 , as well as the formation of a dense char layer.

3.7. Flame retardant mechanism

To further investigate the flame-retardant mechanism of TPU/G-X, the microstructure of the char

residues was analyzed by SEM. Digital photos and SEM images of the char residues of the TPU/G composites are presented in Fig. 8. It is observed that, for TPU/G, the TPU coating applied to the GFC burns out, and the samples show a clear fiber structure. In contrast, the surfaces of TPU/G-X displayed distinct char structures. Notably, for TPU/G-X containing SiAPP (Fig. 8b-f), the expanded char layer tightly covers the surface of the GFC, which is critical in the heat insulation and oxygen barrier during combustion. This phenomenon can be attributed to the formation of polyphosphoric acids in the decomposition process of APP, which can catalyze the decomposition of the TPU matrix and form an expanded carbon layer. Notably, the char residues of TPU/G-SPM-1 exhibit a highly continuous and dense structure. This intense and solid char layer effectively reduces smoke emissions during combustion, which explains the excellent smoke suppression performance of TPU/G-SPM-1.

The degree of graphitization of the TPU composites is typically analyzed by Raman spectroscopy (Fig. 9a-g). The smaller the I_D/I_G ratio, the greater the degree of graphitization is [60]. TPU/G has the I_D/I_G ratio of 2.49. In contrast, TPU/G-X with the addition of SPM (Fig. 9b-d) have the decreased I_D/I_G ratios (2.34, 2.46 and 2.37, respectively for TPU/G-SPM-1, TPU/G-SPM-2 and TPU/G-SPM-3), indicating that the graphitization degree of the TPU composites is improved by the addition of SPM. Furthermore, comparing the I_D/I_G ratios between TPU/G-SPM-1 and TPU/G-SP-1 indicates that the addition of 5 wt% MoO_3 significantly enhances the graphitization degree of the composites, which is consistent with the CCT and TGA results. It is obvious that TPU/G-PM-1 exhibits the lowest I_D/I_G ratio (1.6) among all TPU samples. However, the flame retardant and smoke suppression performances reported in the CCT data is not ideal. This can be attributed to the char residues generated by TPU/G-PM-1, which shows high density of char residues (as shown in Fig. 8g) but lacks the expansion capability. As a result, it is unable to form a continuous and dense char layer during combustion,

leading to relatively poor smoke suppression performance.

FTIR is adopted to study the chemical composition and molecular structure of char residues of the TPU coating. As plotted in Fig. 9h, the characteristic peak at 1601 cm^{-1} for all the samples corresponds to the unsaturated C=C bonds formed by aromatic compounds after TPU combustion [61]. It is observed that after adding SPM retardant into the TPU coating, the new characteristic peaks at 1221 and 970 cm^{-1} are assigned to the stretching vibrations of P=O and P-O-C, respectively [62, 63]. In addition, the characteristic peak at 1071 cm^{-1} corresponds to the Si-O-Si stretching vibration [64]. Combined with the SEM images of char residue, it can be analyzed that the TPU samples containing silica gel decompose at high temperatures to generate phosphoric acid-containing components, which can accelerate the decomposition of the main chain of the TPU and enhance the char formation properties of the TPU composites.

In order to reveal the flame retardant mechanism of the flame retardant TPU coatings, the relationship between the reduction in PHRR and char residue was investigated under the same amount of flame retardant added, as shown in Fig. 9i. It is noted that the correlation coefficient (R_1^2) between values of char residues and PHRR reduction of TPU/G-X is 0.730, indicating the poor linear correlation. In order to further investigate the mechanism of PHRR reduction, the relationship between the PHRR reduction and the contribution value (defined as the sum of the absolute value of char residue and the gas phase index Y) is presented in Fig. 9j [49]. The introduction of the gas phase index shows a clear linear relationship between the PHRR reduction and contribution values ($R_2^2 = 0.999$), indicating the existence of gas phase flame retardant mechanism for TPU/G-X. As shown in Table 6, it can be observed that the gas phase index of TPU/G-PM-1 is 10.62, which is 3 times as that of TPU/G-SPM-1. Notably, this result is very consistent with the proportion of PPNPP flame retardant added. In

addition, TPU/G-SM-1 has a relatively low gas phase index of 0.57. From comparing different samples, it can be seen that the gas phase index of the TPU composites increases linearly and significantly with the increase of PPNPP addition. It can be speculated that PPNPP flame retardant plays a very important role in the gas phase flame mechanism, while the flame retardant mechanism of SiAPP is mainly reflected in the condensed phase.

Based on the results and discussions presented above, the possible mechanism for enhancing the flame retardant and smoke suppression performance of TPU/G-X is proposed (Fig. 9k). After burning, SiAPP and PPNPP rapidly dehydrate and decompose into components, such as phosphoric acid, metaphosphoric acid and polyphosphoric acid, which can accelerate the char formation of the TPU matrix and promote cross-linking of carbonization [65]. Meanwhile, SiO₂ and MoO₃ form a dense oxide film on the surface, preventing O₂ from entering the interior and thus inhibiting the combustion of TPU coating. On the other hand, SiAPP and PPNPP release non-flammable products, such as H₂O and NH₃ upon combustion, which dilute the concentration of flammable gases. Moreover, SiAPP and PPNPP can degrade to generate free radicals i.e. PO• and HPO• at high temperatures, which can capture active radicals such as H• and OH•, thereby reducing the combustion rate and suppressing the emission of toxic and harmful smoke. Overall, the synergistic effect of SPM in the condensed phase and the gas phase can effectively enhance the flame retardant and smoke suppression abilities of flame retardant TPU coatings.

3.8. Mechanical property

To meet the demands of daily applications, it is crucial to overcome the inherent defects of GFC, such as poor abrasion resistance and brittleness. The mechanical properties of the GFC and TPU/G composites are presented in Fig. 10a. The tensile strength and elongation at break of GFC are 64.7

MPa and 3.4%, respectively. After coating with TPU, TPU/G exhibits a tensile strength of 126.9 MPa, representing a 96.1% increase compared to that of pure fabric. However, the elongation at break decreases to 2.6%, which may be due to the higher strength conferred by the TPU coating at the expense of some toughness. It is noted that the mechanical properties of TPU/G-X are generally improved compared to that of the control sample. In order to investigate the effect of different coating ratios on mechanical properties, the fracture surfaces of all samples were observed by SEM (Fig. 10b-h). Notably, the values of tensile strength of TPU/G-X are higher than that of TPU/G, indicating that the addition of SiAPP and PPNPP can enhance the interfacial compatibility of the TPU coating with GFC.

The mechanical strengthening mechanism of TPU coatings is analysed as shown in Fig. 10i-m. The GFC is unable to maintain its original neatly woven structure after being damaged by external forces (Fig. 10i), and the fibres appear to be dispersed. In contrast, TPU/G-SPM-1 (Fig. 10j, k) has dense and compact structure. Moreover, the fracture region of TPU/G-SPM-1 (Fig. 10l) displays that though the external TPU coating is pulled off, the internal GFC still maintains its original structure, indicating that the TPU coating protects the GFC well from damage in the early stage of tensile. Based on the above analysis, the mechanical enhancement mechanism of the TPU coatings is proposed and illustrated in Fig. 10m. Multiple hydrogen bonding interactions are formed between SPM flame retardant and TPU chains before stretching, which makes the composites present 3D morphology. After the tensile force is applied, the TPU chains are straightened, and the hydrogen bonding of the internal connection is broken and slipped. With the continuous application of the external force, the external TPU coating firstly deforms and break down. Subsequently, after the TPU coating is broken, the tensile force is transferred to the GFC, ultimately causing the breakage of GFC.

4. Conclusions

In this work, the novel phosphoramidate flame retardant PPNPP was synthesized by esterification and compounded with SiAPP and MoO₃ added into TPU to prepare TPU flame-retardant coatings, and finally the flame-retardant TPU/G composites were obtained by double-sided coating on the surface of GFC and heat curing. The results indicate that the SPM flame retardant provides the TPU coating with excellent flame-retardant performance. For TPU/G-SPM-1, the PHRR and THR decreased by 57.7% and 36.8%, respectively, compared to TPU/G. Meanwhile, the incorporation of the SPM flame retardant effectively reduces the emission of toxic and harmful smoke during the combustion of the TPU composites. Notably, this coating demonstrated remarkable suppression of CO emissions. For TPU/G-SPM-1, the PCOPR and CO yield decreased by 91.4% and 98.9%, respectively, compared to the pure sample. Furthermore, the TPU/SPM flame-retardant coating also imparts excellent mechanical properties to the GFC. Compared to pure GFC (64.7 MPa), the tensile strength of TPU/G-SPM-1 is improved by 101%, reaching 130.3 MPa. In summary, this work provides a novel approach for the preparation of fire-resistant TPU composites, demonstrating promising applications in the field of cable wrapping materials.

CRedit authorship contribution statement

Yongqian Shi: Writing - Original Draft, Supervision, Funding acquisition; **Songqiong Jiang:** Writing-Review & Editing, Data Curation, Investigation, Formal analysis; **Jinke Wu:** Conceptualization, Data Curation, Visualization; **Zhendong Chen:** Validation, Visualization; **Cancan Zhang:** Writing-Review & Editing, Validation, Visualization, Supervision; **Yun Zhang:** Methodology, Investigation; **Pingan Song:** Methodology, Investigation; **Yan Zhang:** Validation, Visualization.

Declaration of competing interest

The authors declare that they have no known competing financial interests or personal relationships that could have appeared to influence the work reported in this paper.

Acknowledgement

This work was financially supported by the Key research and development projects of Baoying County (Grant No. BY202205) and International Scientific and Technological Cooperation Program of Ningbo (No. 2024H020).

References

- [1] Y. Li, L. Qi, Y. Liu, J. Qiao, M. Wang, X. Liu, S. Li, Recent Advances in Halogen-Free Flame Retardants for Polyolefin Cable Sheath Materials, *Polymers* 14 (2022) 2876.
- [2] W. An, T. Wang, K. Liang, Y. Tang, Z. Wang, Effects of interlayer distance and cable spacing on flame characteristics and fire hazard of multilayer cables in utility tunnel, *Case Stud. Therm. Eng.* 22 (2020) 100784.
- [3] P. Jia, X. Yu, J. Lu, X. Zhou, Z. Yin, G. Tang, T. Lu, L. Guo, L. Song, B. Wang, Y. Hu, The $\text{Re}_2\text{Sn}_2\text{O}_7$ (Re = Nd, Sm, Gd) on the enhancement of fire safety and physical performance of Polyolefin/IFR cable materials, *J. Colloid Interf. Sci.* 608 (2022) 1652-1661.
- [4] A. Vishwakarma, M. Singh, B. Weclawski, V. J. Reddy, B. K. Kandola, G. Manik, A. Dasari, S. Chattopadhyay, Construction of hydrophobic fire retardant coating on cotton fabric using a layer-by-layer spray coating method, *Int. J. Biol. Macromol.* 223 (2022) 1653-1666.
- [5] W. Al-Shatty, D. A. Hill, S. Kiani, A. Stanulis, S. Winston, I. Powner, S. Alexander, A. R. Barron, Superhydrophilic surface modification of fabric via coating with cysteic acid mineral oxide, *Appl. Surf. Sci.* 580 (2022) 152306.
- [6] J.-C. Yang, W. Liao, S.-B. Deng, Z.-J. Cao, Y.-Z. Wang, Flame retardation of cellulose-rich fabrics via a simplified layer-by-layer assembly, *Carbohydr. Polym.* 151 (2016) 434-440.
- [7] L. Lu, C. Hu, Y. Zhu, H. Zhang, R. Li, Y. Xing, Multi-functional finishing of cotton fabrics by water-based layer-by-layer assembly of metal-organic framework, *Cellulose* 25 (2018) 4223-4238.

- [8] D. Ding, Q. Wu, J. Wang, Y. Chen, Q. Li, L. Hou, L. Zhao, Y.-y. Xu, Superhydrophobic encapsulation of flexible Bi₂Te₃/CNT coated thermoelectric fabric via layer-by-layer assembly, *Compos. Commun.* 38 (2023) 101509.
- [9] M. Ayesb, A. R. Horrocks, B. K. Kandola, The effect of combined atmospheric plasma/UV treatments on improving the durability of organophosphorus flame retardants applied to polyester fabrics, *Polym. Degrad. Stab.* 225 (2024) 8737.
- [10] L. Qi, B. Wang, W. Zhang, B. Yu, M. Zhou, Y. Hu, W. Xing, Durable flame retardant and dip-resistant coating of polyester fabrics by plasma surface treatment and UV-curing, *Prog. Org. Coat.* 172 (2022) 107066.
- [11] W. Wu, W. Huang, Y. Tong, J. Huang, J. Wu, X. Cao, Q. Zhang, B. Yu, R. K. Y. Li, Self-assembled double core-shell structured zeolitic imidazole framework-8 as an effective flame retardant and smoke suppression agent for thermoplastic polyurethane, *Appl. Surf. Sci.* 610 (2023) 155540.
- [12] K. Liu, Y. Lu, Y. Cheng, J. Li, G. Zhang, F. Zhang, Flame retardancy and mechanism of polymer flame retardant containing P-N bonds for cotton fabrics modified by chemical surface grafting, *Cellulose* 31 (2024) 3243-3258.
- [13] Y. Ma, Y. Wang, L. Ma, Z. Zhu, Fabrication of hydrophobic and flame-retardant cotton fabric via sol-gel method, *Cellulose* 30 (2023) 11829-11843.
- [14] D. Zhang, B. L. Williams, S. B. Shrestha, Z. Nasir, E. M. Becher, B. J. Lofink, V. H. Santos, H. Patel, X. Peng, L. Sun, Flame retardant and hydrophobic coatings on cotton fabrics via sol-gel and self-assembly techniques, *J. Colloid Interf. Sci.* 505 (2017) 892-899.
- [15] Y. Huang, S. Jiang, R. Liang, P. Sun, Y. Hai, L. Zhang, Thermal-triggered insulating fireproof layers: A novel fire-extinguishing MXene composites coating, *Chem. Eng. J.* 391 (2020) 123621.

- [16] T.-T. Li, S. Chu, X. Hu, H.-T. Ren, C.-W. Lou, J.-H. Lin, Silica Nanoparticle/TPU Coating Imparts Aramid with Puncture Resistance and Anti-corrosion for Personal Protection, *ACS Appl. Nano Mater.* 6 (2023) 16986-16999.
- [17] A. Moiz, R. Padhye, X. Wang, Coating of TPU-PDMS-TMS on Polycotton Fabrics for Versatile Protection, *Polymers* 9 (2017) 660.
- [18] Y. Liu, X. Cao, J. Shi, B. Shen, J. Huang, J. Hu, Z. Chen, Y. Lai, A superhydrophobic TPU/CNTs@SiO₂ coating with excellent mechanical durability and chemical stability for sustainable anti-fouling and anti-corrosion, *Chem. Eng. J.* 434 (2022) 134605.
- [19] Q. He, W. Wu, H. Hu, Z. Rui, J. Ye, Y. Wang, Z. Wang, Achieving superior fire safety for TPU 3D-printed workpiece with EP/PBz/PDMS coating, *J. Appl. Polym. Sci.* 140 (2023) 53858.
- [20] W. Huang, J. Huang, B. Yu, Y. Meng, X. Cao, Q. Zhang, W. Wu, D. Shi, T. Jiang, R. K. Y. Li, Facile preparation of phosphorus containing hyperbranched polysiloxane grafted graphene oxide hybrid toward simultaneously enhanced flame retardancy and smoke suppression of thermoplastic polyurethane nanocomposites, *Compos. Part A Appl. Sci.* 150 (2021), 106614.
- [21] M. Steinmann, M. Wagner, F. R. Wurm, Poly(phosphorodiamidate)s by Olefin Metathesis Polymerization with Precise Degradation, *Chem. Eur. J.* 22 (2016) 17329-17338.
- [22] Y. Xue, Z. Ma, X. Xu, M. Shen, G. Huang, S. Bourbigot, X. Liu, P. Song, Mechanically robust and flame-retardant polylactide composites based on molecularly-engineered polyphosphoramides, *Compos. Part A Appl. Sci.* 144 (2021) 106317.
- [23] Q. Tai, R. K. K. Yuen, L. Song, Y. Hu, A novel polymeric flame retardant and exfoliated clay nanocomposites: Preparation and properties, *Chem. Eng. J.* 183 (2012) 542-549.

- [24] Y. Xue, M. Shen, Y. Zheng, W. Tao, Y. Han, W. Li, P. Song, H. Wang, One-pot scalable fabrication of an oligomeric phosphoramidate towards high-performance flame retardant polylactic acid with a submicron-grained structure, *Compos. B Eng.* 183 (2020) 107695.
- [25] C. Liu, D. Yang, M. Sun, G. Deng, B. Jing, K. Wang, Y. Shi, L. Fu, Y. Feng, Y. Lv, M. Liu, Phosphorous-Nitrogen flame retardants engineering MXene towards highly fire safe thermoplastic polyurethane, *Compos. Commun.* 29 (2022) 101055.
- [26] Y.-R. Li, Y.-M. Li, W.-J. Hu, D.-Y. Wang, Cobalt ions loaded polydopamine nanospheres to construct ammonium polyphosphate for the improvement of flame retardancy of thermoplastic polyurethane elastomer, *Polym. Degrad. Stab.* 202 (2022) 110035.
- [27] M. Wan, C. Shi, X. Qian, Y. Qin, J. Jing, H. Che, F. Ren, J. Li, B. Yu, K. Zhou, Design of novel double-layer coated ammonium polyphosphate and its application in flame retardant thermoplastic polyurethanes, *Chem. Eng. J.* 459 (2023) 141448.
- [28] W. Zhao, J. Liu, H. Peng, J. Liao, X. Wang, Synthesis of a novel PEPA-substituted polyphosphoramidate with high char residues and its performance as an intumescent flame retardant for epoxy resins, *Polym. Degrad. Stab.* 118 (2015) 120-129.
- [29] X. Ye, Y. Wang, Z. Zhao, H. Yan, A novel hyperbranched poly(phosphorodiamidate) with high expansion degree and carbonization efficiency used for improving flame retardancy of APP/PP composites, *Polym. Degrad. Stab.* 142 (2017) 29-41.
- [30] X. Dong, Y. Ma, X. Fan, S. Zhao, Y. Xu, S. Liu, D. Jin, Nickel modified two-dimensional bimetallic nanosheets, $M(OH)(OCH_3)$ ($M=Co, Ni$), for improving fire retardancy and smoke suppression of epoxy resin, *Polymer* 235 (2021) 124263.

- [31] Z. H. Wu, Q. Wang, Q. X. Fan, Y. J. Cai, Y. Q. Zhao, Synergistic effect of Nano-ZnO and intumescent flame retardant on flame retardancy of polypropylene/ethylene-propylene-diene monomer composites using elongational flow field, *Polym. Compos.* 40 (2018) 2819-2833.
- [32] M. Zhang, X. Ding, Y. Zhan, Y. Wang, X. Wang, Improving the flame retardancy of poly(lactic acid) using an efficient ternary hybrid flame retardant by dual modification of graphene oxide with phenylphosphinic acid and nano MOFs, *J. Hazard. Mater.* 384 (2020) 121260.
- [33] W.-Z. Xu, C.-C. Li, Y.-X. Hu, L. Liu, Y. Hu, P.-C. Wang, Synthesis of MoO₃ with different morphologies and their effects on flame retardancy and smoke suppression of polyurethane elastomer, *Polym. Adv. Technol.* 27 (2016) 964-972.
- [34] A. Yao, C. Liu, Y. Ye, Y. Yang, Z. Wang, H. Wang, Y. Feng, J. Gao, Y. Shi, Functionalizing MXenes with molybdenum trioxide towards reducing fire hazards of thermoplastic polyurethane, *New J. Chem.* 46 (2022) 14112-14121.
- [35] G. Zeng, W. Zhang, X. Zhang, W. Zhang, J. Du, J. He, R. Yang, Study on flame retardancy of APP/PEPA/MoO₃ synergism in vinyl ester resins, *J. Appl. Polym. Sci.* 137 (2020) 49026.
- [36] L. Liu, Y. Xu, Y. Pan, M. Xu, Y. Di, B. Li, Facile synthesis of an efficient phosphonamide flame retardant for simultaneous enhancement of fire safety and crystallization rate of poly (lactic acid), *Chem. Eng. J.* 421 (2021) 127761.
- [37] Y. Feng, J. Hu, Y. Xue, C. He, X. Zhou, X. Xie, Y. Ye, Y.-W. Mai, Simultaneous improvement in the flame resistance and thermal conductivity of epoxy/Al₂O₃ composites by incorporating polymeric flame retardant-functionalized graphene, *J. Mater. Chem. A* 5 (2017) 13544-13556.

- [38] K. Chen, Y. Feng, Y. Shi, H. Wang, L. Fu, M. Liu, Y. Lv, F. Yang, B. Yu, M. Liu, P. Song, Flexible and fire safe sandwich structured composites with superior electromagnetic interference shielding properties, *Compos. Part A Appl. Sci.* 160 (2022) 107070.
- [39] M. Z. Rahman, X. Wang, L. Song, Y. Hu, A novel green phosphorus-containing flame retardant finishing on polysaccharide-modified polyamide 66 fabric for improving hydrophilicity and durability, *Int. J. Biol. Macromol.* 239 (2023) 124252.
- [40] C. Gao, Y. Shi, Y. Chen, S. Zhu, Y. Feng, Y. Lv, F. Yang, M. Liu, W. Shui, Constructing segregated polystyrene composites for excellent fire resistance and electromagnetic wave shielding, *J. Colloid Interf. Sci.* 606 (2022) 1193-1204.
- [41] S. Zhang, X. Liu, X. Jin, H. Li, J. Sun, X. Gu, The novel application of chitosan: Effects of cross-linked chitosan on the fire performance of thermoplastic polyurethane, *Carbohydr. Polym.* 189 (2018) 313-321.
- [42] P. Sun, H. Zhang, Y. Leng, Z. Wang, J. Zhang, M. Xu, X. Li, B. Li, Construction of flame retardant functionalized carbon dot with insulation, flame retardancy and thermal conductivity in epoxy resin, *Constr. Build. Mater.* 451 (2024) 138853.
- [43] W. Wu, W. Zhao, X. Gong, Q. Sun, X. Cao, Y. Su, B. Yu, R. K. Y. Li, R. A. L. Vellaisamy, Surface decoration of Halloysite nanotubes with POSS for fire-safe thermoplastic polyurethane nanocomposites, *J. Mater. Sci. Technol.* 101 (2022) 107-117.
- [44] B.-h. Kang, X. Lu, J.-p. Qu, T. Yuan, Synergistic effect of hollow glass beads and intumescent flame retardant on improving the fire safety of biodegradable poly(lactic acid), *Polym. Degrad. Stab.* 164 (2019) 167-176.

- [45] X. Lyu, H. Zhang, Y. Yan, Effect of expandable graphite and molybdenum trioxide in nitrogen/phosphorus synergistic system on acoustic performance and fire safety in rigid polyurethane foam, *J. Appl. Polym. Sci.* 139 (2022) 52488.
- [46] T. Tanaka, O. Terakado, M. Hirasawa, Flame retardancy in fabric consisting of cellulosic fiber and modacrylic fiber containing fine-grained MoO_3 particles, *Fire Mater.* 40 (2015) 612-621.
- [47] H. Xu, C. Peng, L. Xia, Z. Miao, S. He, C. Chi, W. Luo, G. Chen, B. Zeng, S. Wang, L. Dai, A Novel Anderson-Type POMs-Based Hybrids Flame Retardant for Reducing Smoke Release and Toxicity of Epoxy Resins, *Macromol. Rapid Commun.* 44 (2023) 2300162.
- [48] B. Yu, Y. Shi, B. Yuan, S. Qiu, W. Xing, W. Hu, L. Song, S. Lo, Y. Hu, Enhanced thermal and flame retardant properties of flame-retardant-wrapped graphene/epoxy resin nanocomposites, *J. Mater. Chem. A* 3 (2015) 8034-8044.
- [49] C. Liu, K. Xu, Y. Shi, J. Wang, S. Ma, Y. Feng, Y. Lv, F. Yang, M. Liu, P. Song, Fire-safe, mechanically strong and tough thermoplastic Polyurethane/MXene nanocomposites with exceptional smoke suppression, *Mater. Today Phys.* 22 (2022) 100607.
- [50] W. Cai, Z. Li, T. Cui, X. Feng, L. Song, Y. Hu, X. Wang, Self-assembly of hierarchical MXene@ SnO_2 nanostructure for enhancing the flame retardancy, solar de-icing, and mechanical property of polyurethane resin, *Compos. B Eng.* 244 (2022) 15.
- [51] Y. Hou, C. Liao, S. Qiu, Z. Xu, X. Mu, Z. Gui, L. Song, Y. Hu, W. Hu, Preparation of soybean root-like CNTs/bimetallic oxides hybrid to enhance fire safety and mechanical performance of thermoplastic polyurethane, *Chem. Eng. J.* 428 (2022) 132338.
- [52] W. Cai, T. Cai, L. He, F. Chu, X. Mu, L. Han, Y. Hu, B. Wang, W. Hu, Natural antioxidant functionalization for fabricating ambient-stable black phosphorus nanosheets toward enhancing

- flame retardancy and toxic gases suppression of polyurethane, *J. Hazard. Mater.* 387 (2020) 121971.
- [53] K. Zhou, Z. Gui, Y. Hu, S. Jiang, G. Tang, The influence of cobalt oxide–graphene hybrids on thermal degradation, fire hazards and mechanical properties of thermoplastic polyurethane composites, *Compos. Part A Appl. Sci.* 88 (2016) 10-18.
- [54] C. Nie, Y. Shi, S. Jiang, H. Wang, M. Liu, R. Huang, Y. Feng, L. Fu, F. Yang, Constructing Fireproof MXene-Based Cotton Fabric/Thermoplastic Polyurethane Hierarchical Composites via Encapsulation Strategy, *ACS Appl. Polym. Mater.* 5 (2023) 7229-7239.
- [55] C. Liu, W. Wu, Y. Shi, F. Yang, M. Liu, Z. Chen, B. Yu, Y. Feng, Creating MXene/reduced graphene oxide hybrid towards highly fire safe thermoplastic polyurethane nanocomposites, *Compos. B Eng.* 203 (2020) 108486.
- [56] J. Wang, Y. Hu, W. Cai, B. Yuan, Y. Zhang, W. Guo, W. Hu, L. Song, Atherton–Todd reaction assisted synthesis of functionalized multicomponent MoSe₂/CNTs nanoarchitecture towards the fire safety enhancement of polymer, *Compos. Part A Appl. Sci.* 112 (2018) 271-282.
- [57] C. Wang, W. Xu, L. Qi, H. Ding, W. Cai, G. Jiang, Y. Hu, W. Xing, B. Yu, Hierarchical NiO/Al₂O₃ nanostructure for highly effective smoke and toxic gases suppression of polymer Materials: Experimental and theoretical investigation, *Compos. Part A Appl. Sci.* 175 (2023) 107807.
- [58] X. Chen, Z. Wei, W. Wang, C. Jiao, Properties of flame-retardant TPU based on para-aramid fiber modified with iron diethyl phosphinate, *Polym. Adv. Technol.* 30 (2018) 170-178.
- [59] H. Ren, K. Qing, Y. Chen, Y. Lin, X. Duan, Smoke suppressant in flame retarded thermoplastic polyurethane composites: Synergistic effect and mechanism study, *Nano Res.* 14 (2021) 3926-3934.

- [60] H. Li, D. Meng, P. Qi, J. Sun, H. Li, X. Gu, S. Zhang, Fabrication of a hybrid from metal organic framework and sepiolite (ZIF-8@SEP) for reducing the fire hazards in thermoplastic polyurethane, *Appl. Clay Sci.* 216 (2022) 106376.
- [61] H. Wang, H. Qiao, J. Guo, J. Sun, H. Li, S. Zhang, X. Gu, Preparation of cobalt-based metal organic framework and its application as synergistic flame retardant in thermoplastic polyurethane (TPU), *Compos. B Eng.* 182 (2020) 2036-2045.
- [62] S. Wang, Q. Fang, C. Liu, J. Zhang, Y. Jiang, Y. Huang, M. Yang, Z. Tan, Y. He, B. Ji, C. Qi, Y. Chen, Biomass tannic acid intermediated surface functionalization of ammonium polyphosphate for enhancing fire safety and smoke suppression of thermoplastic polyurethane, *Eur. Polym. J.* 187 (2023) 111897.
- [63] S.-C. Huang, C. Deng, S.-X. Wang, W.-C. Wei, H. Chen, Y.-Z. Wang, Electrostatic action induced interfacial accumulation of layered double hydroxides towards highly efficient flame retardance and mechanical enhancement of thermoplastic polyurethane/ammonium polyphosphate, *Polym. Degrad. Stab.* 165 (2019) 126-136.
- [64] Y. Zhu, H. Wang, L. Fu, P. Xu, G. Rao, W. Xiao, L. Wang, Y. Shi, Interface engineering of multi-component core-shell flame retardant towards enhancing fire safety of thermoplastic polyurethane and mechanism investigation, *Appl. Mater. Today* 38 (2024) 1106-1114.
- [65] M. Yang, X. Li, W. Qin, Y. Wang, C. Gu, L. Feng, Z. Tian, H. Qiao, J. Chen, J. Chen, S. Yin, Multifunctional thermoplastic polyurethane composites with excellent flame retardancy, strain-sensitivity, water penetration resistance and breathability, *Eur. Polym. J.* 195 (2023) 112227.

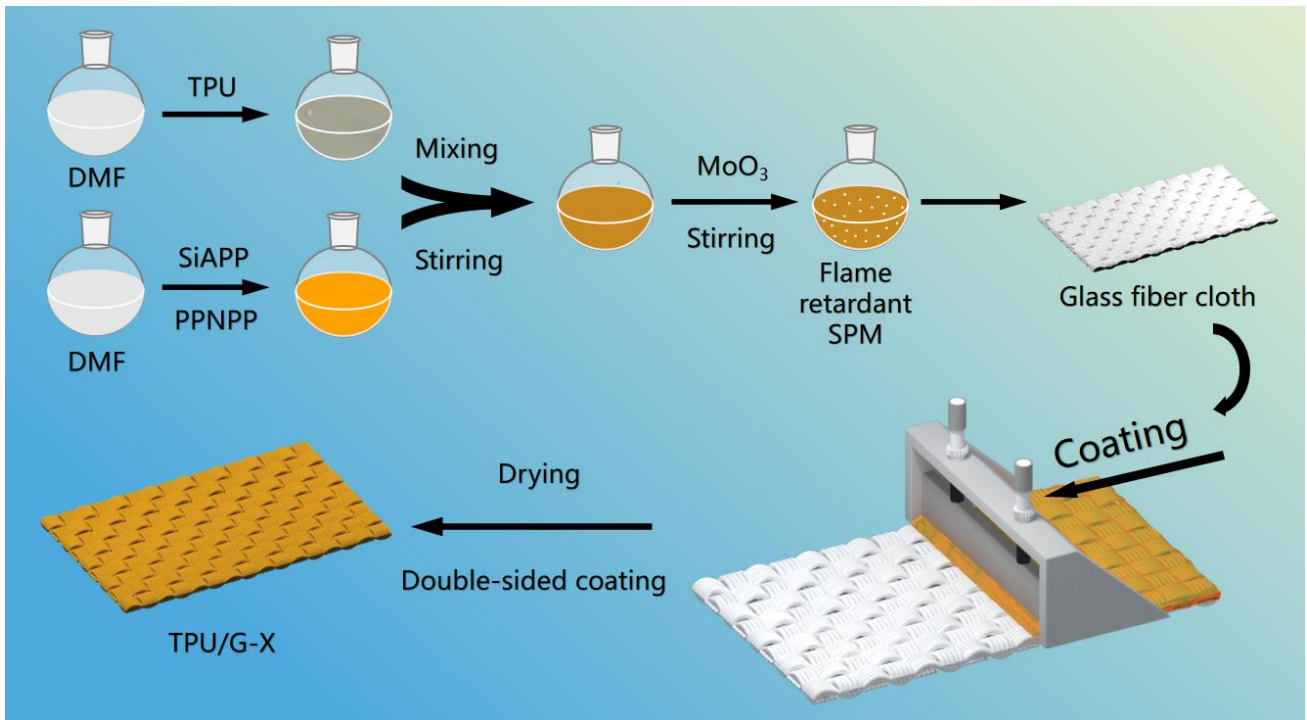


Fig. 1. Schematic diagram for preparation of TPU/G-X.

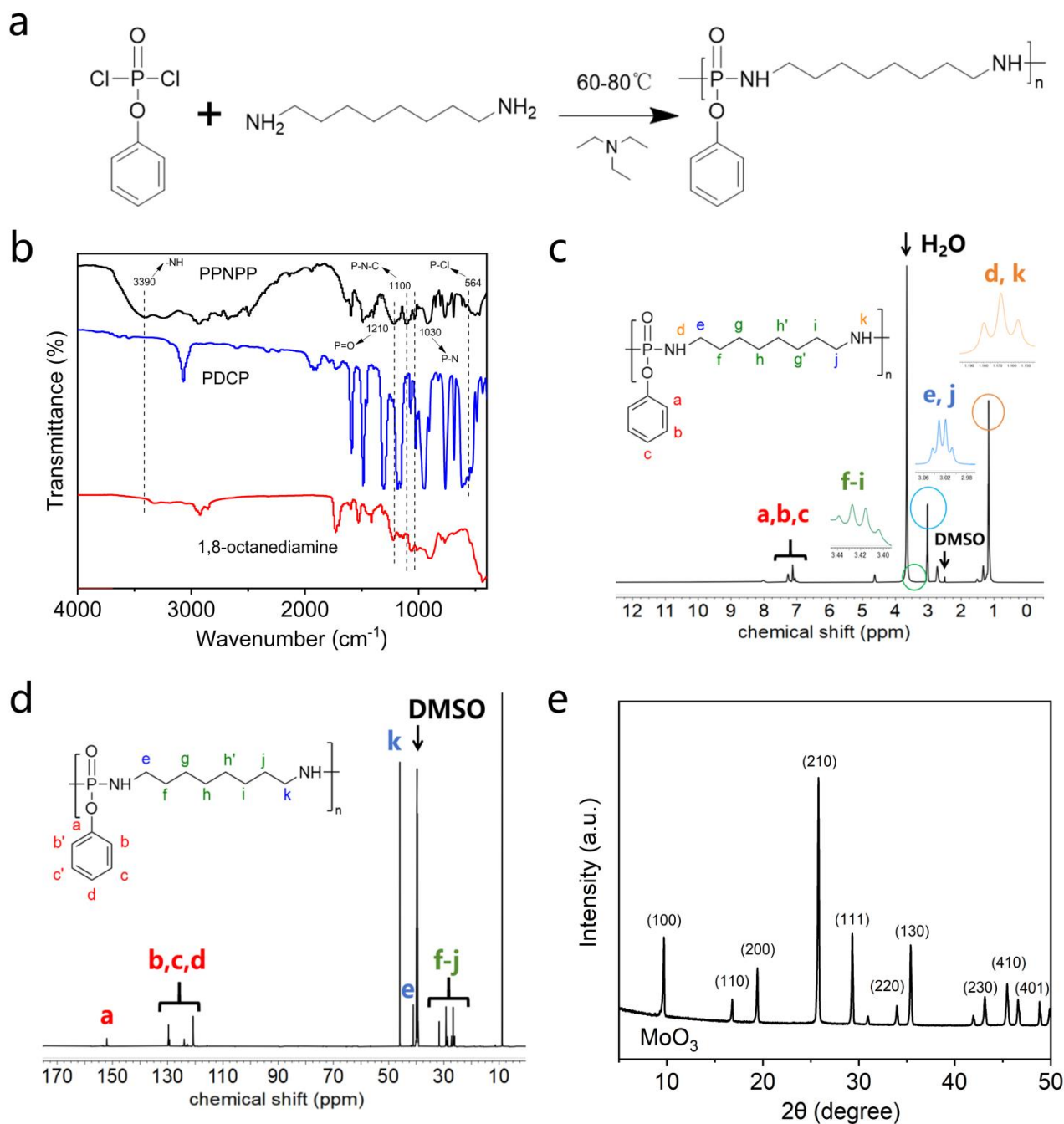


Fig. 2. (a) Preparation route of PPNPP; (b) FTIR spectra of PPNPP and PDCP and 1,8-octanediamine; (c) ^1H NMR and (d) ^{13}C NMR spectra of PPNPP; (e) XRD patterns of MoO_3 .

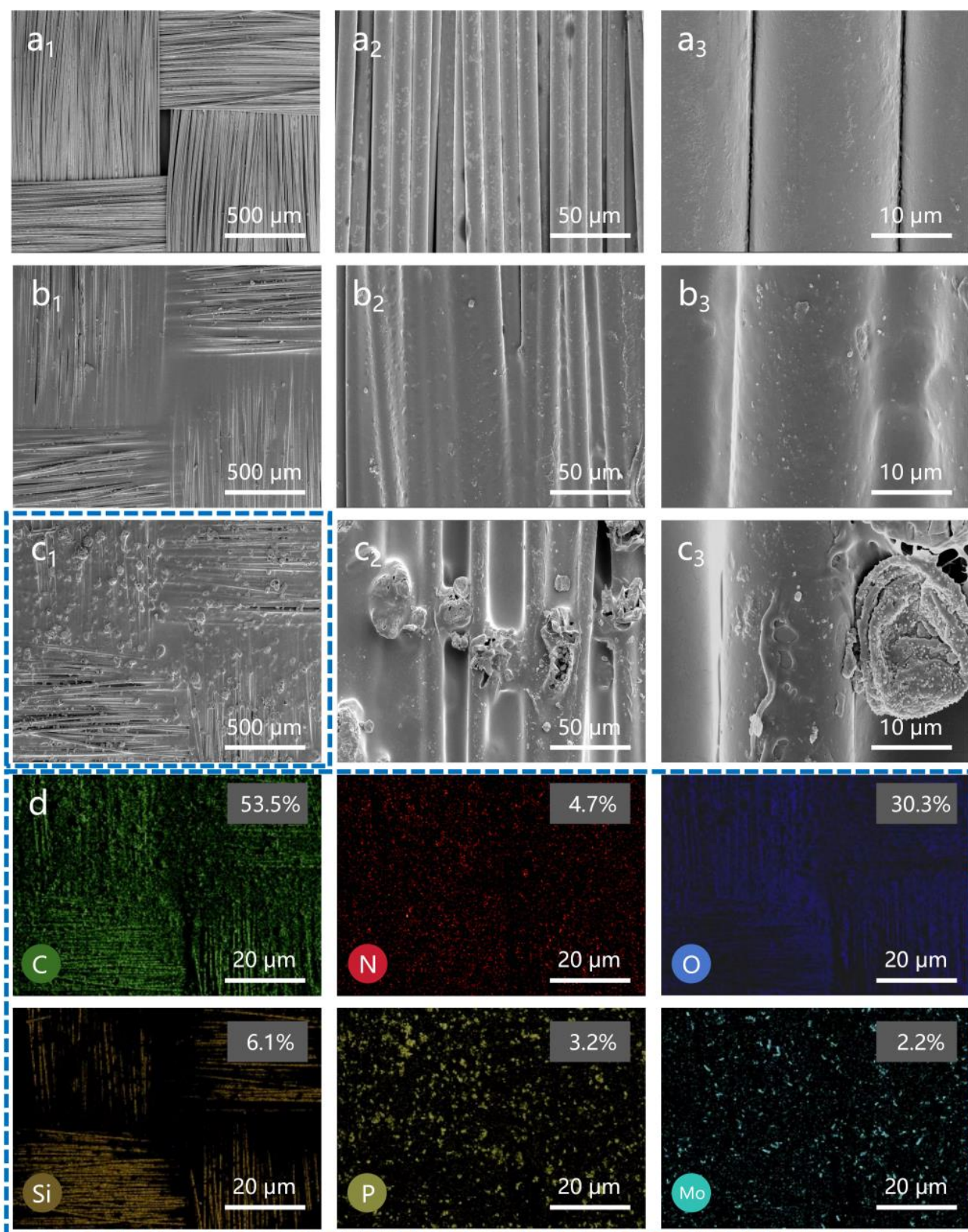


Fig. 3. SEM images of surface of (a) GFC, (b) TPU/G, and (c) TPU/G-SPM-1; (d) Element distribution images of TPU/G-SPM-1(c₁).

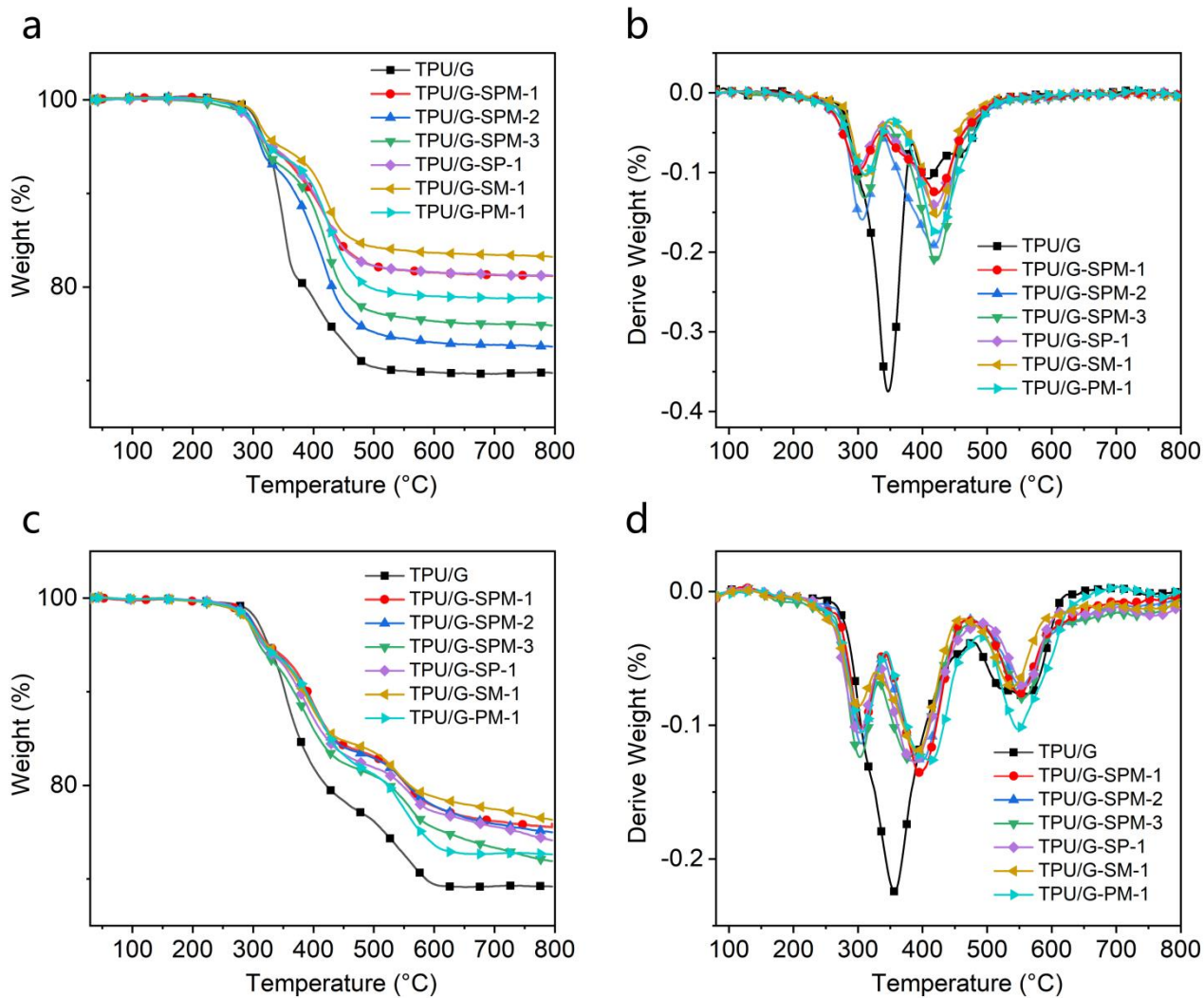
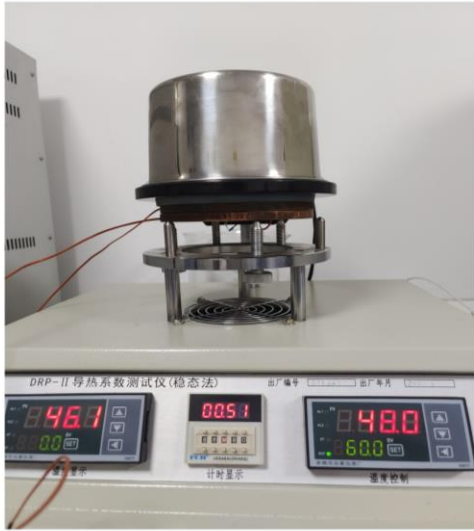


Fig. 4. TGA and DTG curves of the TPU/G composites in (a, b) Ar and (c, d) air atmospheres.

a



b

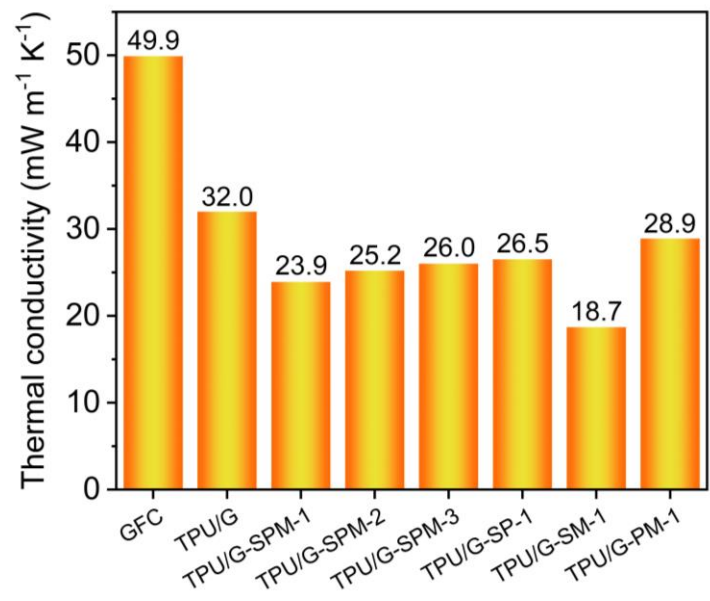


Fig. 5. (a) Photograph of thermal conductivity tester; (b) Thermal conductivity of GFC and the TPU/G composites.

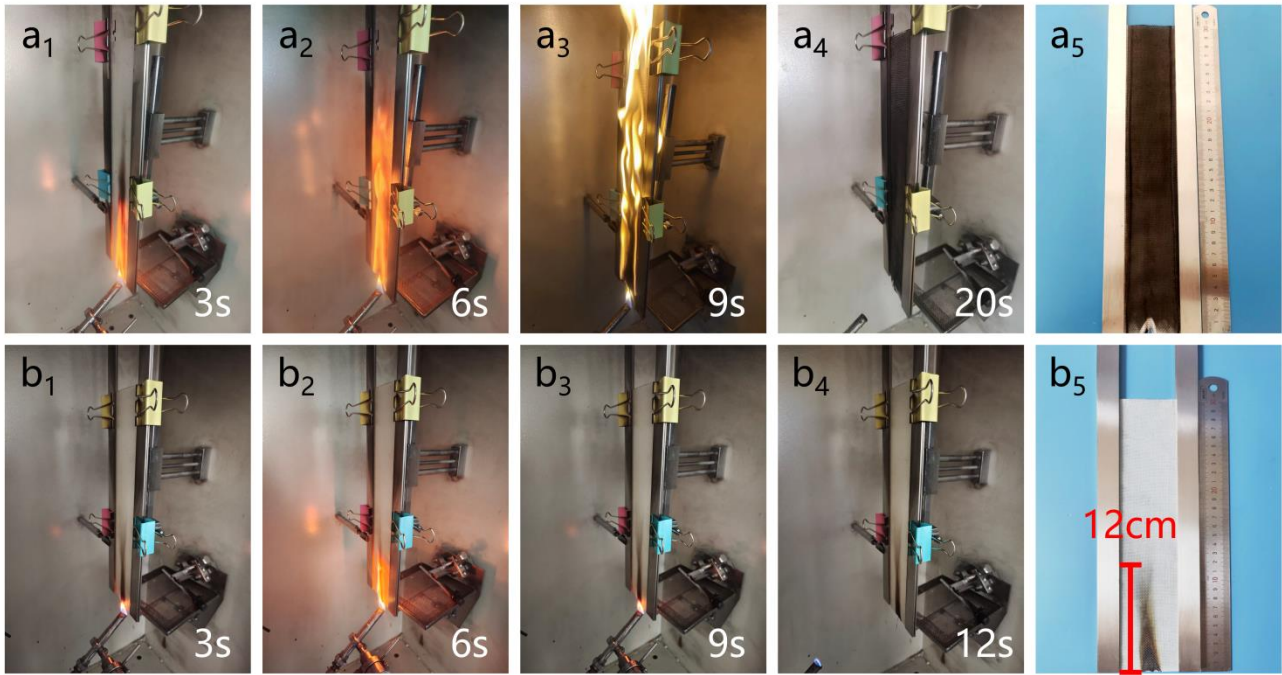


Fig. 6. Photographs of the vertical burning tests for (a) TPU/G and (b) TPU/G-SPM-1.

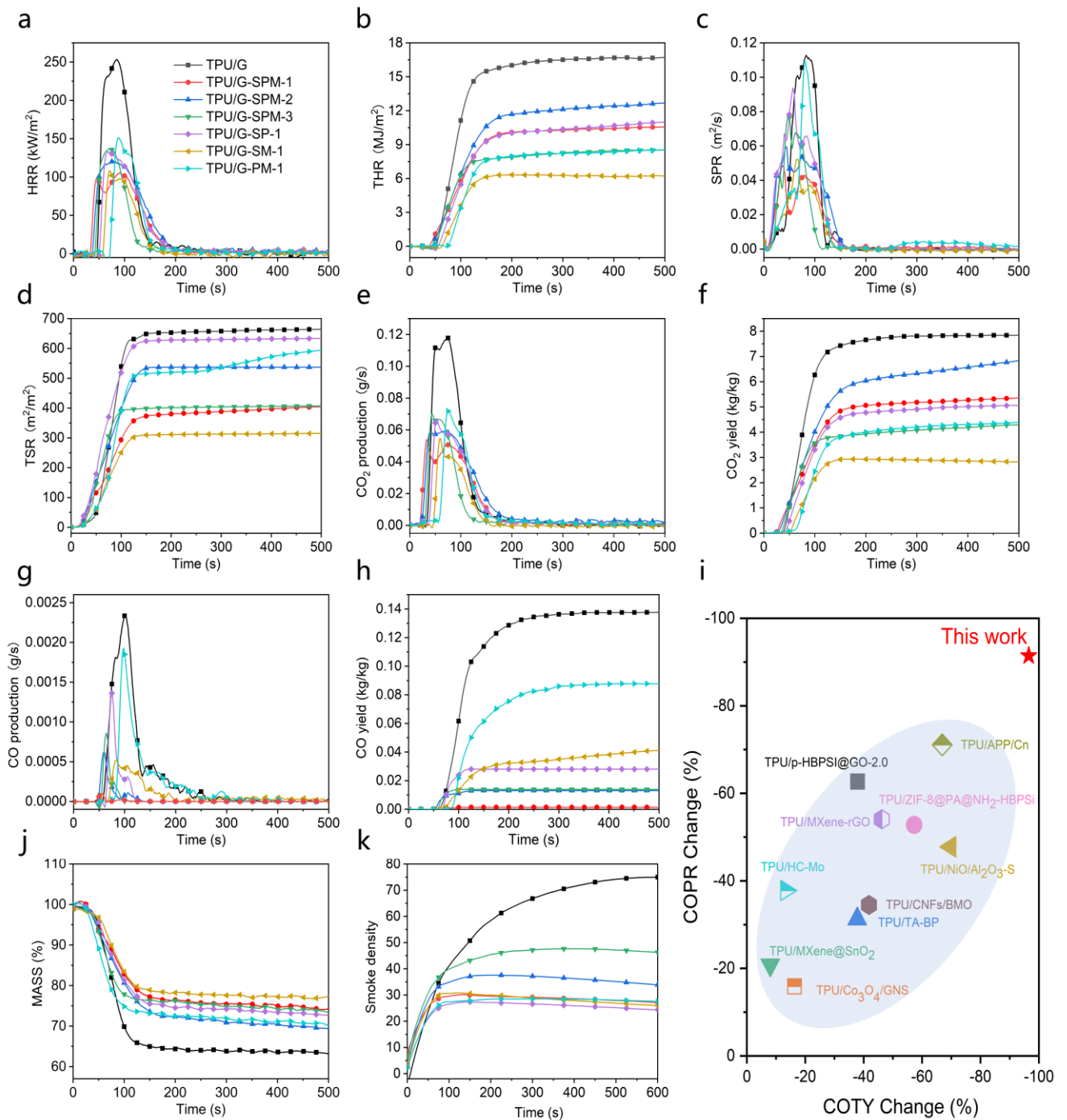


Fig. 7. CCT data: (a) HRR, (b) THR, (c) SPR, (d) TSR, (e) CO₂PR, (f) CO₂TY, (g) COPR, and (h) COTY; (i) Comparison of COPR and COTY reductions with previous works; (j) Weight loss and (k) Smoke density.

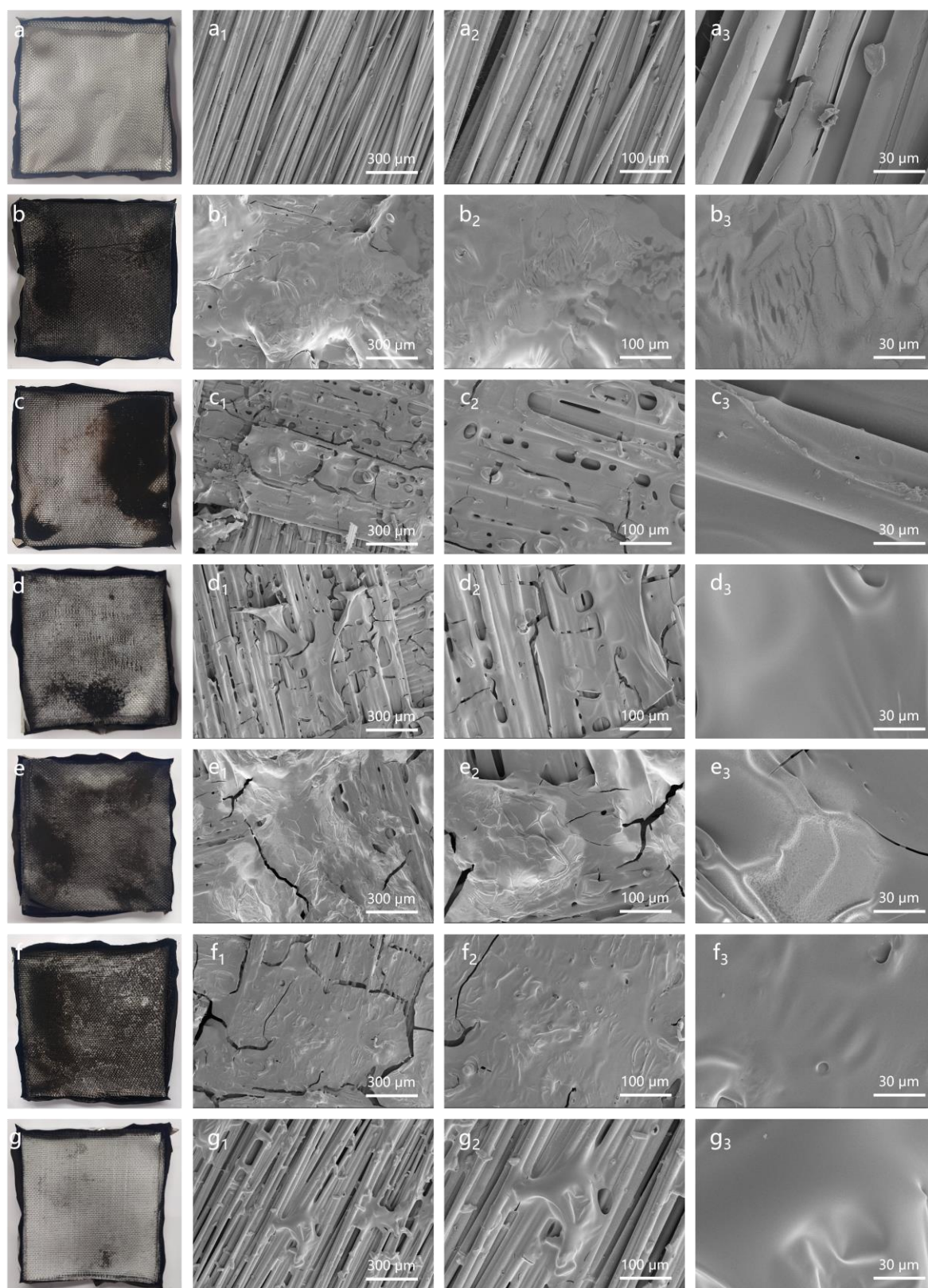


Fig. 8. Digital photos and SEM images of char residues of the TPU/G composites: (a) TPU/G, (b) TPU/G-SPM-1, (c) TPU/G-SPM-2, (d) TPU/G-SPM-3, (e) TPU/G-SP-1, (f) TPU/G-SM-1, and (g) TPU/G-PM-1.

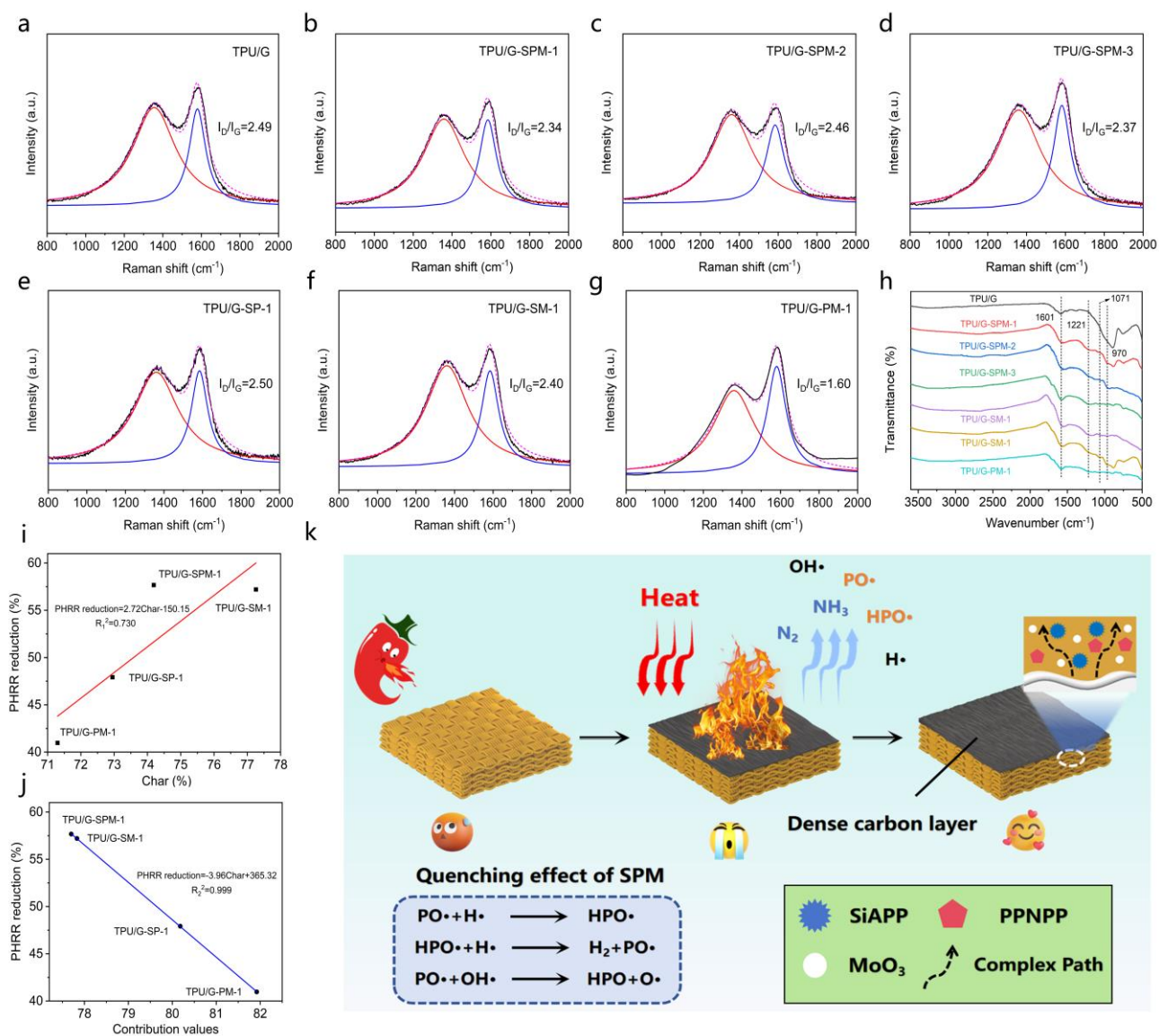


Fig. 9. Raman spectra of char residues of the TPU/G composites: (a) TPU/G, (b) TPU/G-SPM-1, (c) TPU/G-SPM-2, (d) TPU/G-SPM-3, (e) TPU/G-SP-1, (f) TPU/G-SM-1, (g) TPU/G-PM-1, (h) FTIR spectra of char residues of the TPU/G composites; (i) Correlation between the char residues from CCT and PHRR reduction; (j) Correlation between the contributions values and PHRR reduction; (k) Flame retardant mechanism of TPU/G-X.

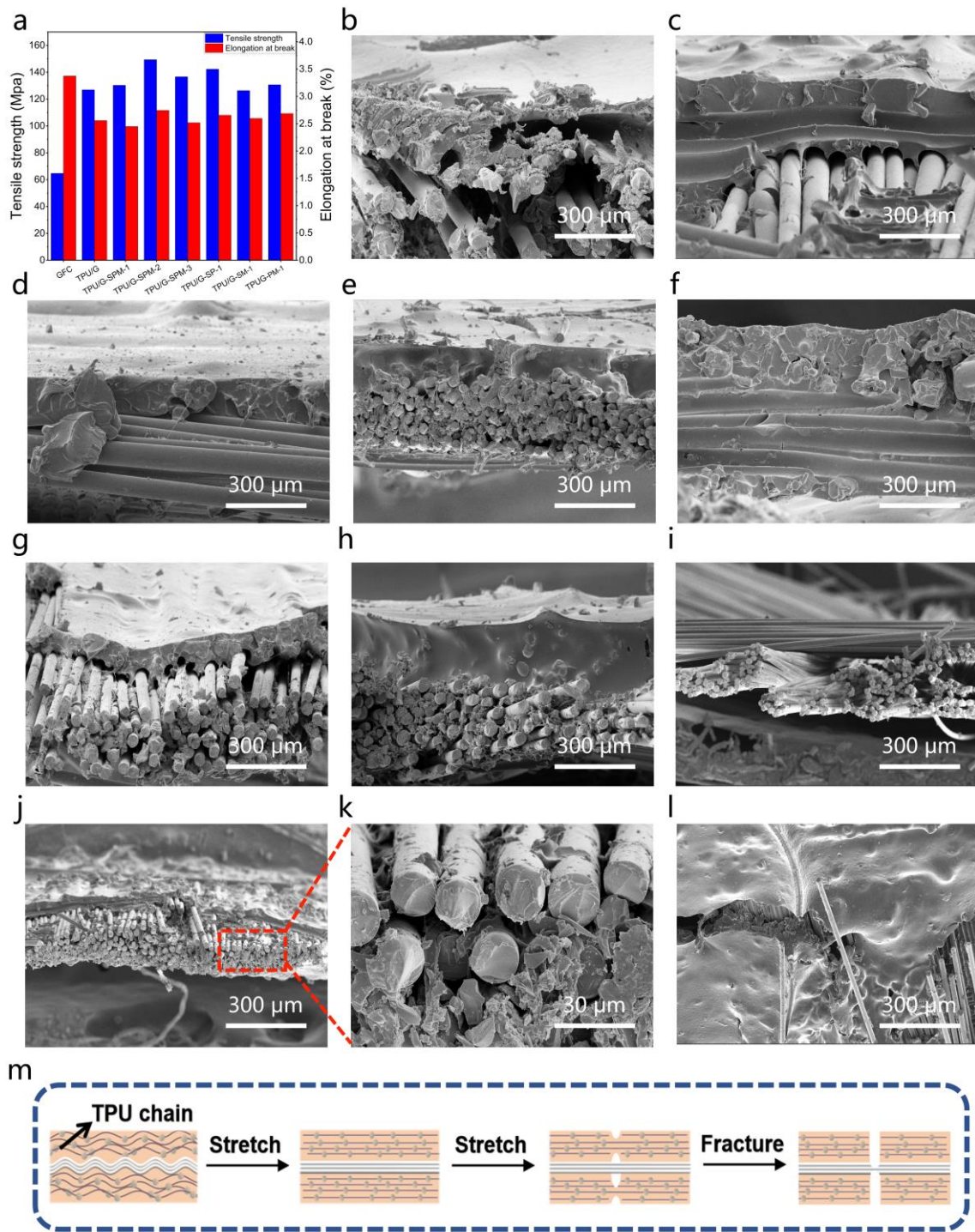


Fig. 10. (a) Tensile strength and elongation of the GFC and TPU/G composites; SEM images of fracture surface of (b) TPU/G, (c) TPU/G-SPM-1, (d) TPU/G-SPM-2, (e) TPU/G-SPM-3, (f) TPU/G-SP-1, (g) TPU/G-SM-1, (h) TPU/G-PM-1, (i) GFC (Flat view), (j, k) TPU/G-SPM-1 (Flat view), and (l) TPU/G-SPM-1 (Top view); (m) Schematic diagram for the mechanical failure process of the TPU/G composites.

Table 1. Formulation of the TPU/G composites.

Samples No.	TPU (g)	SiAPP (g)	PPNPP (g)	MoO ₃ (g)
TPU	100	-	-	-
TPU/SPM-1	80	10	5	5
TPU/SPM-2	84	8	4	4
TPU/SPM-3	88	6	3	3
TPU/SP-1	80	10	10	-
TPU/SM-1	80	15	-	5
TPU/PM-1	80	-	15	5

Table 2. TGA data of the TPU/G composites in air and Ar atmospheres.

Samples No.	$T_{5\%}$ (°C)		T_{max1} (°C)		T_{max2} (°C)		T_{max3} (°C)	Char residue at 800 °C (wt%)	
	Air	Ar	Air	Ar	Air	Ar	Air	Air	Ar
TPU/G	296.5	298.3	355.1	345.7	552.9	408.4		69.20	70.82
TPU/G-SPM-1	277.4	276.7	306.8	299.1	394.4	418.7	550.2	75.54	81.19
TPU/G-SPM-2	281.6	288.7	303.0	304.8	395.7	418.3	554.0	75.00	73.63
TPU/G-SPM-3	273.9	278.1	301.8	308.7	384.1	420.6	554.1	71.91	75.90
TPU/G-SP-1	275.3	273.3	301.8	300.8	387.1	418.7	560.0	74.13	81.23
TPU/G-SM-1	264.7	292.2	305.8	310.2	413.7	422.7	546.8	76.33	83.23
TPU/G-PM-1	277.1	278.6	299.9	308.9	390.4	419.9	539.2	72.64	78.84

Table 3. LOI values and damaged length for the TPU/G composites during vertical burning tests.

Samples No.	LOI (%)	Damaged length (mm)
TPU/G	23.3 ± 0.1	Burn out
TPU/G-SPM-1	28.1 ± 0.2	120 ± 2
TPU/G-SPM-2	27.4 ± 0.2	220 ± 2
TPU/G-SPM-3	27.0 ± 0.2	200 ± 2
TPU/G-SP-1	28.5 ± 0.2	120 ± 5
TPU/G-SM-1	30.8 ± 0.2	110 ± 2
TPU/G-PM-1	26.1 ± 0.2	Burn out

Table 4. Cone calorimetric results for the TPU/G composites.

Samples No.	TTI (s)	PHRR (kW m ⁻²)	THR (MJ m ⁻²)	PSPR (m ² s ⁻¹)	TSR (m ² m ⁻²)	PCOPR (g s ⁻¹)	PCO ₂ PR (g s ⁻¹)	COTY (kg kg ⁻¹)	CO ₂ TY (kg kg ⁻¹)	Char residue (wt%)
TPU/G	47	260	16.7	0.1222	664.5	0.00245	0.1208	0.1377	7.84	63.89
TPU/G-SPM-1	31	110	10.6	0.0658	404.2	0.00021	0.0560	0.0014	5.36	74.19
TPU/G-SPM-2	36	126	12.7	0.0865	537.2	0.00095	0.0629	0.0131	6.83	70.23
TPU/G-SPM-3	41	144	8.5	0.1110	407.4	0.00124	0.0720	0.0138	4.29	73.53
TPU/G-SP-1	50	135	11.0	0.1169	633.6	0.00163	0.0672	0.0280	5.07	72.95
TPU/G-SM-1	59	111	6.3	0.0749	315.0	0.00066	0.0572	0.0411	2.94	77.26
TPU/G-PM-1	41	154	8.5	0.1200	593.8	0.00205	0.0726	0.0878	4.39	71.3

Table 5. Smoke density results for the TPU/G composites.

Samples No.	TPU/G	TPU/G-SPM-1	TPU/G-SPM-2	TPU/G-SPM-3	TPU/G-SP-1	TPU/G-SM-1	TPU/G-PM-1
D,10	74.8	27.1	34.1	51.3	24.5	26	27.6
D,max	75.1	30.4	37.6	53.5	27.5	30.8	28.5

Table 6. The detailed information about contribution values.

Samples No.	Char	Y	Contribution values
TPU/G-SPM-1	74.19	3.51	77.70
TPU/G-SP-1	72.95	7.23	80.18
TPU/G-SM-1	77.26	0.57	77.83
TPU/G-PM-1	71.30	10.62	81.92

Response to Reviewers' comments:

Reviewer #2: In this manuscript, the authors prepared a new type of flame-retardant TPU coating through solution mixing and applied it to the surface of glass fiber cloth to obtain a novel flame-retardant cable taping material. The prepared TPU/G composites exhibit excellent flame-retardant and smoke suppression properties and effectively improve the mechanical properties of the glass fiber cloth, introducing a new concept for environmentally friendly flame-retardant cable wrapping tape. Therefore, it is recommended that this paper be published in the Composites Communications with minor modifications. The authors may consider adopting the following suggestions.

Q1. Some expressions in the text lack articles. For example, on Page 4, "is primary method for enhancing" should be changed to "is the primary method for enhancing".

It is recommended to double-check such problems.

Response: Thank you very much for your kind comments.

Modified section: We have added the missing articles and rechecked the entire article. (Please see Page 4, Line 15 in the revised manuscript).

Q2. It is recommended that proper nouns, such as $T_{5\%}$ and T_{\max} , be briefly explained upon their first appearance to enhance the article's readability.

Response: Thank you very much for your kind comments.

Modified section: We have added explanations of proper nouns when they first appeared in the text and double-checked for similar issues. (Please see Page 12, Line 19 and Page 13, Line 11 in the revised manuscript).

Q3. Revise the use of certain grammatical structures in the article

Response: Thank you very much for your kind comments. The grammar of the entire article has been scrutinized and revised once again by a professional English researcher.

Q4. On Page 14, "these results indicates" should be replaced with "these results indicate", and it is recommended to double-check such problems.

Response: Thank you very much for your kind comments.

Modified section: We have repeatedly checked similar issues in the text and made the necessary corrections. (Please see Page 6, Line 8 and Page 14, Line 14 in the revised manuscript).

Q5. Research articles on flame retardancy and smoke suppression may be added as appropriate.

Response: Thank you very much for your kind comments.

Modified section: To strengthen the discussion on flame retardancy and smoke suppression, we have added relevant research articles in the CCT test (e.g., (Citation 44, Citation 45)). These references further support our findings and provide a broader context for our study.

Reviewer #3: In this manuscript, the authors synthesized a novel phosphoramidite flame retardant, PPNPP, and compounded SiAPP and MoO₃ into liquid TPU to prepare flame-retardant TPU coatings. The flame-retardant system exhibits excellent flame-retardant and smoke-suppressing properties, particularly effective in inhibiting CO emissions. Moreover, the flame-retardant coating effectively enhances the mechanical properties of GFC. Essentially, this work further broadens the application prospects of TPU. However, I have a few questions about the manuscript.

Q1. It is recommended that the thermal conductivity of the GFC be added as a blank control group in the thermal conductivity test.

Response: Thank you very much for your kind comments.

Modified section: We have added the thermal conductivity of the GFC in Fig. 5 (Please see Fig. 5b).

Q2. It is recommended to add the content of each element in the element distribution images.

Response: Thank you very much for your kind comments.

Modified section: We have provided the elemental content in Fig. 3d. (Please see Fig. 3d).

Q3. What are the advantages of the cable taping materials prepared in this study compared with the traditional cable taping materials?

Response: Thank you for your careful reading of the article. Thank you for your careful reading of the article. The cable taping materials developed in this research have the following significant advantages over traditional materials: (1)

Multi-functional synergistic optimization: It breaks through the technical bottleneck of traditional flame-retardant taping materials, which can be difficult to balance flame-retardant and insulating properties, and at the same time solves the environmental protection problem of the release of volatile organic compounds (VOCs) during processing; (2) Comprehensive performance enhancement: Through the composite design of flame-retardant modified thermoplastic polyurethane (TPU) and glass fiber cloth (GFC), synergistic enhancement of material performance has been realized. The composite is characterized by halogen-free flame retardant, efficient smoke suppression, excellent abrasion resistance, low thermal conductivity, and high mechanical strength, and its comprehensive performance far exceeds that of traditional cable taping materials; (3) Advantage of industrialized application: The solution coating-heat curing process is characterized by easy operation, low energy consumption, large-scale production, and low cost, which has promising market prospects.

Q4. Authors should pay attention to the singular and plural forms in the text. For example, “developed for modifying fiber” in Page 4 should be changed to “developed for modifying fibers” , and it is recommended to double-check this type of question.

Response: Thank you very much for your kind comments.

Modified section: We have thoroughly checked the text for similar issues and made the necessary corrections accordingly. (Please see Page 4, Line 1 and Page 13, Lines 17-20 in the revised manuscript).

Q5. Page 12, the first occurrence of a proper noun, e.g., T_{5%}, should be explained, and it is recommended to double-check such questions.

Response: Thank you very much for your kind comments.

Modified section: We have added the definition of "T_{5%}" as it first appears on Page 12, Line 19. In addition, we have double-checked the text for similar issues and made revisions.

Constructing Efficient Flame-Retardant Thermoplastic Polyurethane Coatings with Smoke-Suppression to Enhance the Performance of Glass Fiber Cloth

Yongqian Shi ^{a,*}, Songqiong Jiang ^a, Jinke Wu ^a, Zhendong Chen ^a, Cancan Zhang ^b, Yun Zhang ^{c,*}, Pingan Song ^d, and Yan Zhang ^{e,*}

^a College of Environment and Safety Engineering, Fuzhou University, 2 Xueyuan Road, Fuzhou 350116, China.

^b Jiangsu Xinchanya New Material Co., Ltd, Liuhe Road North Side and Hexiang Road West Side, Baoying Economic Development Zone, Yangzhou 225800, China.

^c Yangzhou Tengfei Electric Cable and Appliance Materials Co., Ltd, 8 Qixin Road, Anyi Industrial Zone, Yangzhou 225800, China.

^d School of Agriculture and Environmental Science, University of Southern Queensland, Springfield, QLD 4300, Australia.

^e Laboratory of Polymer Materials and Engineering, NingboTech University, Ningbo 315100, China.

* Corresponding authors: Prof. Yongqian Shi, Mr Yun Zhang and Prof. Yan Zhang

E-mail addresses: shiyq1986@fzu.edu.cn (Y. Shi), Yangzhoutengfei@126.com (Y. Zhang),

hnpdszy@163.com (Y. Zhang)

Abstract

In order to meet the application requirements for cables in different environments, it is imperative to develop cable tapes with insulation, flame retardancy, and high strength. In this work, a new type of halogen-free flame-retardant and high-strength coating was prepared by synthesizing a new phosphoramidate flame retardant phenyl P-methyl-N-(8-(methylamino)octyl) phosphonamidate (PPNPP) compounded with silicon wrapped ammonium polyphosphate (SiAPP) and molybdenum trioxide (MoO_3) added into thermoplastic polyurethane (TPU), and TPU/glass fiber cloth (TPU/G) composites were obtained by double-sided coating on the surface of glass fiber cloth (GFC) and heat curing. Compared with those of the pure TPU-coated sample, the peak of heat release rate (PHRR) and total heat release (THR) results of the TPU/G composite containing 20 wt% SiAPP-PPNPP- MoO_3 (TPU/G-SPM-1) decreased by 57.7% and 36.8%, respectively. In addition, the TPU/G-SPM-1 sample showed an excellent toxic gases suppression effect, i.e. the peak of carbon monoxide production rate (PCOPR) and total carbon monoxide yield (COTY) decreased by 91.4% and 98.9%, respectively, compared with the pure sample. The coating also imparted excellent mechanical properties to the GFC, which overcame the original defects of glass fiber such as poor abrasion resistance and brittleness, and the tensile strength of TPU/G-SPM-1 was increased by 101% compared with that of pure GFC. This work presents a new method for the preparation of flame-retardant and mechanically strong TPU/G composites used as cable tapes.

Keywords: Thermoplastic polyurethane; Interface engineering; Flame-retardancy; High-strength; Smoke suppression; Glass fiber cloth.

1. Introduction

In recent years, the installation scale of urban cables has been increasing, and cables, as a kind of wire product that transmits signals, conveys electricity or facilitates electromagnetic transformation, are the fundamental assurance for the stable operation of society. However, due to overloading, short circuit, aging and other reasons, cable fire will inevitably occur [1]. Once a cable fire occurs, the consequences are often severe owing to the imperceptibility, rapid spread and the toxicity of the smoke of cable combustion [2, 3]. Therefore, preventing cable fires or effectively controlling their spread is an urgent problem that needs to be addressed.

Cable core tape plays a crucial role in cables. The flame-retardant modification of cable core tapes is an effective measure to prevent cable fires. The common cable core wrapping tape on the market is mainly made of organic materials, for example polyvinyl chloride (PVC), thermoplastic polyurethane (TPU), polypropylene (PP) and polytetrafluoroethylene (PTFE), as the main matrix, and adding flame retardant and adhesive which has the advantages of simple preparation process, low cost and convenient processing. However, due to the single insulation or flame retardant performance, its applicability is limited. In recent years, some organic-inorganic composite products have gradually appeared both domestically and internationally, such products not only inherit the advantages of organic materials, but also integrate the characteristics of inorganic materials, such as excellent mechanical strength, insulation, corrosion resistance and high temperature resistance.

Glass fiber cloth (GFC), an inorganic material known for its excellent insulation, heat resistance, and corrosion resistance, is highly suitable for cable core winding tape. However, its inherent poor abrasion resistance and brittleness limit its service life. To meet the demands of industrial applications, there is an urgent need to improve flame-retardant and mechanical properties of GFC. Various methods

have been developed for modifying fibers, including solution dipping and spraying [4, 5], layer-by-layer assembly (LBL) [6-8], plasma treatment [9, 10], chemical surface grafting [11, 12], and sol-gel reaction [13, 14], etc. Among these, applying appropriate flame retardant coatings is considered as a straightforward and effective approach. Flame retardant coatings can significantly inhibit or slow the spread of flames and the release of toxic smoke. When the flame-retardant materials are concentrated on the surface, they maximize flame retardant efficiency without compromising the mechanical properties of the fabric [15]. Consequently, developing a suitable coating is the current problem that needs to be solved.

TPU is an excellent candidate for coatings due to its remarkable wear resistance, hardness, elasticity and easy processing, etc. Recently, researchers have increasingly applied TPU coatings to improve the hydrophobicity, flame retardancy, mechanical properties, and corrosion resistance of various materials [16-19]. However, the inherent flammability of TPU and heavy smoke release upon burning, significantly limit its applications [11, 20]. Hence, it is critical for finding a suitable way to reduce the fire risk of TPU.

The introduction of flame retardants is the primary method for enhancing the flame retardant properties of TPU. Traditional halogen-containing flame retardants are being phased out due to the release of corrosive gases and fumes during thermal decomposition. In recent years, phosphorous-nitrogen flame retardants have emerged as a preferred alternative, having the advantages of halogen-free, easy to obtain, low toxicity and cost effectiveness. Among all the phosphorous-nitrogen flame retardants, phosphoramidate flame retardants have garnered significant attention from researchers due to their high flame retardancy, low smoke production, as well as the strong interfacial adhesive with the polymeric matrix [21-23]. For example, Xue et al. synthesized an oligomeric phosphoramidate (PPP),

using a one-pot method, and found that PPP was well distributed in polylactic acid (PLA). Besides, the addition of 3 wt% PPP endowed the PLA sample with UL-94 V-0 rating, and the limiting oxygen index (LOI) increased from 20.5% to 32.5% [24]. Liu et al. developed a novel phosphoramidate flame retardant, $\text{Ti}_3\text{C}_2\text{Tx-PPPA}$, followed by incorporating it into TPU. At a 1.0 wt% addition, the total heat release (THR) and total smoke release (TSR) of the TPU composites were reduced by 32.6% and 54.4%, respectively, demonstrating effective flame retardancy and smoke suppression [25]. However, phosphoramidate flame retardants often fail to meet the demands of practical applications when used alone. In order to utilize the advantages of phosphoramidate-based compounds, researchers have considered combining them with other flame retardants to improve flame retardant efficiency. Ammonium polyphosphate (APP) is a halogen-free flame retardant rich in phosphorus and nitrogen, with excellent flame retardant properties due to its ability of release inert gases during combustion and excellent catalytic carbonation properties [26]. As an effective flame retardant, APP can be used alone or in combination with other flame retardants. Some studies have reported that the compounding of APP and phosphoramidate flame retardants could achieve outstanding flame-retardant effects [27]. For instance, Wei et al. synthesized a novel phosphonamide (PSA) through solution polycondensation and incorporated it with APP into epoxy resin (EP). The results indicated that the addition of 12.5 wt% PSA could endow the EP sample with a LOI value of 32%. Besides, the peak of heat release rate (PHRR) and THR of the EP/PSA decreased by 71.9% and 67.8%, respectively [28]. Ye et al. reported a hyperbranched flame retardant (HBPPDA) through polymerization, which significantly improved the flame-retardant performance of APP when 6.25 wt% of HBPPDA was added. The LOI value of the PP composites reached 30.6% with the content of 25 wt% flame retardant. Additionally, the PHRR and THR of the PP composite were reduced by 76.2% and 41.5%, respectively, compared to those of pure

PP [29]. Although several studies have confirmed that the addition of APP-modified phosphoramidites to polymers can achieve significant synergistic flame retardant effects. Unfortunately, there are still few reports on the application of such flame retardants to TPU.

In cable fire accidents, more than 2/3 of the deaths were caused by toxic and harmful smoke, therefore it is very important to inhibit the emission of smoke during cable combustion. Various studies have shown that the incorporation of small amounts of nanofillers (<5 wt%) into polymers can provides excellent flame retardancy and smoke suppression [30-32], which can be attributed to the advantages of small size, large surface area and good thermal conductivity of nanofillers. In addition, there is a synergistic effect between nanofillers and phosphorous-nitrogen flame retardants, due to the fact that the nanofillers with high thermal oxidative resistance can effectively enhance the char quality of the polymer during combustion, leading to an improvement in flame retardancy [15]. Molybdenum trioxide (MoO_3), as a traditional smoke suppression agent, exhibits excellent flame retardant and smoke suppressant effects by promoting the generation of carbon layer on top of polymers during combustion, and has been widely used for smoke suppression of various polymers. For example, Xu et al. prepared different forms of MoO_3 by high-temperature calcination and hydrothermal method, respectively, and added them into polyurethane elastomer (PUE) to study the flame retardant and smoke suppression properties of PUE composites. When the amount of 1 wt% was added, the PHRR of the PUE composite was reduced by 61.0%. As for smoke suppression, at 5 wt% addition, the smoke density of the PUE composites was reduced by 41.3% compared to that of pure PUE sample [33]. Yao et al. prepared $\text{Ti}_3\text{C}_2\text{T}_x\text{-MoO}_3$ flame retardant through electrostatic interactions, and added it into TPU by melt blending, and found that the PHRR and peak of smoke production rate (PSPR) of the TPU composite decreased by 26.2% and 42.9% respectively when the addition amount was 2 wt% [34].

Zeng et al. added three flame retardants, i.e. APP, PEPA and MoO₃, into vinyl ester resins (VERs), and found that the LOI value of VERs composites reached 31% at the addition levels of 10% APP, 10% PEPA and 5% MoO₃, respectively, besides the UL-94 V-0 rating, which showed excellent synergistic flame retardant properties [35].

In this study, a novel phosphoramidate flame retardant phenyl P-methyl-N-(8-(methylamino)octyl) phosphonamidate (PPNPP) was firstly synthesized via the esterification, and subsequently the flame retardant silicon wrapped ammonium polyphosphate (SiAPP)-PPNPP-MoO₃ (SPM) was prepared by solution mixing and incorporated into liquid TPU to create a flame retardant and high-strength TPU coating. This coating was then applied onto the surface of the GFC by brushing and heat curing processes to form the TPU/glass fiber cloth (TPU/G) composites. The synthesized flame retardants were characterised, and the morphological information, the flame retardant and mechanical properties of the TPU/G composites were investigated. In addition, the enhancement mechanism of the coating for flame retardancy and mechanical properties were discussed. This study proposes a novel idea for the development of new flame-retardant cable wrapping tape, which further broadens the application scope of TPU composites.

2. Experimental section

2.1. Materials

TPU (65E85) was produced by Bangtai Chemical Industry Co., Ltd. (Baoding, China). SiAPP (203) was purchased from Shenfang Changfeng Chemical Co., Ltd. (Shenfang, China). 1,8-octanediamine (98%), triethylamine (TEA, AR), acetonitrile (AR), phenyl dichlorophosphate (PDCP, 98%), ammonium molybdate tetrahydrate ((NH₄)₆Mo₇O₂₄•4H₂O, 99.9%), nitric acid (HNO₃, 66.5%), and N, N-Dimethylformamide (DMF, AR) were obtained from Aladdin Reagent Co., Ltd. (Shanghai,

China). GFC ($125 \pm 2 \text{ g/m}^2$) was purchased from Hebei Fuhua new building Materials Co., Ltd. (Langfang, China).

2.2. Synthesis of PPNPP

Typically, 8.64 g 1,8-octanediamine, 80 mL acetonitrile, and 18.40 g TEA were poured into the 500 mL three-neck flask equipped with a mechanical stirrer, condenser, and thermometer. Subsequently, 13.86 g PDCP and 40 mL acetonitrile were slowly added into the above solution with mechanical stirring for 1.5 h under ice bath. After that, the mixture was stirred at 60 °C for 3 h, and then heated to 80 °C and kept stirring for 3 h. Finally, the organic phase was separated and washed three times with deionized water and petroleum ether, and dried for 24 h in a vacuum oven.

2.3. Preparation of MoO₃

20.00 g $(\text{NH}_4)_6\text{Mo}_7\text{O}_{24}\cdot 4\text{H}_2\text{O}$ was dissolved in 200 mL deionized water with mechanical stirring for 30 min under room temperature, and then 6.55 mL HNO_3 was added into the above solution. After that, the mixture was transferred into a reaction kettle at 180 °C for 24 h. Finally, the precipitate was separated by filtration, washed with ethanol and deionized water after being cooled down to room temperature, and the product was dried at 60 °C in a vacuum oven for 24 h.

2.4. Fabrication of TPU/G composites

To prepare the fire-retardant coating (TPU/SPM-1.0), 20.00 g TPU was mixed with 60 mL DMF at 80 °C until TPU completely dissolved to liquid. Subsequently, 2.50 g SiAPP and 1.25 g PPNPP were dissolved in 20 mL DMF and thereby added to the TPU solution with mechanical stirring for 10 min. Then, 1.25 g MoO₃ was added into the mixture with ultrasonic mixing for 20 min. Finally, the coating was applied to the surface of GFC by double-sided coating and heat curing processes to prepare TPU/G-SPM-1.0. For the designation of the TPU/G composites, GFC coated with pure TPU is defined

as TPU/G and the composites with added flame retardants are defined as TPU/G-X, the X stands for different ratios of flame retardants. The schematic diagram for preparation of TPU/G-X is shown in Fig. 1, and Table 1 summarizes the formulations of the TPU/G composites.

2.5. Characterization

Fourier transform infrared spectra (FTIR) of the samples were estimated on a Nicolet IS50 spectrometer (Nicolet Instrument Company, USA) with a wavenumber range of 4000 to 400 cm^{-1} . ^1H NMR and ^{13}C NMR were measured on a fully digitalized nuclear magnetic resonance spectrometer (NMR, AVANCE NEO 600, Switzerland) at 600 MHz using DMSO- d_6 as a solvent. X-ray diffraction (XRD) results of samples were obtained using a DY1602/Empyrean x-ray diffractometer ($\lambda = 1.54178$ Å). Scanning electron microscope (SEM, Verios G4, USA) was used to observe the surface morphologies of the GFC and TPU/G composites. The surface elemental distribution of TPU/G-X microstructure and char residues were observed by energy dispersive spectrometer (EDS). Thermal conductivity data were obtained by a thermal conductivity tester (DRP-II, Xiangtan Xiangyi Instrument Co., Ltd.). The combustion behavior of the TPU/G composites was estimated by TTech-GBT16172-2 cone calorimeter (CCT) (TESTech, Suzhou, China) according to the ISO 5660 standard under a heat flux of 35 kW/m^2 . Each sample with a size of 100 mm \times 100 mm \times 0.2 mm and stacked in 10 layers (2 mm). Thermogravimetric analysis (TGA) of the TPU/G composites was performed by thermal analyzer (TA Q5000, USA) from room temperature to 800 $^\circ\text{C}$ with 20 $^\circ\text{C}/\text{min}$ heating rate under Ar and air conditions. Smoke density data of the samples were obtained by plastic smoke density tester (JSC-2), according to GB/T 8323-2008. Each sample with dimensions of 75 mm \times 75 mm \times 0.2 mm and exposed horizontally to an external heat flux of 25 kW/m^2 with the application of no pilot flame. Mechanical properties of the GFC and TPU/G samples were tested by an electronic universal

testing machine (JPL-1000N) with a tensile rate of 20 mm/min according to GB/T12914-2018. LOI values of the samples were tested by the LOI analyzer (HC-2, Nanjing, China) according to GB/T5454-1997 with specimen dimensions of 150 mm × 58 mm × 0.2 mm. The vertical burning test was carried out by vertical combustion tester (CZF-II, Jiangning Analytical Instruments Co., Ltd.) according to GB/T5455-2014, and each sample with dimensions of 300 mm × 89 mm × 0.2 mm. Raman spectroscopy was provided by a Renishaw Invia Raman Microscope (Invia Reflex, Britain) with a 532 nm argon ion laser.

3. Results and discussion

3.1. Characterization of flame retardants

Fig. 2a shows the preparation route of PPNPP, which was synthesized via the esterification of 1,8-octanediamine and PDCP. Fig. 2b shows the FTIR spectra of PPNPP and its raw materials. The absorption peaks at 3200-3500 cm^{-1} are ascribed to the stretching vibration of primary amine in the 1,8-octanediamine [25]. For PDCP, the peaks at 564 cm^{-1} and 1210 cm^{-1} typically are associated with the stretching vibrations of the P-Cl and P=O bonds, respectively [36]. In contrast to the FTIR spectra of raw materials, the disappearance of P-Cl and primary amine bonds, and the formation of a new peak of secondary amine at 3390 cm^{-1} indicate the complete reaction between 1,8-octanediamine and PDCP [37]. Besides, the new peaks generated at 1100 and 1030 cm^{-1} are ascribed to P-N-C and P-N, respectively [29], which further confirms the successful synthesis of PPNPP.

To further verify the structure of PPNPP, the products were characterized by ^1H and ^{13}C NMR tests. Fig. 2c is the ^1H NMR spectrum of PPNPP, showing that the resonance signals in the range of 7.05-7.22 ppm are attributed to the aromatic protons on the benzene ring (labeled a, b, c), and the signal around 1.17 ppm corresponds to the imine structure on the main chain of PPNPP (labeled d, k) [28].

In addition, the weak signals in the range of 2.98-3.06 ppm and 3.40-3.44 ppm are attributed to the methylene structure on the carbon chain (labeled e-j) [22]. Fig. 2d presents the ^{13}C NMR spectrum. The signal at 150.5 ppm supports the aromatic carbon structure at the junction of the benzene ring and the main chain of PPNPP (labeled a), while the signals in the range of 120.0-130.0 ppm are ascribed to the remaining aromatic structures on the benzene ring (labeled b, c, d). In addition, the signals at 41.0 ppm, 46.2 ppm, and the range of 25.0-32.5 ppm are attributed to the methylene structures on the main carbon chain (labeled e-k). The results above confirm the successful synthesis of PPNPP.

The XRD patterns of MoO_3 nanorods are plotted in Fig. 2e. It can be seen from the XRD patterns that the reflection peaks located at $2\theta = 9.7^\circ$, 19.4° , 25.8° , and 45.5° correspond to the (100), (200), (210), and (410) crystal planes of MoO_3 nanorods, which are consistent with the standard card (JCPDS: 83-1176) [33], proving the successful synthesis of MoO_3 nanorods.

3.2. Surface morphology and element composition

The micromorphology of flame-retardant coating on the GFC was studied by SEM. As shown in Fig. 3a₁-a₃, the pristine GFC has a smooth and flat surface, and a complete fiber structure can be observed. After the introduction of the TPU coating, the surface of the GFC becomes more consistent and rougher (Fig. 3b₁-b₃). It is noted that a thin film is attached onto the surface of the GFC. In comparison to TPU/G, a large number of micro/nano-scale hierarchical structures are obtained on the surface of TPU/G-SPM-1 (Fig. 3c₁-c₃), which can be attributed to the deposition of SPM flame retardant. In addition, the element distribution mapping images for the surface of TPU/G-SPM-1 are shown in Fig. 3d, revealing the homogeneous distributions of C, N, O, Si, P and Mo elements in the flame retardant coating. Meanwhile, these distributions of different elements exhibit a clear fiber shape similar to the GFC, further indicating that the TPU/SPM flame retardant coating have been

successfully applied to the surface of the GFC.

3.3. Thermal stability

The thermal degradation behavior of the TPU/G composites with different coatings was studied through TGA technique. The degradation curves of the TPU/G composites under Ar (a) and air (b) atmosphere are plotted in Fig. 4 (since the test temperature did not reach the degradation temperature of the GFC, this discussion focuses solely on the thermal degradation performance of the TPU flame-retardant coating), and the related thermal data are shown in Table 2. As displayed in Fig. 4a, the thermal degradation of all samples under the Ar atmosphere presents two typical weight loss stages. The first stage involves the degradation of the hard segments of the TPU main chain to diols and diisocyanates, while the second stage is attributed to the further breakdown of isocyanates and polyols in the soft segments of TPU chains [38]. However, the thermal oxidative degradation processes of TPU/G-X under the air atmosphere occur in three different stages (Fig. 4c). In addition to the two thermal degradation stages mentioned above, the final stage can be lied to the further thermal oxidative degradation of the char residues produced in the first stage [39]. As observed from Table 2, the **initial decomposition temperature ($T_{5\%}$)** of TPU/G-X decreases significantly, compared to that of TPU/G. This may be due to SPM flame retardant can catalyze the decomposition of polyurethane bonds into isocyanates, alcohols, and carbon dioxide at lower temperatures, which can delay heat transfer and decrease the fire hazard of TPU/G-X [40, 41]. After the thermal degradation stages, the char yields of TPU/G under the air and Ar atmospheres are 69.20% and 70.82%, respectively. Notably, the char residues of TPU/G-X at 800 °C are significantly higher than TPU/G, indicating that SPM flame retardant effectively enhances the thermal stability of the TPU coating. Furthermore, by comparing the char yield of different samples, it is noted that under the same loading conditions, TPU/G-SM-1

exhibits the highest char yield at 800 °C in both air and Ar atmospheres, indicating that SiAPP actually performs better char formation ability than PPNPP. This phenomenon can be attributed to SiAPP acting as a suitable acid source and demonstrating superior flame retardant performance in the condensed phase.

Additionally, from the differential thermal gravity (DTG) curves in Fig. 4b, d, it can be seen that the main thermal degradation peaks of TPU/G-X are significantly lower than TPU/G, and the corresponding **maximum decomposition rate temperature (T_{max})** is also lower than the control one. This is primarily related to the increase in char yield, as SPM flame retardant effectively improves the stability of the char layer formed during combustion, physically hindering heat transfer and enhancing the fire resistance of the composites.

3.4. Thermal conductivity

The thermal conductivity serves as an important index to evaluate the heat transfer performance of materials, which can be tested by thermal conductivity tester (Fig. 5a). **As shown in Fig. 5b, GFC exhibits high thermal conductivity ($49.9 \text{ mW m}^{-1} \text{ K}^{-1}$), while TPU/G has a thermal conductivity of $32.0 \text{ mW m}^{-1} \text{ K}^{-1}$. In contrast, the thermal conductivity of TPU/G-X samples is reduced to varying degrees.** The comparison of different samples reveals that the thermal conductivity of the TPU/G-SPM composites tends to increase as the amount of SPM flame retardant decreases, indicating that the incorporation of SPM flame retardant effectively enhances the thermal insulation properties of the coating, potentially reducing the rate of heat transfer during combustion, and thereby improving fire safety. It is evident that TPU/G-SM-1 has the lowest thermal conductivity ($16.7 \text{ mW m}^{-1} \text{ K}^{-1}$). This phenomenon can be attributed to the reason that introduction of SiAPP alters the arrangement of TPU molecules, resulting in a denser structure that hinders the establishment of an efficient heat channel

[42]. In addition, this leads to the thermal conductivity of TPU/G-PM-1 higher than that of TPU/G-SM-1.

3.5. Flame retardant performance

To evaluate the flame retardant performance of the materials, the LOI and vertical burning test are usually employed to assess flammability of polymeric materials. The relevant flammability data are presented in Table 3. The LOI value of the pristine TPU/G sample is 23.3%, indicating a high fire risk. In contrast, the LOI value of TPU/G-SPM-3 reaches 27%. This means that the TPU coating transforms from a flammable material into a highly flame-retardant one at a low load of SPM. Meanwhile, the LOI value of the TPU composites increases with increasing content of SPM, which indicate a significant improvement in the flame retardant properties of the coating. Moreover, as shown in the digital photographs in Fig. 6, TPU/G is ignited rapidly after encountering fire, which eventually burns all the TPU coating on the sample within 20 s. In contrast, TPU/G-SPM-1 passes the vertical burning test, and self-extinguishes immediately after 6 s of ignition with the char residues morphology remaining intact with a small damaged length (120 ± 2 mm). In summary, [these results indicate](#) that the TPU coating added with SPM improves flame retardancy of the TPU/G composites.

The CCT is an instrument for evaluating the combustion behavior of materials, which collects the combustion parameters of composites by simulating the fire scenario to comprehensively evaluate the flame retardancy and smoke suppression properties of materials [43]. As shown in Fig. 7 and Table 4, the time to ignition (TTI) of TPU/G is 47s. In contrast, the TTI of composites incorporating only two types of flame retardants exhibits varying trends (TPU/G-SP-1, TPU/G-SM-1 increasing and TPU/G-PM-1 decreasing) compared to the control one. After comparing different samples, it can be found that the TTI of the composites gradually increases with the increase of SiAPP flame retardant. This

phenomenon can be attributed to the higher thermal stability of SiAPP than PPNPP, which is well consistent with the trends observed in thermal conductivity tests. Furthermore, the TTI values of the TPU composites containing SPM flame retardant are all less than 47 s, and gradually decrease with the increase of SPM addition, indicating that SPM flame retardant can catalyze the early decomposition of the TPU coating.

The PHRR is an important parameter for assessing the fire hazard of composites after combustion [44]. The HRR and THR curves are shown in Fig. 7a, b. Due to the high flammability of TPU, TPU/G exhibits high PHRR of 260 kW/m² and THR of 16.7 MJ/m². In contrast, the incorporation of the SPM flame retardant significantly reduces the PHRR and THR of the composites. Particularly, the PHRR and THR of TPU/G-SPM-1 are 110 kW/m² and 10.6 MJ/m², respectively, which are 57.7% and 36.8% lower than those of TPU/G. Notably, TPU/G-SM-1 shows the lowest THR of 6.3 MJ/m², which can be attributed to the high flame retardant efficiency of SiAPP, significantly shortening the combustion time of the composites. Combined with the CCT data, it is concluded that SPM significantly reduces the fire hazard of the TPU coating, which is in good agreement with the results of the TGA and LOI tests.

The impact of cable combustion is often severe due to its imperceptible, rapidly spreading and the emission of large quantities of toxic and harmful smoke. Therefore, it is extremely important to improve the smoke suppression performance of cable materials. The SPR and TSR data of different samples are presented in Fig. 7c, d. TPU/G shows high PSPR (0.1222 m²/s) and TSR (664.5 m²/m²). In comparison, the PSPR and TSR values of TPU/G-SPM-1 are 0.0658 m²/s and 404.2 m²/m², respectively, which are 46.2% and 39.2% lower than those of TPU/G. However, the PSPR (0.1169 m²/s) and TSR (633.6 m²/m²) of TPU/G-SP-1 respectively decrease by only 4.3% and 4.7%, compared to those of the control one, indicating that the incorporation of a small amount of MoO₃ can effectively

enhance the smoke suppression performance of the TPU coating. This can be due to the explanation that MoO_3 , as an inorganic nanofiller, has been shown to synergize with phosphorous-nitrogen flame retardants in polymers (such as VERs and rigid polyurethane foam) to promote the formation of carbon layer, which enables the composites to exhibit excellent smoke suppression [35, 45-47].

The toxic and harmful gases suppression curves of the TPU composites are shown in Fig. 7e-h. The peak of the carbon dioxide production rate (PCO_2PR) and total carbon dioxide yield (CO_2TY) of TPU/G-X are significantly lower than those of TPU/G. Notably, TPU/G-SPM-1 demonstrates the lowest PCO_2PR (0.0560 g/s), which is 53.6% lower than that of the control sample. However, TPU/G-SM-1 exhibits a lower CO_2TY (2.94 kg/kg). Additionally, carbon monoxide (CO) is one of the deadliest gases in a fire hazard. When CO level in the air reaches 1%, it can cause loss of consciousness [48]. The pristine TPU/G shows high peak of carbon monoxide production rate (PCOPR) (0.00245 g/s) and total carbon monoxide yield (COTY) (0.1377 kg/kg). In contrast, TPU/G-X with varying proportions of SPM (12 wt%, 16 wt%, and 20 wt%) show a reduction of over 90% in COTY compared to TPU/G. Specially, TPU/G-SPM-1 shows significant reductions in PCOPR (0.00021 g/s) and COTY (0.0014 kg/kg) by 91.43% and 99.0%, respectively, compared with the control one. This excellent toxic and harmful smoke suppression performance can be attributed to the synergistic effect of SPM in both the condensed and gas phases. Other studies on CO suppression of TPU composites are listed in Fig. 7i, further demonstrating the superiority of this work in terms of toxic gas inhibition performance [11, 20, 49-57].

The mass loss after combustion is an important factor affecting the flame retardant and smoke suppression performance of the composites, as shown in Fig. 7j, the residual mass of TPU/G only 63.89%, and with the addition of SPM flame retardant, the mass loss of TPU/G-X showed a significant

reduction trend. Among them, TPU/G/SM-1 exhibits the highest residual mass (77.26%), which can be attributed to the excellent performance of SiAPP in the condensed phase, which is consistent with the previous analysis. The addition of flame retardant can well catalyse the TPU matrix to generate a dense and stable carbon layer in combustion, which can well reduce the heat conduction and smoke emission in combustion, and reduce the fire hazard of composites.

3.6. Smoke density test

Smoke density testing simulates the smoke density and concentration released by burning materials under fire conditions, which is crucial for ensuring people's health and safety [58, 59]. The smoke density curves of the TPU/G composites are portrayed in Fig. 7k and Table 5. The $D_{s,10}$ and $D_{s,max}$ are defined as smoke density at 10 min and the maximum smoke density, respectively. For TPU/G, $D_{s,10}$ and $D_{s,max}$ are 74.8 and 75.1, indicating that the pure TPU coating emits large amounts of smoke during combustion. In contrast, with the increase of SPM flame retardant addition, the $D_{s,max}$ values of TPU/G-SPM-3, TPU/G-SPM-2 and TPU/G-SPM-1 are 53.5, 37.6 and 30.4, respectively, which are 28.8%, 49.9% and 59.5% less than that of the control sample, demonstrating that SPM flame retardant effectively reduces the concentration of smoke. Notably, the $D_{s,10}$ and $D_{s,max}$ of TPU/G-X show a similar decreasing pattern when the flame retardants are added in equal amounts, suggesting that either SiAPP or PPNPP in combination with MoO_3 can effectively reduce the smoke density of the TPU coatings during combustion. This phenomenon may be attributed to the quenching effects generated during combustion by the phosphorus-nitrogen flame retardant and MoO_3 , as well as the formation of a dense char layer.

3.7. Flame retardant mechanism

To further investigate the flame-retardant mechanism of TPU/G-X, the microstructure of the char

residues was analyzed by SEM. Digital photos and SEM images of the char residues of the TPU/G composites are presented in Fig. 8. It is observed that, for TPU/G, the TPU coating applied to the GFC burns out, and the samples show a clear fiber structure. In contrast, the surfaces of TPU/G-X displayed distinct char structures. Notably, for TPU/G-X containing SiAPP (Fig. 8b-f), the expanded char layer tightly covers the surface of the GFC, which is critical in the heat insulation and oxygen barrier during combustion. This phenomenon can be attributed to the formation of polyphosphoric acids in the decomposition process of APP, which can catalyze the decomposition of the TPU matrix and form an expanded carbon layer. Notably, the char residues of TPU/G-SPM-1 exhibit a highly continuous and dense structure. This intense and solid char layer effectively reduces smoke emissions during combustion, which explains the excellent smoke suppression performance of TPU/G-SPM-1.

The degree of graphitization of the TPU composites is typically analyzed by Raman spectroscopy (Fig. 9a-g). The smaller the I_D/I_G ratio, the greater the degree of graphitization is [60]. TPU/G has the I_D/I_G ratio of 2.49. In contrast, TPU/G-X with the addition of SPM (Fig. 9b-d) have the decreased I_D/I_G ratios (2.34, 2.46 and 2.37, respectively for TPU/G-SPM-1, TPU/G-SPM-2 and TPU/G-SPM-3), indicating that the graphitization degree of the TPU composites is improved by the addition of SPM. Furthermore, comparing the I_D/I_G ratios between TPU/G-SPM-1 and TPU/G-SP-1 indicates that the addition of 5 wt% MoO_3 significantly enhances the graphitization degree of the composites, which is consistent with the CCT and TGA results. It is obvious that TPU/G-PM-1 exhibits the lowest I_D/I_G ratio (1.6) among all TPU samples. However, the flame retardant and smoke suppression performances reported in the CCT data is not ideal. This can be attributed to the char residues generated by TPU/G-PM-1, which shows high density of char residues (as shown in Fig. 8g) but lacks the expansion capability. As a result, it is unable to form a continuous and dense char layer during combustion,

leading to relatively poor smoke suppression performance.

FTIR is adopted to study the chemical composition and molecular structure of char residues of the TPU coating. As plotted in Fig. 9h, the characteristic peak at 1601 cm^{-1} for all the samples corresponds to the unsaturated C=C bonds formed by aromatic compounds after TPU combustion [61]. It is observed that after adding SPM retardant into the TPU coating, the new characteristic peaks at 1221 and 970 cm^{-1} are assigned to the stretching vibrations of P=O and P-O-C, respectively [62, 63]. In addition, the characteristic peak at 1071 cm^{-1} corresponds to the Si-O-Si stretching vibration [64]. Combined with the SEM images of char residue, it can be analyzed that the TPU samples containing silica gel decompose at high temperatures to generate phosphoric acid-containing components, which can accelerate the decomposition of the main chain of the TPU and enhance the char formation properties of the TPU composites.

In order to reveal the flame retardant mechanism of the flame retardant TPU coatings, the relationship between the reduction in PHRR and char residue was investigated under the same amount of flame retardant added, as shown in Fig. 9i. It is noted that the correlation coefficient (R_1^2) between values of char residues and PHRR reduction of TPU/G-X is 0.730, indicating the poor linear correlation. In order to further investigate the mechanism of PHRR reduction, the relationship between the PHRR reduction and the contribution value (defined as the sum of the absolute value of char residue and the gas phase index Y) is presented in Fig. 9j [49]. The introduction of the gas phase index shows a clear linear relationship between the PHRR reduction and contribution values ($R_2^2 = 0.999$), indicating the existence of gas phase flame retardant mechanism for TPU/G-X. As shown in Table 6, it can be observed that the gas phase index of TPU/G-PM-1 is 10.62, which is 3 times as that of TPU/G-SPM-1. Notably, this result is very consistent with the proportion of PPNPP flame retardant added. In

addition, TPU/G-SM-1 has a relatively low gas phase index of 0.57. From comparing different samples, it can be seen that the gas phase index of the TPU composites increases linearly and significantly with the increase of PPNPP addition. It can be speculated that PPNPP flame retardant plays a very important role in the gas phase flame mechanism, while the flame retardant mechanism of SiAPP is mainly reflected in the condensed phase.

Based on the results and discussions presented above, the possible mechanism for enhancing the flame retardant and smoke suppression performance of TPU/G-X is proposed (Fig. 9k). After burning, SiAPP and PPNPP rapidly dehydrate and decompose into components, such as phosphoric acid, metaphosphoric acid and polyphosphoric acid, which can accelerate the char formation of the TPU matrix and promote cross-linking of carbonization [65]. Meanwhile, SiO₂ and MoO₃ form a dense oxide film on the surface, preventing O₂ from entering the interior and thus inhibiting the combustion of TPU coating. On the other hand, SiAPP and PPNPP release non-flammable products, such as H₂O and NH₃ upon combustion, which dilute the concentration of flammable gases. Moreover, SiAPP and PPNPP can degrade to generate free radicals i.e. PO• and HPO• at high temperatures, which can capture active radicals such as H• and OH•, thereby reducing the combustion rate and suppressing the emission of toxic and harmful smoke. Overall, the synergistic effect of SPM in the condensed phase and the gas phase can effectively enhance the flame retardant and smoke suppression abilities of flame retardant TPU coatings.

3.8. Mechanical property

To meet the demands of daily applications, it is crucial to overcome the inherent defects of GFC, such as poor abrasion resistance and brittleness. The mechanical properties of the GFC and TPU/G composites are presented in Fig. 10a. The tensile strength and elongation at break of GFC are 64.7

MPa and 3.4%, respectively. After coating with TPU, TPU/G exhibits a tensile strength of 126.9 MPa, representing a 96.1% increase compared to that of pure fabric. However, the elongation at break decreases to 2.6%, which may be due to the higher strength conferred by the TPU coating at the expense of some toughness. It is noted that the mechanical properties of TPU/G-X are generally improved compared to that of the control sample. In order to investigate the effect of different coating ratios on mechanical properties, the fracture surfaces of all samples were observed by SEM (Fig. 10b-h). Notably, the values of tensile strength of TPU/G-X are higher than that of TPU/G, indicating that the addition of SiAPP and PPNPP can enhance the interfacial compatibility of the TPU coating with GFC.

The mechanical strengthening mechanism of TPU coatings is analysed as shown in Fig. 10i-m. The GFC is unable to maintain its original neatly woven structure after being damaged by external forces (Fig. 10i), and the fibres appear to be dispersed. In contrast, TPU/G-SPM-1 (Fig. 10j, k) has dense and compact structure. Moreover, the fracture region of TPU/G-SPM-1 (Fig. 10l) displays that though the external TPU coating is pulled off, the internal GFC still maintains its original structure, indicating that the TPU coating protects the GFC well from damage in the early stage of tensile. Based on the above analysis, the mechanical enhancement mechanism of the TPU coatings is proposed and illustrated in Fig. 10m. Multiple hydrogen bonding interactions are formed between SPM flame retardant and TPU chains before stretching, which makes the composites present 3D morphology. After the tensile force is applied, the TPU chains are straightened, and the hydrogen bonding of the internal connection is broken and slipped. With the continuous application of the external force, the external TPU coating firstly deforms and break down. Subsequently, after the TPU coating is broken, the tensile force is transferred to the GFC, ultimately causing the breakage of GFC.

4. Conclusions

In this work, the novel phosphoramidate flame retardant PPNPP was synthesized by esterification and compounded with SiAPP and MoO₃ added into TPU to prepare TPU flame-retardant coatings, and finally the flame-retardant TPU/G composites were obtained by double-sided coating on the surface of GFC and heat curing. The results indicate that the SPM flame retardant provides the TPU coating with excellent flame-retardant performance. For TPU/G-SPM-1, the PHRR and THR decreased by 57.7% and 36.8%, respectively, compared to TPU/G. Meanwhile, the incorporation of the SPM flame retardant effectively reduces the emission of toxic and harmful smoke during the combustion of the TPU composites. Notably, this coating demonstrated remarkable suppression of CO emissions. For TPU/G-SPM-1, the PCOPR and CO yield decreased by 91.4% and 98.9%, respectively, compared to the pure sample. Furthermore, the TPU/SPM flame-retardant coating also imparts excellent mechanical properties to the GFC. Compared to pure GFC (64.7 MPa), the tensile strength of TPU/G-SPM-1 is improved by 101%, reaching 130.3 MPa. In summary, this work provides a novel approach for the preparation of fire-resistant TPU composites, demonstrating promising applications in the field of cable wrapping materials.

CRedit authorship contribution statement

Yongqian Shi: Writing - Original Draft, Supervision, Funding acquisition; **Songqiong Jiang:** Writing-Review & Editing, Data Curation, Investigation, Formal analysis; **Jinke Wu:** Conceptualization, Data Curation, Visualization; **Zhendong Chen:** Validation, Visualization; **Cancan Zhang:** Writing-Review & Editing, Validation, Visualization, Supervision; **Yun Zhang:** Methodology, Investigation; **Pingan Song:** Methodology, Investigation; **Yan Zhang:** Validation, Visualization.

Declaration of competing interest

The authors declare that they have no known competing financial interests or personal relationships that could have appeared to influence the work reported in this paper.

Acknowledgement

This work was financially supported by the Key research and development projects of Baoying County (Grant No. BY202205) and International Scientific and Technological Cooperation Program of Ningbo (No. 2024H020).

References

- [1] Y. Li, L. Qi, Y. Liu, J. Qiao, M. Wang, X. Liu, S. Li, Recent Advances in Halogen-Free Flame Retardants for Polyolefin Cable Sheath Materials, *Polymers* 14 (2022) 2876.
- [2] W. An, T. Wang, K. Liang, Y. Tang, Z. Wang, Effects of interlayer distance and cable spacing on flame characteristics and fire hazard of multilayer cables in utility tunnel, *Case Stud. Therm. Eng.* 22 (2020) 100784.
- [3] P. Jia, X. Yu, J. Lu, X. Zhou, Z. Yin, G. Tang, T. Lu, L. Guo, L. Song, B. Wang, Y. Hu, The $\text{Re}_2\text{Sn}_2\text{O}_7$ (Re = Nd, Sm, Gd) on the enhancement of fire safety and physical performance of Polyolefin/IFR cable materials, *J. Colloid Interf. Sci.* 608 (2022) 1652-1661.
- [4] A. Vishwakarma, M. Singh, B. Weclawski, V. J. Reddy, B. K. Kandola, G. Manik, A. Dasari, S. Chattopadhyay, Construction of hydrophobic fire retardant coating on cotton fabric using a layer-by-layer spray coating method, *Int. J. Biol. Macromol.* 223 (2022) 1653-1666.
- [5] W. Al-Shatty, D. A. Hill, S. Kiani, A. Stanulis, S. Winston, I. Powner, S. Alexander, A. R. Barron, Superhydrophilic surface modification of fabric via coating with cysteic acid mineral oxide, *Appl. Surf. Sci.* 580 (2022) 152306.
- [6] J.-C. Yang, W. Liao, S.-B. Deng, Z.-J. Cao, Y.-Z. Wang, Flame retardation of cellulose-rich fabrics via a simplified layer-by-layer assembly, *Carbohydr. Polym.* 151 (2016) 434-440.
- [7] L. Lu, C. Hu, Y. Zhu, H. Zhang, R. Li, Y. Xing, Multi-functional finishing of cotton fabrics by water-based layer-by-layer assembly of metal-organic framework, *Cellulose* 25 (2018) 4223-4238.

- [8] D. Ding, Q. Wu, J. Wang, Y. Chen, Q. Li, L. Hou, L. Zhao, Y.-y. Xu, Superhydrophobic encapsulation of flexible Bi₂Te₃/CNT coated thermoelectric fabric via layer-by-layer assembly, *Compos. Commun.* 38 (2023) 101509.
- [9] M. Ayesh, A. R. Horrocks, B. K. Kandola, The effect of combined atmospheric plasma/UV treatments on improving the durability of organophosphorus flame retardants applied to polyester fabrics, *Polym. Degrad. Stab.* 225 (2024) 8737.
- [10] L. Qi, B. Wang, W. Zhang, B. Yu, M. Zhou, Y. Hu, W. Xing, Durable flame retardant and dip-resistant coating of polyester fabrics by plasma surface treatment and UV-curing, *Prog. Org. Coat.* 172 (2022) 107066.
- [11] W. Wu, W. Huang, Y. Tong, J. Huang, J. Wu, X. Cao, Q. Zhang, B. Yu, R. K. Y. Li, Self-assembled double core-shell structured zeolitic imidazole framework-8 as an effective flame retardant and smoke suppression agent for thermoplastic polyurethane, *Appl. Surf. Sci.* 610 (2023) 155540.
- [12] K. Liu, Y. Lu, Y. Cheng, J. Li, G. Zhang, F. Zhang, Flame retardancy and mechanism of polymer flame retardant containing P-N bonds for cotton fabrics modified by chemical surface grafting, *Cellulose* 31 (2024) 3243-3258.
- [13] Y. Ma, Y. Wang, L. Ma, Z. Zhu, Fabrication of hydrophobic and flame-retardant cotton fabric via sol-gel method, *Cellulose* 30 (2023) 11829-11843.
- [14] D. Zhang, B. L. Williams, S. B. Shrestha, Z. Nasir, E. M. Becher, B. J. Lofink, V. H. Santos, H. Patel, X. Peng, L. Sun, Flame retardant and hydrophobic coatings on cotton fabrics via sol-gel and self-assembly techniques, *J. Colloid Interf. Sci.* 505 (2017) 892-899.
- [15] Y. Huang, S. Jiang, R. Liang, P. Sun, Y. Hai, L. Zhang, Thermal-triggered insulating fireproof layers: A novel fire-extinguishing MXene composites coating, *Chem. Eng. J.* 391 (2020) 123621.

- [16] T.-T. Li, S. Chu, X. Hu, H.-T. Ren, C.-W. Lou, J.-H. Lin, Silica Nanoparticle/TPU Coating Imparts Aramid with Puncture Resistance and Anti-corrosion for Personal Protection, *ACS Appl. Nano Mater.* 6 (2023) 16986-16999.
- [17] A. Moiz, R. Padhye, X. Wang, Coating of TPU-PDMS-TMS on Polycotton Fabrics for Versatile Protection, *Polymers* 9 (2017) 660.
- [18] Y. Liu, X. Cao, J. Shi, B. Shen, J. Huang, J. Hu, Z. Chen, Y. Lai, A superhydrophobic TPU/CNTs@SiO₂ coating with excellent mechanical durability and chemical stability for sustainable anti-fouling and anti-corrosion, *Chem. Eng. J.* 434 (2022) 134605.
- [19] Q. He, W. Wu, H. Hu, Z. Rui, J. Ye, Y. Wang, Z. Wang, Achieving superior fire safety for TPU 3D-printed workpiece with EP/PBz/PDMS coating, *J. Appl. Polym. Sci.* 140 (2023) 53858.
- [20] W. Huang, J. Huang, B. Yu, Y. Meng, X. Cao, Q. Zhang, W. Wu, D. Shi, T. Jiang, R. K. Y. Li, Facile preparation of phosphorus containing hyperbranched polysiloxane grafted graphene oxide hybrid toward simultaneously enhanced flame retardancy and smoke suppression of thermoplastic polyurethane nanocomposites, *Compos. Part A Appl. Sci.* 150 (2021), 106614.
- [21] M. Steinmann, M. Wagner, F. R. Wurm, Poly(phosphorodiamidate)s by Olefin Metathesis Polymerization with Precise Degradation, *Chem. Eur. J.* 22 (2016) 17329-17338.
- [22] Y. Xue, Z. Ma, X. Xu, M. Shen, G. Huang, S. Bourbigot, X. Liu, P. Song, Mechanically robust and flame-retardant polylactide composites based on molecularly-engineered polyphosphoramides, *Compos. Part A Appl. Sci.* 144 (2021) 106317.
- [23] Q. Tai, R. K. K. Yuen, L. Song, Y. Hu, A novel polymeric flame retardant and exfoliated clay nanocomposites: Preparation and properties, *Chem. Eng. J.* 183 (2012) 542-549.

- [24] Y. Xue, M. Shen, Y. Zheng, W. Tao, Y. Han, W. Li, P. Song, H. Wang, One-pot scalable fabrication of an oligomeric phosphoramidate towards high-performance flame retardant polylactic acid with a submicron-grained structure, *Compos. B Eng.* 183 (2020) 107695.
- [25] C. Liu, D. Yang, M. Sun, G. Deng, B. Jing, K. Wang, Y. Shi, L. Fu, Y. Feng, Y. Lv, M. Liu, Phosphorous-Nitrogen flame retardants engineering MXene towards highly fire safe thermoplastic polyurethane, *Compos. Commun.* 29 (2022) 101055.
- [26] Y.-R. Li, Y.-M. Li, W.-J. Hu, D.-Y. Wang, Cobalt ions loaded polydopamine nanospheres to construct ammonium polyphosphate for the improvement of flame retardancy of thermoplastic polyurethane elastomer, *Polym. Degrad. Stab.* 202 (2022) 110035.
- [27] M. Wan, C. Shi, X. Qian, Y. Qin, J. Jing, H. Che, F. Ren, J. Li, B. Yu, K. Zhou, Design of novel double-layer coated ammonium polyphosphate and its application in flame retardant thermoplastic polyurethanes, *Chem. Eng. J.* 459 (2023) 141448.
- [28] W. Zhao, J. Liu, H. Peng, J. Liao, X. Wang, Synthesis of a novel PEPA-substituted polyphosphoramidate with high char residues and its performance as an intumescent flame retardant for epoxy resins, *Polym. Degrad. Stab.* 118 (2015) 120-129.
- [29] X. Ye, Y. Wang, Z. Zhao, H. Yan, A novel hyperbranched poly(phosphorodiamidate) with high expansion degree and carbonization efficiency used for improving flame retardancy of APP/PP composites, *Polym. Degrad. Stab.* 142 (2017) 29-41.
- [30] X. Dong, Y. Ma, X. Fan, S. Zhao, Y. Xu, S. Liu, D. Jin, Nickel modified two-dimensional bimetallic nanosheets, $M(OH)(OCH_3)$ ($M=Co, Ni$), for improving fire retardancy and smoke suppression of epoxy resin, *Polymer* 235 (2021) 124263.

- [31] Z. H. Wu, Q. Wang, Q. X. Fan, Y. J. Cai, Y. Q. Zhao, Synergistic effect of Nano-ZnO and intumescent flame retardant on flame retardancy of polypropylene/ethylene-propylene-diene monomer composites using elongational flow field, *Polym. Compos.* 40 (2018) 2819-2833.
- [32] M. Zhang, X. Ding, Y. Zhan, Y. Wang, X. Wang, Improving the flame retardancy of poly(lactic acid) using an efficient ternary hybrid flame retardant by dual modification of graphene oxide with phenylphosphinic acid and nano MOFs, *J. Hazard. Mater.* 384 (2020) 121260.
- [33] W.-Z. Xu, C.-C. Li, Y.-X. Hu, L. Liu, Y. Hu, P.-C. Wang, Synthesis of MoO₃ with different morphologies and their effects on flame retardancy and smoke suppression of polyurethane elastomer, *Polym. Adv. Technol.* 27 (2016) 964-972.
- [34] A. Yao, C. Liu, Y. Ye, Y. Yang, Z. Wang, H. Wang, Y. Feng, J. Gao, Y. Shi, Functionalizing MXenes with molybdenum trioxide towards reducing fire hazards of thermoplastic polyurethane, *New J. Chem.* 46 (2022) 14112-14121.
- [35] G. Zeng, W. Zhang, X. Zhang, W. Zhang, J. Du, J. He, R. Yang, Study on flame retardancy of APP/PEPA/MoO₃ synergism in vinyl ester resins, *J. Appl. Polym. Sci.* 137 (2020) 49026.
- [36] L. Liu, Y. Xu, Y. Pan, M. Xu, Y. Di, B. Li, Facile synthesis of an efficient phosphonamide flame retardant for simultaneous enhancement of fire safety and crystallization rate of poly (lactic acid), *Chem. Eng. J.* 421 (2021) 127761.
- [37] Y. Feng, J. Hu, Y. Xue, C. He, X. Zhou, X. Xie, Y. Ye, Y.-W. Mai, Simultaneous improvement in the flame resistance and thermal conductivity of epoxy/Al₂O₃ composites by incorporating polymeric flame retardant-functionalized graphene, *J. Mater. Chem. A* 5 (2017) 13544-13556.

- [38] K. Chen, Y. Feng, Y. Shi, H. Wang, L. Fu, M. Liu, Y. Lv, F. Yang, B. Yu, M. Liu, P. Song, Flexible and fire safe sandwich structured composites with superior electromagnetic interference shielding properties, *Compos. Part A Appl. Sci.* 160 (2022) 107070.
- [39] M. Z. Rahman, X. Wang, L. Song, Y. Hu, A novel green phosphorus-containing flame retardant finishing on polysaccharide-modified polyamide 66 fabric for improving hydrophilicity and durability, *Int. J. Biol. Macromol.* 239 (2023) 124252.
- [40] C. Gao, Y. Shi, Y. Chen, S. Zhu, Y. Feng, Y. Lv, F. Yang, M. Liu, W. Shui, Constructing segregated polystyrene composites for excellent fire resistance and electromagnetic wave shielding, *J. Colloid Interf. Sci.* 606 (2022) 1193-1204.
- [41] S. Zhang, X. Liu, X. Jin, H. Li, J. Sun, X. Gu, The novel application of chitosan: Effects of cross-linked chitosan on the fire performance of thermoplastic polyurethane, *Carbohydr. Polym.* 189 (2018) 313-321.
- [42] P. Sun, H. Zhang, Y. Leng, Z. Wang, J. Zhang, M. Xu, X. Li, B. Li, Construction of flame retardant functionalized carbon dot with insulation, flame retardancy and thermal conductivity in epoxy resin, *Constr. Build. Mater.* 451 (2024) 138853.
- [43] W. Wu, W. Zhao, X. Gong, Q. Sun, X. Cao, Y. Su, B. Yu, R. K. Y. Li, R. A. L. Vellaisamy, Surface decoration of Halloysite nanotubes with POSS for fire-safe thermoplastic polyurethane nanocomposites, *J. Mater. Sci. Technol.* 101 (2022) 107-117.
- [44] B.-h. Kang, X. Lu, J.-p. Qu, T. Yuan, Synergistic effect of hollow glass beads and intumescent flame retardant on improving the fire safety of biodegradable poly(lactic acid), *Polym. Degrad. Stab.* 164 (2019) 167-176.

- [45] X. Lyu, H. Zhang, Y. Yan, Effect of expandable graphite and molybdenum trioxide in nitrogen/phosphorus synergistic system on acoustic performance and fire safety in rigid polyurethane foam, *J. Appl. Polym. Sci.* 139 (2022) 52488.
- [46] T. Tanaka, O. Terakado, M. Hirasawa, Flame retardancy in fabric consisting of cellulosic fiber and modacrylic fiber containing fine-grained MoO_3 particles, *Fire Mater.* 40 (2015) 612-621.
- [47] H. Xu, C. Peng, L. Xia, Z. Miao, S. He, C. Chi, W. Luo, G. Chen, B. Zeng, S. Wang, L. Dai, A Novel Anderson-Type POMs-Based Hybrids Flame Retardant for Reducing Smoke Release and Toxicity of Epoxy Resins, *Macromol. Rapid Commun.* 44 (2023) 2300162.
- [48] B. Yu, Y. Shi, B. Yuan, S. Qiu, W. Xing, W. Hu, L. Song, S. Lo, Y. Hu, Enhanced thermal and flame retardant properties of flame-retardant-wrapped graphene/epoxy resin nanocomposites, *J. Mater. Chem. A* 3 (2015) 8034-8044.
- [49] C. Liu, K. Xu, Y. Shi, J. Wang, S. Ma, Y. Feng, Y. Lv, F. Yang, M. Liu, P. Song, Fire-safe, mechanically strong and tough thermoplastic Polyurethane/MXene nanocomposites with exceptional smoke suppression, *Mater. Today Phys.* 22 (2022) 100607.
- [50] W. Cai, Z. Li, T. Cui, X. Feng, L. Song, Y. Hu, X. Wang, Self-assembly of hierarchical MXene@ SnO_2 nanostructure for enhancing the flame retardancy, solar de-icing, and mechanical property of polyurethane resin, *Compos. B Eng.* 244 (2022) 15.
- [51] Y. Hou, C. Liao, S. Qiu, Z. Xu, X. Mu, Z. Gui, L. Song, Y. Hu, W. Hu, Preparation of soybean root-like CNTs/bimetallic oxides hybrid to enhance fire safety and mechanical performance of thermoplastic polyurethane, *Chem. Eng. J.* 428 (2022) 132338.
- [52] W. Cai, T. Cai, L. He, F. Chu, X. Mu, L. Han, Y. Hu, B. Wang, W. Hu, Natural antioxidant functionalization for fabricating ambient-stable black phosphorus nanosheets toward enhancing

- flame retardancy and toxic gases suppression of polyurethane, *J. Hazard. Mater.* 387 (2020) 121971.
- [53] K. Zhou, Z. Gui, Y. Hu, S. Jiang, G. Tang, The influence of cobalt oxide–graphene hybrids on thermal degradation, fire hazards and mechanical properties of thermoplastic polyurethane composites, *Compos. Part A Appl. Sci.* 88 (2016) 10-18.
- [54] C. Nie, Y. Shi, S. Jiang, H. Wang, M. Liu, R. Huang, Y. Feng, L. Fu, F. Yang, Constructing Fireproof MXene-Based Cotton Fabric/Thermoplastic Polyurethane Hierarchical Composites via Encapsulation Strategy, *ACS Appl. Polym. Mater.* 5 (2023) 7229-7239.
- [55] C. Liu, W. Wu, Y. Shi, F. Yang, M. Liu, Z. Chen, B. Yu, Y. Feng, Creating MXene/reduced graphene oxide hybrid towards highly fire safe thermoplastic polyurethane nanocomposites, *Compos. B Eng.* 203 (2020) 108486.
- [56] J. Wang, Y. Hu, W. Cai, B. Yuan, Y. Zhang, W. Guo, W. Hu, L. Song, Atherton–Todd reaction assisted synthesis of functionalized multicomponent MoSe₂/CNTs nanoarchitecture towards the fire safety enhancement of polymer, *Compos. Part A Appl. Sci.* 112 (2018) 271-282.
- [57] C. Wang, W. Xu, L. Qi, H. Ding, W. Cai, G. Jiang, Y. Hu, W. Xing, B. Yu, Hierarchical NiO/Al₂O₃ nanostructure for highly effective smoke and toxic gases suppression of polymer Materials: Experimental and theoretical investigation, *Compos. Part A Appl. Sci.* 175 (2023) 107807.
- [58] X. Chen, Z. Wei, W. Wang, C. Jiao, Properties of flame-retardant TPU based on para-aramid fiber modified with iron diethyl phosphinate, *Polym. Adv. Technol.* 30 (2018) 170-178.
- [59] H. Ren, K. Qing, Y. Chen, Y. Lin, X. Duan, Smoke suppressant in flame retarded thermoplastic polyurethane composites: Synergistic effect and mechanism study, *Nano Res.* 14 (2021) 3926-3934.

- [60] H. Li, D. Meng, P. Qi, J. Sun, H. Li, X. Gu, S. Zhang, Fabrication of a hybrid from metal organic framework and sepiolite (ZIF-8@SEP) for reducing the fire hazards in thermoplastic polyurethane, *Appl. Clay Sci.* 216 (2022) 106376.
- [61] H. Wang, H. Qiao, J. Guo, J. Sun, H. Li, S. Zhang, X. Gu, Preparation of cobalt-based metal organic framework and its application as synergistic flame retardant in thermoplastic polyurethane (TPU), *Compos. B Eng.* 182 (2020) 2036-2045.
- [62] S. Wang, Q. Fang, C. Liu, J. Zhang, Y. Jiang, Y. Huang, M. Yang, Z. Tan, Y. He, B. Ji, C. Qi, Y. Chen, Biomass tannic acid intermediated surface functionalization of ammonium polyphosphate for enhancing fire safety and smoke suppression of thermoplastic polyurethane, *Eur. Polym. J.* 187 (2023) 111897.
- [63] S.-C. Huang, C. Deng, S.-X. Wang, W.-C. Wei, H. Chen, Y.-Z. Wang, Electrostatic action induced interfacial accumulation of layered double hydroxides towards highly efficient flame retardance and mechanical enhancement of thermoplastic polyurethane/ammonium polyphosphate, *Polym. Degrad. Stab.* 165 (2019) 126-136.
- [64] Y. Zhu, H. Wang, L. Fu, P. Xu, G. Rao, W. Xiao, L. Wang, Y. Shi, Interface engineering of multi-component core-shell flame retardant towards enhancing fire safety of thermoplastic polyurethane and mechanism investigation, *Appl. Mater. Today* 38 (2024) 1106-1114.
- [65] M. Yang, X. Li, W. Qin, Y. Wang, C. Gu, L. Feng, Z. Tian, H. Qiao, J. Chen, J. Chen, S. Yin, Multifunctional thermoplastic polyurethane composites with excellent flame retardancy, strain-sensitivity, water penetration resistance and breathability, *Eur. Polym. J.* 195 (2023) 112227.

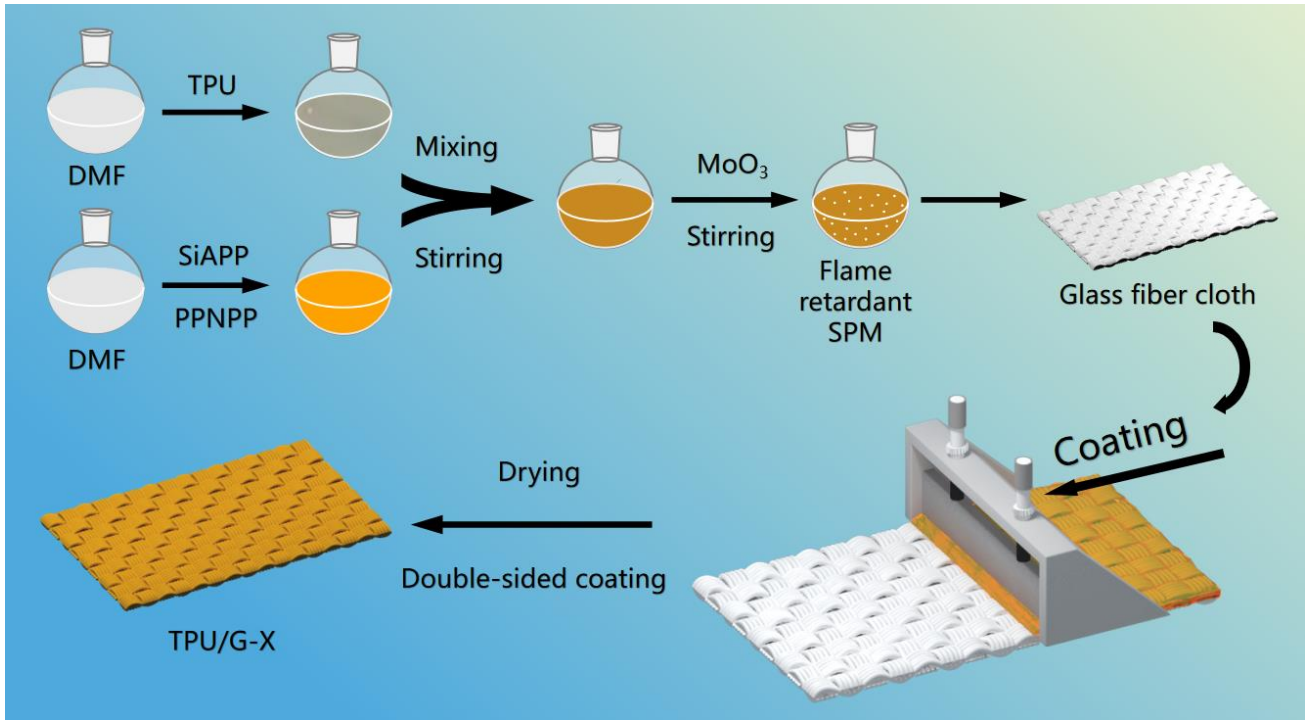


Fig. 1. Schematic diagram for preparation of TPU/G-X.

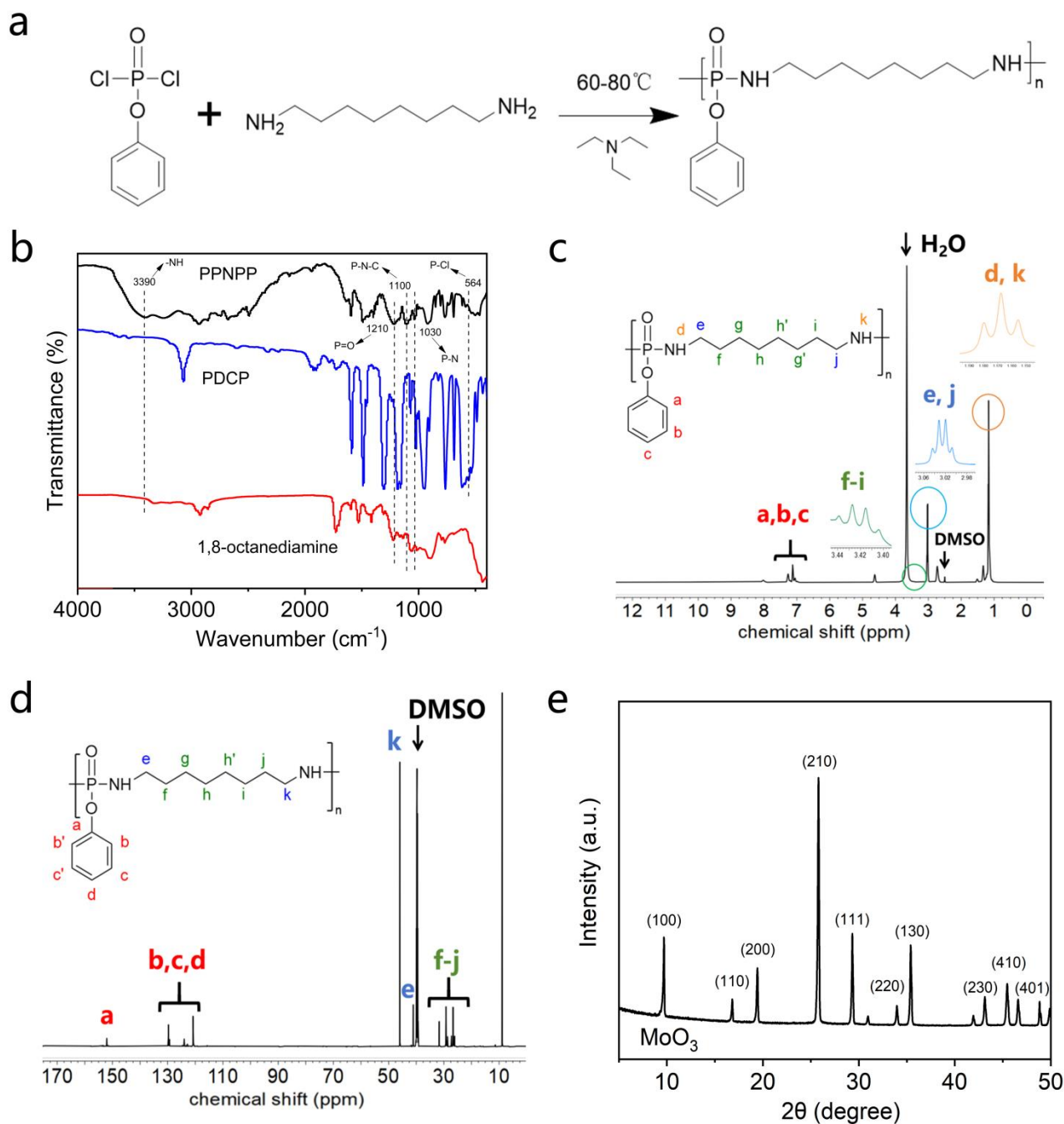


Fig. 2. (a) Preparation route of PPNPP; (b) FTIR spectra of PPNPP and PDCP and 1,8-octanediamine; (c) ^1H NMR and (d) ^{13}C NMR spectra of PPNPP; (e) XRD patterns of MoO_3 .

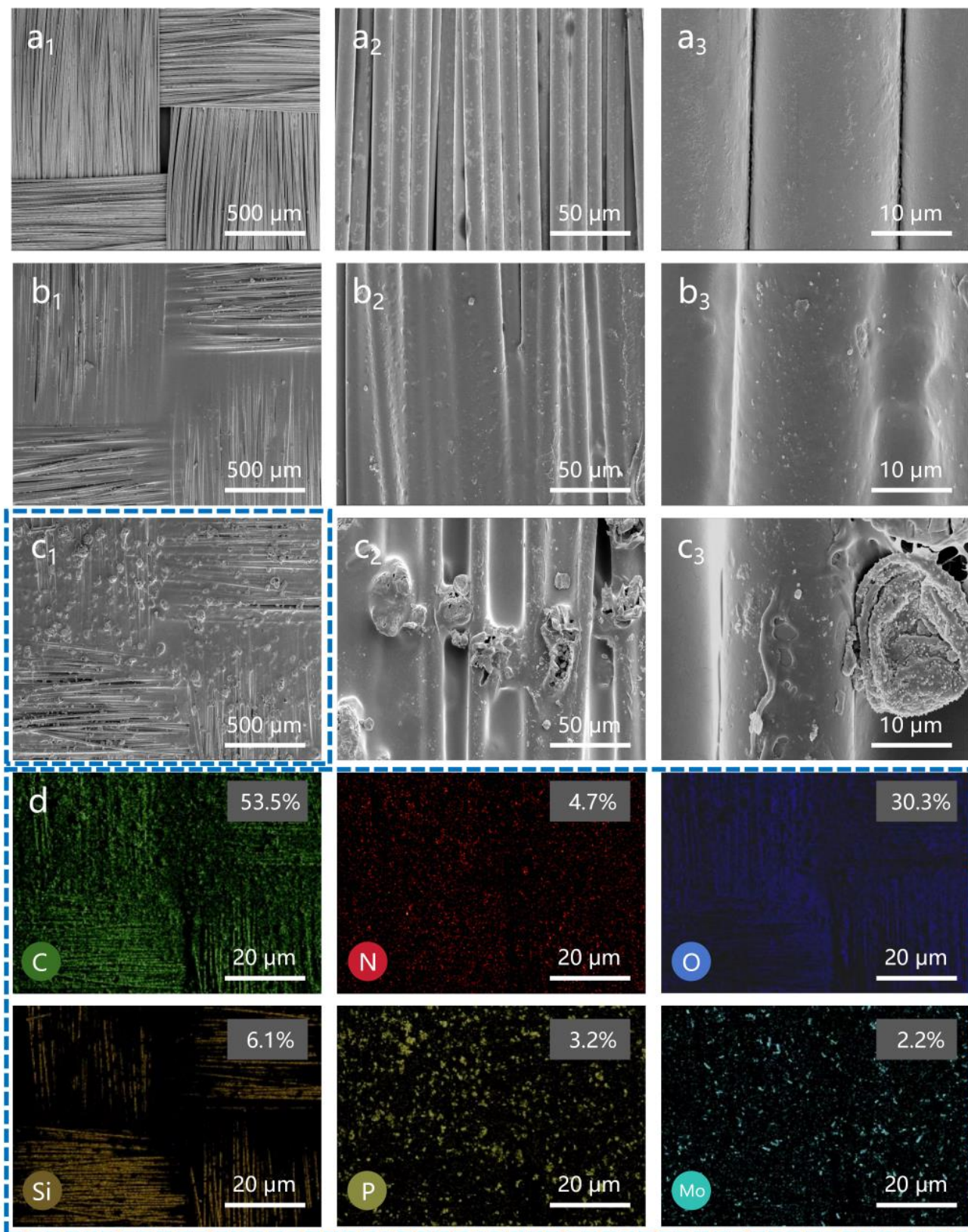


Fig. 3. SEM images of surface of (a) GFC, (b) TPU/G, and (c) TPU/G-SPM-1; (d) Element distribution images of TPU/G-SPM-1(c₁).

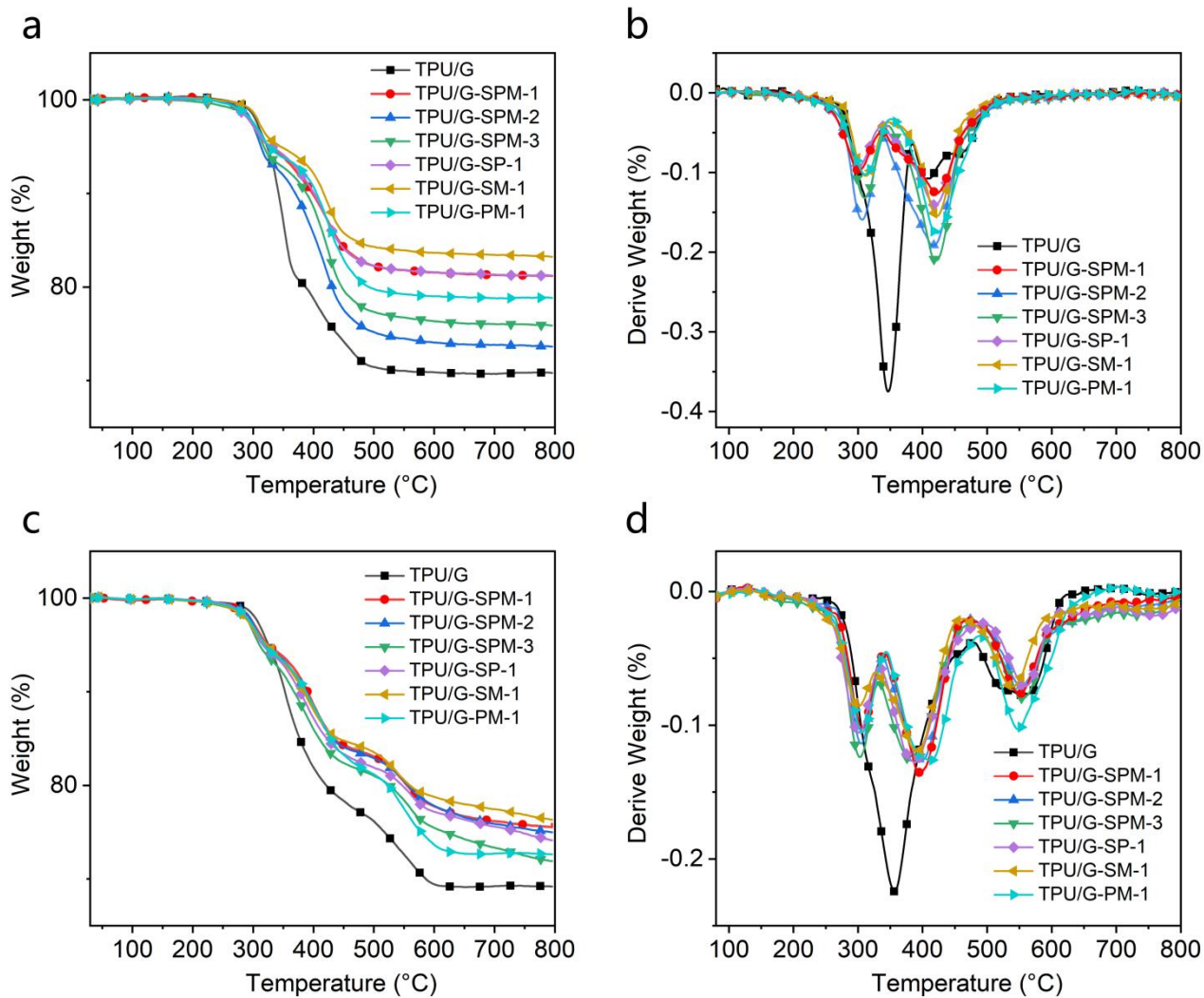
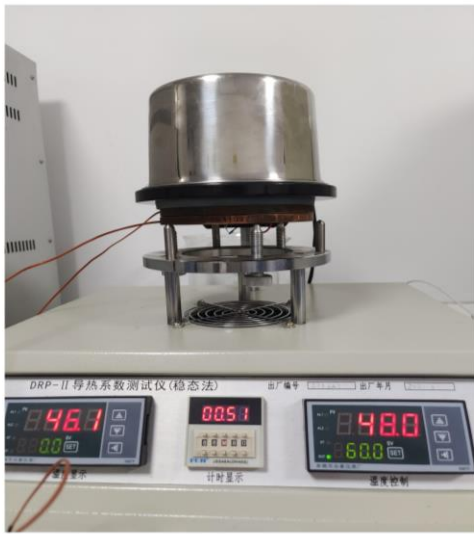


Fig. 4. TGA and DTG curves of the TPU/G composites in (a, b) Ar and (c, d) air atmospheres.

a



b

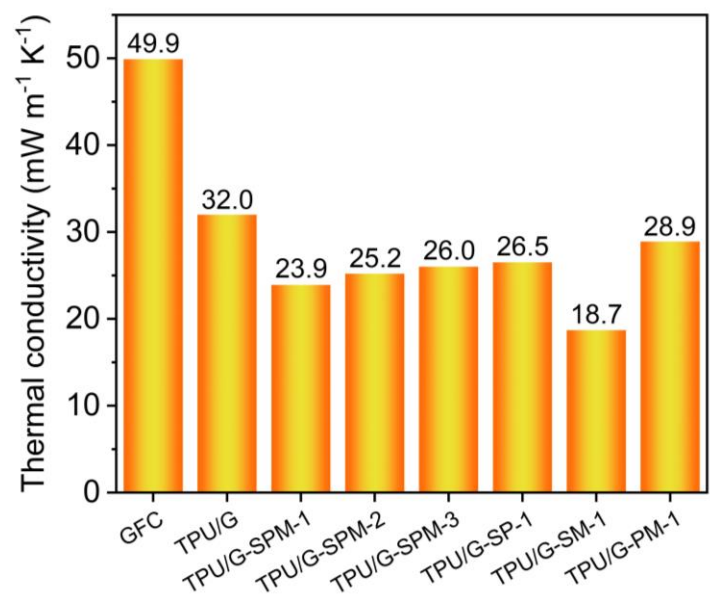


Fig. 5. (a) Photograph of thermal conductivity tester; (b) Thermal conductivity of GFC and the TPU/G composites.

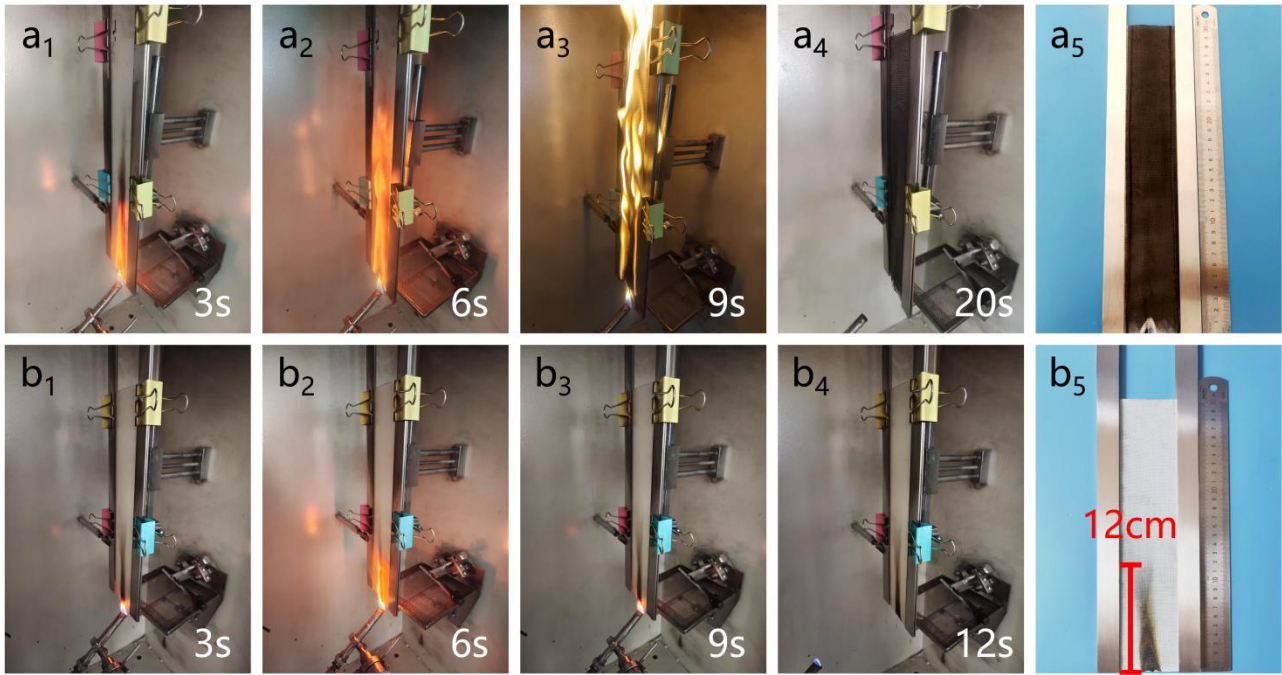


Fig. 6. Photographs of the vertical burning tests for (a) TPU/G and (b) TPU/G-SPM-1.

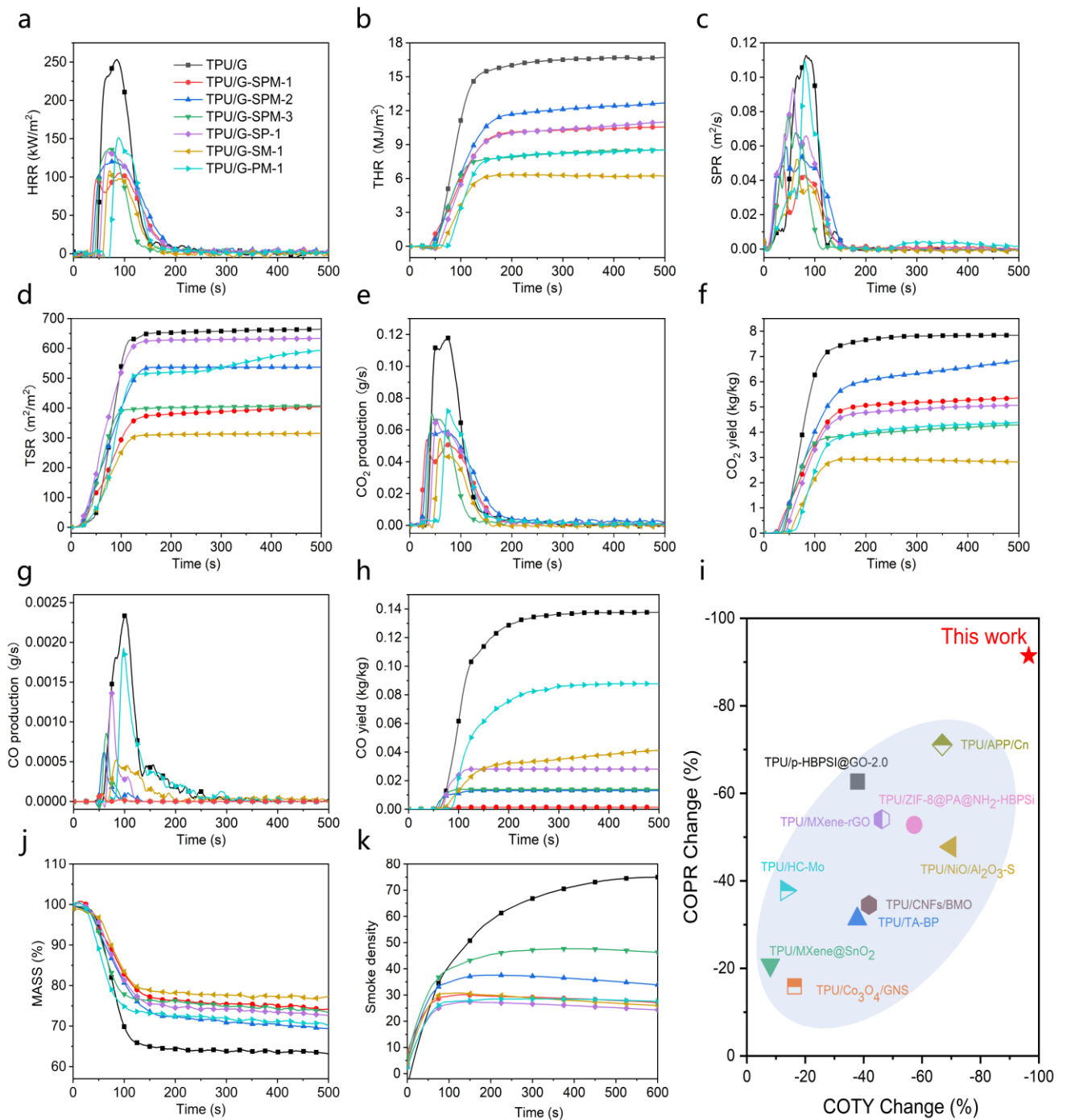


Fig. 7. CCT data: (a) HRR, (b) THR, (c) SPR, (d) TSR, (e) CO₂PR, (f) CO₂TY, (g) COPR, and (h) COTY; (i) Comparison of COPR and COTY reductions with previous works; (j) Weight loss and (k) Smoke density.

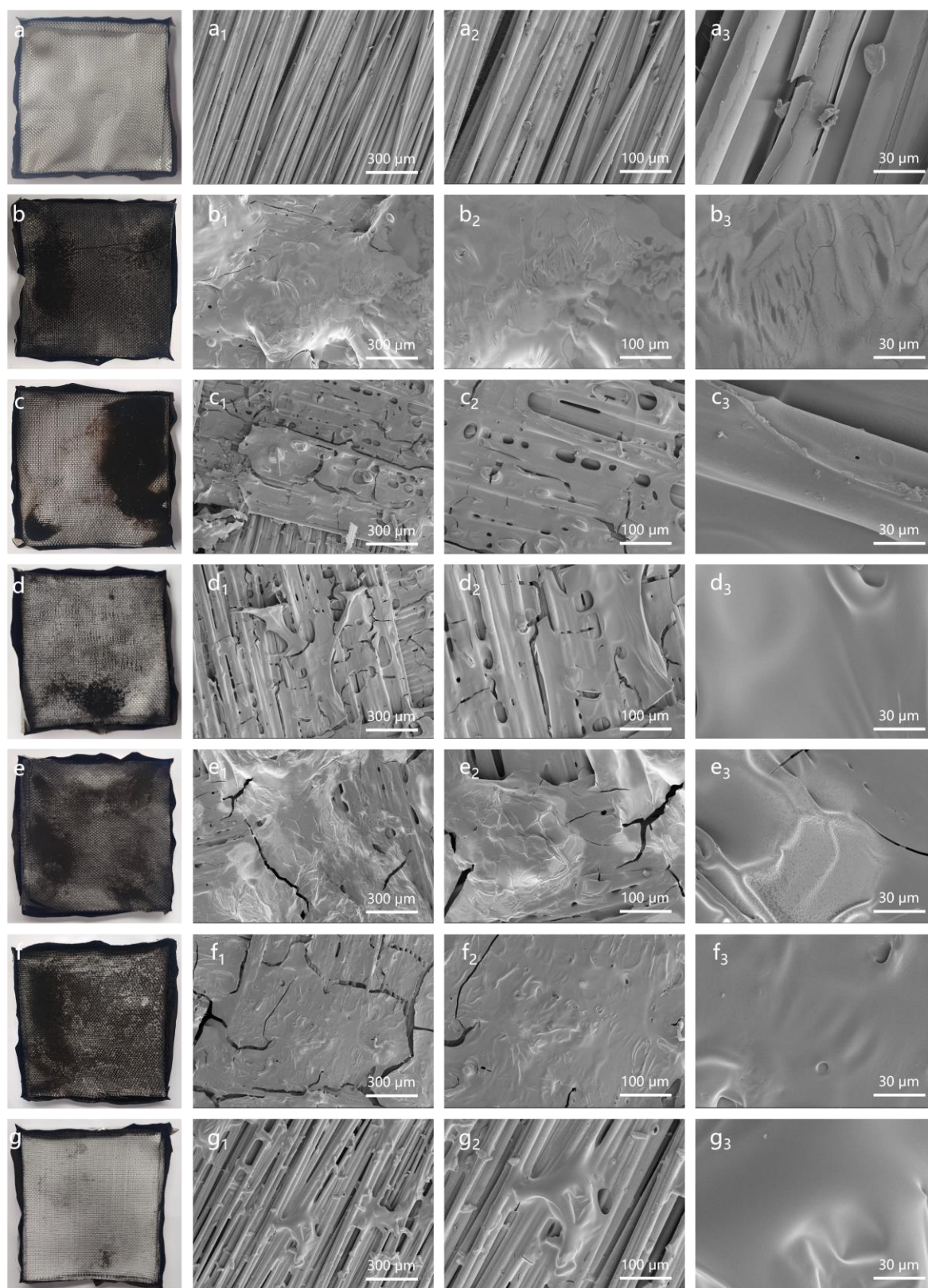


Fig. 8. Digital photos and SEM images of char residues of the TPU/G composites: (a) TPU/G, (b) TPU/G-SPM-1, (c) TPU/G-SPM-2, (d) TPU/G-SPM-3, (e) TPU/G-SP-1, (f) TPU/G-SM-1, and (g) TPU/G-PM-1.

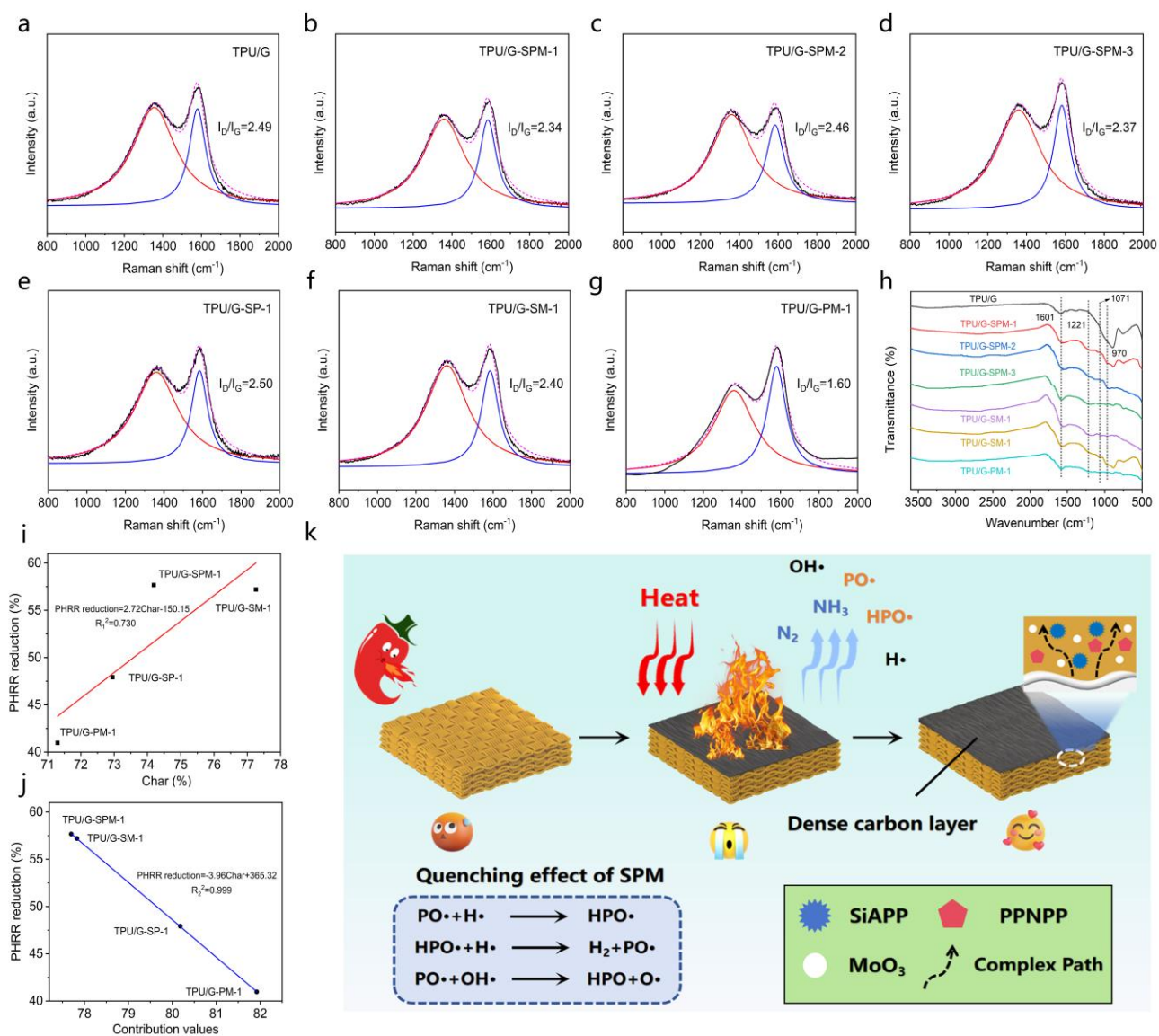


Fig. 9. Raman spectra of char residues of the TPU/G composites: (a) TPU/G, (b) TPU/G-SPM-1, (c) TPU/G-SPM-2, (d) TPU/G-SPM-3, (e) TPU/G-SP-1, (f) TPU/G-SM-1, (g) TPU/G-PM-1, (h) FTIR spectra of char residues of the TPU/G composites; (i) Correlation between the char residues from CCT and PHRR reduction; (j) Correlation between the contributions values and PHRR reduction; (k) Flame retardant mechanism of TPU/G-X.

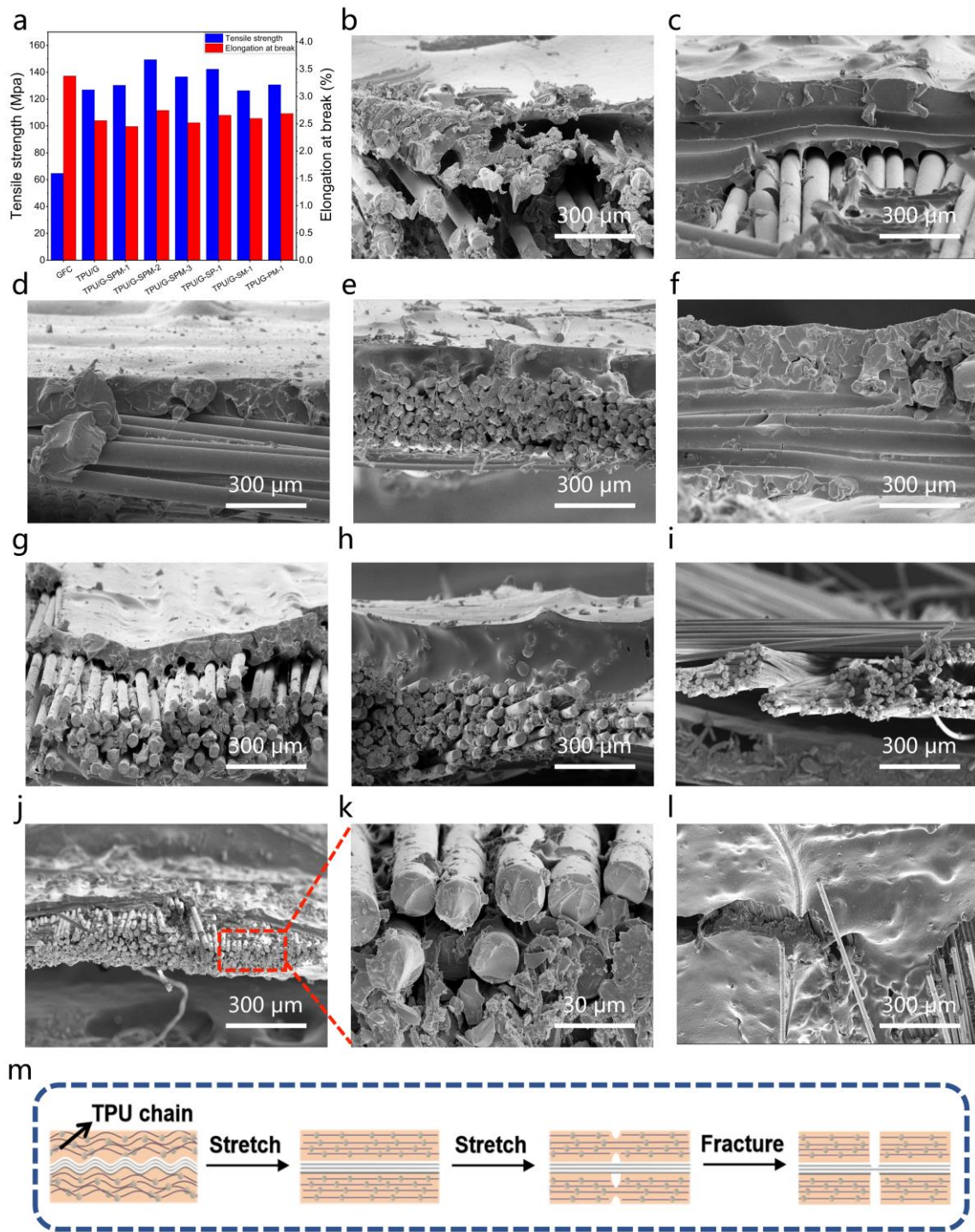


Fig. 10. (a) Tensile strength and elongation of the GFC and TPU/G composites; SEM images of fracture surface of (b) TPU/G, (c) TPU/G-SPM-1, (d) TPU/G-SPM-2, (e) TPU/G-SPM-3, (f) TPU/G-SP-1, (g) TPU/G-SM-1, (h) TPU/G-PM-1, (i) GFC (Flat view), (j, k) TPU/G-SPM-1 (Flat view), and (l) TPU/G-SPM-1 (Top view); (m) Schematic diagram for the mechanical failure process of the TPU/G composites.

Table 1. Formulation of the TPU/G composites.

Samples No.	TPU (g)	SiAPP (g)	PPNPP (g)	MoO ₃ (g)
TPU	100	-	-	-
TPU/SPM-1	80	10	5	5
TPU/SPM-2	84	8	4	4
TPU/SPM-3	88	6	3	3
TPU/SP-1	80	10	10	-
TPU/SM-1	80	15	-	5
TPU/PM-1	80	-	15	5

Table 2. TGA data of the TPU/G composites in air and Ar atmospheres.

Samples No.	$T_{5\%}$ (°C)		T_{max1} (°C)		T_{max2} (°C)		T_{max3} (°C)	Char residue at 800 °C (wt%)	
	Air	Ar	Air	Ar	Air	Ar	Air	Air	Ar
TPU/G	296.5	298.3	355.1	345.7	552.9	408.4		69.20	70.82
TPU/G-SPM-1	277.4	276.7	306.8	299.1	394.4	418.7	550.2	75.54	81.19
TPU/G-SPM-2	281.6	288.7	303.0	304.8	395.7	418.3	554.0	75.00	73.63
TPU/G-SPM-3	273.9	278.1	301.8	308.7	384.1	420.6	554.1	71.91	75.90
TPU/G-SP-1	275.3	273.3	301.8	300.8	387.1	418.7	560.0	74.13	81.23
TPU/G-SM-1	264.7	292.2	305.8	310.2	413.7	422.7	546.8	76.33	83.23
TPU/G-PM-1	277.1	278.6	299.9	308.9	390.4	419.9	539.2	72.64	78.84

Table 3. LOI values and damaged length for the TPU/G composites during vertical burning tests.

Samples No.	LOI (%)	Damaged length (mm)
TPU/G	23.3 ± 0.1	Burn out
TPU/G-SPM-1	28.1 ± 0.2	120 ± 2
TPU/G-SPM-2	27.4 ± 0.2	220 ± 2
TPU/G-SPM-3	27.0 ± 0.2	200 ± 2
TPU/G-SP-1	28.5 ± 0.2	120 ± 5
TPU/G-SM-1	30.8 ± 0.2	110 ± 2
TPU/G-PM-1	26.1 ± 0.2	Burn out

Table 4. Cone calorimetric results for the TPU/G composites.

Samples No.	TTI (s)	PHRR (kW m ⁻²)	THR (MJ m ⁻²)	PSPR (m ² s ⁻¹)	TSR (m ² m ⁻²)	PCOPR (g s ⁻¹)	PCO ₂ PR (g s ⁻¹)	COTY (kg kg ⁻¹)	CO ₂ TY (kg kg ⁻¹)	Char residue (wt%)
TPU/G	47	260	16.7	0.1222	664.5	0.00245	0.1208	0.1377	7.84	63.89
TPU/G-SPM-1	31	110	10.6	0.0658	404.2	0.00021	0.0560	0.0014	5.36	74.19
TPU/G-SPM-2	36	126	12.7	0.0865	537.2	0.00095	0.0629	0.0131	6.83	70.23
TPU/G-SPM-3	41	144	8.5	0.1110	407.4	0.00124	0.0720	0.0138	4.29	73.53
TPU/G-SP-1	50	135	11.0	0.1169	633.6	0.00163	0.0672	0.0280	5.07	72.95
TPU/G-SM-1	59	111	6.3	0.0749	315.0	0.00066	0.0572	0.0411	2.94	77.26
TPU/G-PM-1	41	154	8.5	0.1200	593.8	0.00205	0.0726	0.0878	4.39	71.3

Table 5. Smoke density results for the TPU/G composites.

Samples No.	TPU/G	TPU/G-SPM-1	TPU/G-SPM-2	TPU/G-SPM-3	TPU/G-SP-1	TPU/G-SM-1	TPU/G-PM-1
D,10	74.8	27.1	34.1	51.3	24.5	26	27.6
D,max	75.1	30.4	37.6	53.5	27.5	30.8	28.5

Table 6. The detailed information about contribution values.

Samples No.	Char	Y	Contribution values
TPU/G-SPM-1	74.19	3.51	77.70
TPU/G-SP-1	72.95	7.23	80.18
TPU/G-SM-1	77.26	0.57	77.83
TPU/G-PM-1	71.30	10.62	81.92

Constructing Efficient Flame-Retardant Thermoplastic Polyurethane Coatings with Smoke-Suppression to Enhance the Performance of Glass Fiber Cloth

Yongqian Shi ^{a,*}, Songqiong Jiang ^a, Jinke Wu ^a, Zhendong Chen ^a, Cancan Zhang ^b, Yun Zhang ^{c,*}, Pingan Song ^d, and Yan Zhang ^{e,*}

^a College of Environment and Safety Engineering, Fuzhou University, 2 Xueyuan Road, Fuzhou 350116, China.

^b Jiangsu Xinchanya New Material Co., Ltd, Liuhe Road North Side and Hexiang Road West Side, Baoying Economic Development Zone, Yangzhou 225800, China.

^c Yangzhou Tengfei Electric Cable and Appliance Materials Co., Ltd, 8 Qixin Road, Anyi Industrial Zone, Yangzhou 225800, China.

^d School of Agriculture and Environmental Science, University of Southern Queensland, Springfield, QLD 4300, Australia.

^e Laboratory of Polymer Materials and Engineering, NingboTech University, Ningbo 315100, China.

* Corresponding authors: Prof. Yongqian Shi, Mr Yun Zhang and Prof. Yan Zhang

E-mail addresses: shiyq1986@fzu.edu.cn (Y. Shi), Yangzhoutengfei@126.com (Y. Zhang),

hnpdszy@163.com (Y. Zhang)

Abstract

In order to meet the application requirements for cables in different environments, it is imperative to develop cable tapes with insulation, flame retardancy, and high strength. In this work, a new type of halogen-free flame-retardant and high-strength coating was prepared by synthesizing a new phosphoramidate flame retardant phenyl P-methyl-N-(8-(methylamino)octyl) phosphonamidate (PPNPP) compounded with silicon wrapped ammonium polyphosphate (SiAPP) and molybdenum trioxide (MoO_3) added into thermoplastic polyurethane (TPU), and TPU/glass fiber cloth (TPU/G) composites were obtained by double-sided coating on the surface of glass fiber cloth (GFC) and heat curing. Compared with those of the pure TPU-coated sample, the peak of heat release rate (PHRR) and total heat release (THR) results of the TPU/G composite containing 20 wt% SiAPP-PPNPP- MoO_3 (TPU/G-SPM-1) decreased by 57.7% and 36.8%, respectively. In addition, the TPU/G-SPM-1 sample showed an excellent toxic gases suppression effect, i.e. the peak of carbon monoxide production rate (PCOPR) and total carbon monoxide yield (COTY) decreased by 91.4% and 98.9%, respectively, compared with the pure sample. The coating also imparted excellent mechanical properties to the GFC, which overcame the original defects of glass fiber such as poor abrasion resistance and brittleness, and the tensile strength of TPU/G-SPM-1 was increased by 101% compared with that of pure GFC. This work presents a new method for the preparation of flame-retardant and mechanically strong TPU/G composites used as cable tapes.

Keywords: Thermoplastic polyurethane; Interface engineering; Flame-retardancy; High-strength; Smoke suppression; Glass fiber cloth.

1. Introduction

In recent years, the installation scale of urban cables has been increasing, and cables, as a kind of wire product that transmits signals, conveys electricity or facilitates electromagnetic transformation, are the fundamental assurance for the stable operation of society. However, due to overloading, short circuit, aging and other reasons, cable fire will inevitably occur [1]. Once a cable fire occurs, the consequences are often severe owing to the imperceptibility, rapid spread and the toxicity of the smoke of cable combustion [2, 3]. Therefore, preventing cable fires or effectively controlling their spread is an urgent problem that needs to be addressed.

Cable core tape plays a crucial role in cables. The flame-retardant modification of cable core tapes is an effective measure to prevent cable fires. The common cable core wrapping tape on the market is mainly made of organic materials, for example polyvinyl chloride (PVC), thermoplastic polyurethane (TPU), polypropylene (PP) and polytetrafluoroethylene (PTFE), as the main matrix, and adding flame retardant and adhesive which has the advantages of simple preparation process, low cost and convenient processing. However, due to the single insulation or flame retardant performance, its applicability is limited. In recent years, some organic-inorganic composite products have gradually appeared both domestically and internationally, such products not only inherit the advantages of organic materials, but also integrate the characteristics of inorganic materials, such as excellent mechanical strength, insulation, corrosion resistance and high temperature resistance.

Glass fiber cloth (GFC), an inorganic material known for its excellent insulation, heat resistance, and corrosion resistance, is highly suitable for cable core winding tape. However, its inherent poor abrasion resistance and brittleness limit its service life. To meet the demands of industrial applications, there is an urgent need to improve flame-retardant and mechanical properties of GFC. Various methods

have been developed for modifying fibers, including solution dipping and spraying [4, 5], layer-by-layer assembly (LBL) [6-8], plasma treatment [9, 10], chemical surface grafting [11, 12], and sol-gel reaction [13, 14], etc. Among these, applying appropriate flame retardant coatings is considered as a straightforward and effective approach. Flame retardant coatings can significantly inhibit or slow the spread of flames and the release of toxic smoke. When the flame-retardant materials are concentrated on the surface, they maximize flame retardant efficiency without compromising the mechanical properties of the fabric [15]. Consequently, developing a suitable coating is the current problem that needs to be solved.

TPU is an excellent candidate for coatings due to its remarkable wear resistance, hardness, elasticity and easy processing, etc. Recently, researchers have increasingly applied TPU coatings to improve the hydrophobicity, flame retardancy, mechanical properties, and corrosion resistance of various materials [16-19]. However, the inherent flammability of TPU and heavy smoke release upon burning, significantly limit its applications [11, 20]. Hence, it is critical for finding a suitable way to reduce the fire risk of TPU.

The introduction of flame retardants is the primary method for enhancing the flame retardant properties of TPU. Traditional halogen-containing flame retardants are being phased out due to the release of corrosive gases and fumes during thermal decomposition. In recent years, phosphorous-nitrogen flame retardants have emerged as a preferred alternative, having the advantages of halogen-free, easy to obtain, low toxicity and cost effectiveness. Among all the phosphorous-nitrogen flame retardants, phosphoramidate flame retardants have garnered significant attention from researchers due to their high flame retardancy, low smoke production, as well as the strong interfacial adhesive with the polymeric matrix [21-23]. For example, Xue et al. synthesized an oligomeric phosphoramidate (PPP),

using a one-pot method, and found that PPP was well distributed in polylactic acid (PLA). Besides, the addition of 3 wt% PPP endowed the PLA sample with UL-94 V-0 rating, and the limiting oxygen index (LOI) increased from 20.5% to 32.5% [24]. Liu et al. developed a novel phosphoramidate flame retardant, $\text{Ti}_3\text{C}_2\text{Tx-PPPA}$, followed by incorporating it into TPU. At a 1.0 wt% addition, the total heat release (THR) and total smoke release (TSR) of the TPU composites were reduced by 32.6% and 54.4%, respectively, demonstrating effective flame retardancy and smoke suppression [25]. However, phosphoramidate flame retardants often fail to meet the demands of practical applications when used alone. In order to utilize the advantages of phosphoramidate-based compounds, researchers have considered combining them with other flame retardants to improve flame retardant efficiency. Ammonium polyphosphate (APP) is a halogen-free flame retardant rich in phosphorus and nitrogen, with excellent flame retardant properties due to its ability of release inert gases during combustion and excellent catalytic carbonation properties [26]. As an effective flame retardant, APP can be used alone or in combination with other flame retardants. Some studies have reported that the compounding of APP and phosphoramidate flame retardants could achieve outstanding flame-retardant effects [27]. For instance, Wei et al. synthesized a novel phosphonamide (PSA) through solution polycondensation and incorporated it with APP into epoxy resin (EP). The results indicated that the addition of 12.5 wt% PSA could endow the EP sample with a LOI value of 32%. Besides, the peak of heat release rate (PHRR) and THR of the EP/PSA decreased by 71.9% and 67.8%, respectively [28]. Ye et al. reported a hyperbranched flame retardant (HBPPDA) through polymerization, which significantly improved the flame-retardant performance of APP when 6.25 wt% of HBPPDA was added. The LOI value of the PP composites reached 30.6% with the content of 25 wt% flame retardant. Additionally, the PHRR and THR of the PP composite were reduced by 76.2% and 41.5%, respectively, compared to those of pure

PP [29]. Although several studies have confirmed that the addition of APP-modified phosphoramidites to polymers can achieve significant synergistic flame retardant effects. Unfortunately, there are still few reports on the application of such flame retardants to TPU.

In cable fire accidents, more than 2/3 of the deaths were caused by toxic and harmful smoke, therefore it is very important to inhibit the emission of smoke during cable combustion. Various studies have shown that the incorporation of small amounts of nanofillers (<5 wt%) into polymers can provide excellent flame retardancy and smoke suppression [30-32], which can be attributed to the advantages of small size, large surface area and good thermal conductivity of nanofillers. In addition, there is a synergistic effect between nanofillers and phosphorous-nitrogen flame retardants, due to the fact that the nanofillers with high thermal oxidative resistance can effectively enhance the char quality of the polymer during combustion, leading to an improvement in flame retardancy [15]. Molybdenum trioxide (MoO_3), as a traditional smoke suppression agent, exhibits excellent flame retardant and smoke suppressant effects by promoting the generation of carbon layer on top of polymers during combustion, and has been widely used for smoke suppression of various polymers. For example, Xu et al. prepared different forms of MoO_3 by high-temperature calcination and hydrothermal method, respectively, and added them into polyurethane elastomer (PUE) to study the flame retardant and smoke suppression properties of PUE composites. When the amount of 1 wt% was added, the PHRR of the PUE composite was reduced by 61.0%. As for smoke suppression, at 5 wt% addition, the smoke density of the PUE composites was reduced by 41.3% compared to that of pure PUE sample [33]. Yao et al. prepared $\text{Ti}_3\text{C}_2\text{T}_x\text{-MoO}_3$ flame retardant through electrostatic interactions, and added it into TPU by melt blending, and found that the PHRR and peak of smoke production rate (PSPR) of the TPU composite decreased by 26.2% and 42.9% respectively when the addition amount was 2 wt% [34].

Zeng et al. added three flame retardants, i.e. APP, PEPA and MoO₃, into vinyl ester resins (VERs), and found that the LOI value of VERs composites reached 31% at the addition levels of 10% APP, 10% PEPA and 5% MoO₃, respectively, besides the UL-94 V-0 rating, which showed excellent synergistic flame retardant properties [35].

In this study, a novel phosphoramidate flame retardant phenyl P-methyl-N-(8-(methylamino)octyl) phosphonamidate (PPNPP) was firstly synthesized via the esterification, and subsequently the flame retardant silicon wrapped ammonium polyphosphate (SiAPP)-PPNPP-MoO₃ (SPM) was prepared by solution mixing and incorporated into liquid TPU to create a flame retardant and high-strength TPU coating. This coating was then applied onto the surface of the GFC by brushing and heat curing processes to form the TPU/glass fiber cloth (TPU/G) composites. The synthesized flame retardants were characterised, and the morphological information, the flame retardant and mechanical properties of the TPU/G composites were investigated. In addition, the enhancement mechanism of the coating for flame retardancy and mechanical properties were discussed. This study proposes a novel idea for the development of new flame-retardant cable wrapping tape, which further broadens the application scope of TPU composites.

2. Experimental section

2.1. Materials

TPU (65E85) was produced by Bangtai Chemical Industry Co., Ltd. (Baoding, China). SiAPP (203) was purchased from Shenfang Changfeng Chemical Co., Ltd. (Shenfang, China). 1,8-octanediamine (98%), triethylamine (TEA, AR), acetonitrile (AR), phenyl dichlorophosphate (PDCP, 98%), ammonium molybdate tetrahydrate ((NH₄)₆Mo₇O₂₄•4H₂O, 99.9%), nitric acid (HNO₃, 66.5%), and N, N-Dimethylformamide (DMF, AR) were obtained from Aladdin Reagent Co., Ltd. (Shanghai,

China). GFC ($125 \pm 2 \text{ g/m}^2$) was purchased from Hebei Fuhua new building Materials Co., Ltd. (Langfang, China).

2.2. Synthesis of PPNPP

Typically, 8.64 g 1,8-octanediamine, 80 mL acetonitrile, and 18.40 g TEA were poured into the 500 mL three-neck flask equipped with a mechanical stirrer, condenser, and thermometer. Subsequently, 13.86 g PDCP and 40 mL acetonitrile were slowly added into the above solution with mechanical stirring for 1.5 h under ice bath. After that, the mixture was stirred at 60 °C for 3 h, and then heated to 80 °C and kept stirring for 3 h. Finally, the organic phase was separated and washed three times with deionized water and petroleum ether, and dried for 24 h in a vacuum oven.

2.3. Preparation of MoO₃

20.00 g $(\text{NH}_4)_6\text{Mo}_7\text{O}_{24}\cdot 4\text{H}_2\text{O}$ was dissolved in 200 mL deionized water with mechanical stirring for 30 min under room temperature, and then 6.55 mL HNO_3 was added into the above solution. After that, the mixture was transferred into a reaction kettle at 180 °C for 24 h. Finally, the precipitate was separated by filtration, washed with ethanol and deionized water after being cooled down to room temperature, and the product was dried at 60 °C in a vacuum oven for 24 h.

2.4. Fabrication of TPU/G composites

To prepare the fire-retardant coating (TPU/SPM-1.0), 20.00 g TPU was mixed with 60 mL DMF at 80 °C until TPU completely dissolved to liquid. Subsequently, 2.50 g SiAPP and 1.25 g PPNPP were dissolved in 20 mL DMF and thereby added to the TPU solution with mechanical stirring for 10 min. Then, 1.25 g MoO₃ was added into the mixture with ultrasonic mixing for 20 min. Finally, the coating was applied to the surface of GFC by double-sided coating and heat curing processes to prepare TPU/G-SPM-1.0. For the designation of the TPU/G composites, GFC coated with pure TPU is defined

as TPU/G and the composites with added flame retardants are defined as TPU/G-X, the X stands for different ratios of flame retardants. The schematic diagram for preparation of TPU/G-X is shown in Fig. 1, and Table 1 summarizes the formulations of the TPU/G composites.

2.5. Characterization

Fourier transform infrared spectra (FTIR) of the samples were estimated on a Nicolet IS50 spectrometer (Nicolet Instrument Company, USA) with a wavenumber range of 4000 to 400 cm^{-1} . ^1H NMR and ^{13}C NMR were measured on a fully digitalized nuclear magnetic resonance spectrometer (NMR, AVANCE NEO 600, Switzerland) at 600 MHz using DMSO- d_6 as a solvent. X-ray diffraction (XRD) results of samples were obtained using a DY1602/Empyrean x-ray diffractometer ($\lambda = 1.54178$ Å). Scanning electron microscope (SEM, Verios G4, USA) was used to observe the surface morphologies of the GFC and TPU/G composites. The surface elemental distribution of TPU/G-X microstructure and char residues were observed by energy dispersive spectrometer (EDS). Thermal conductivity data were obtained by a thermal conductivity tester (DRP-II, Xiangtan Xiangyi Instrument Co., Ltd.). The combustion behavior of the TPU/G composites was estimated by TTech-GBT16172-2 cone calorimeter (CCT) (TESTech, Suzhou, China) according to the ISO 5660 standard under a heat flux of 35 kW/m^2 . Each sample with a size of 100 mm \times 100 mm \times 0.2 mm and stacked in 10 layers (2 mm). Thermogravimetric analysis (TGA) of the TPU/G composites was performed by thermal analyzer (TA Q5000, USA) from room temperature to 800 $^\circ\text{C}$ with 20 $^\circ\text{C}/\text{min}$ heating rate under Ar and air conditions. Smoke density data of the samples were obtained by plastic smoke density tester (JSC-2), according to GB/T 8323-2008. Each sample with dimensions of 75 mm \times 75 mm \times 0.2 mm and exposed horizontally to an external heat flux of 25 kW/m^2 with the application of no pilot flame. Mechanical properties of the GFC and TPU/G samples were tested by an electronic universal

testing machine (JPL-1000N) with a tensile rate of 20 mm/min according to GB/T12914-2018. LOI values of the samples were tested by the LOI analyzer (HC-2, Nanjing, China) according to GB/T5454-1997 with specimen dimensions of 150 mm × 58 mm × 0.2 mm. The vertical burning test was carried out by vertical combustion tester (CZF-II, Jiangning Analytical Instruments Co., Ltd.) according to GB/T5455-2014, and each sample with dimensions of 300 mm × 89 mm × 0.2 mm. Raman spectroscopy was provided by a Renishaw Invia Raman Microscope (Invia Reflex, Britain) with a 532 nm argon ion laser.

3. Results and discussion

3.1. Characterization of flame retardants

Fig. 2a shows the preparation route of PPNPP, which was synthesized via the esterification of 1,8-octanediamine and PDCP. Fig. 2b shows the FTIR spectra of PPNPP and its raw materials. The absorption peaks at 3200-3500 cm^{-1} are ascribed to the stretching vibration of primary amine in the 1,8-octanediamine [25]. For PDCP, the peaks at 564 cm^{-1} and 1210 cm^{-1} typically are associated with the stretching vibrations of the P-Cl and P=O bonds, respectively [36]. In contrast to the FTIR spectra of raw materials, the disappearance of P-Cl and primary amine bonds, and the formation of a new peak of secondary amine at 3390 cm^{-1} indicate the complete reaction between 1,8-octanediamine and PDCP [37]. Besides, the new peaks generated at 1100 and 1030 cm^{-1} are ascribed to P-N-C and P-N, respectively [29], which further confirms the successful synthesis of PPNPP.

To further verify the structure of PPNPP, the products were characterized by ^1H and ^{13}C NMR tests. Fig. 2c is the ^1H NMR spectrum of PPNPP, showing that the resonance signals in the range of 7.05-7.22 ppm are attributed to the aromatic protons on the benzene ring (labeled a, b, c), and the signal around 1.17 ppm corresponds to the imine structure on the main chain of PPNPP (labeled d, k) [28].

In addition, the weak signals in the range of 2.98-3.06 ppm and 3.40-3.44 ppm are attributed to the methylene structure on the carbon chain (labeled e-j) [22]. Fig. 2d presents the ^{13}C NMR spectrum. The signal at 150.5 ppm supports the aromatic carbon structure at the junction of the benzene ring and the main chain of PPNPP (labeled a), while the signals in the range of 120.0-130.0 ppm are ascribed to the remaining aromatic structures on the benzene ring (labeled b, c, d). In addition, the signals at 41.0 ppm, 46.2 ppm, and the range of 25.0-32.5 ppm are attributed to the methylene structures on the main carbon chain (labeled e-k). The results above confirm the successful synthesis of PPNPP.

The XRD patterns of MoO_3 nanorods are plotted in Fig. 2e. It can be seen from the XRD patterns that the reflection peaks located at $2\theta = 9.7^\circ$, 19.4° , 25.8° , and 45.5° correspond to the (100), (200), (210), and (410) crystal planes of MoO_3 nanorods, which are consistent with the standard card (JCPDS: 83-1176) [33], proving the successful synthesis of MoO_3 nanorods.

3.2. Surface morphology and element composition

The micromorphology of flame-retardant coating on the GFC was studied by SEM. As shown in Fig. 3a₁-a₃, the pristine GFC has a smooth and flat surface, and a complete fiber structure can be observed. After the introduction of the TPU coating, the surface of the GFC becomes more consistent and rougher (Fig. 3b₁-b₃). It is noted that a thin film is attached onto the surface of the GFC. In comparison to TPU/G, a large number of micro/nano-scale hierarchical structures are obtained on the surface of TPU/G-SPM-1 (Fig. 3c₁-c₃), which can be attributed to the deposition of SPM flame retardant. In addition, the element distribution mapping images for the surface of TPU/G-SPM-1 are shown in Fig. 3d, revealing the homogeneous distributions of C, N, O, Si, P and Mo elements in the flame retardant coating. Meanwhile, these distributions of different elements exhibit a clear fiber shape similar to the GFC, further indicating that the TPU/SPM flame retardant coating have been

successfully applied to the surface of the GFC.

3.3. Thermal stability

The thermal degradation behavior of the TPU/G composites with different coatings was studied through TGA technique. The degradation curves of the TPU/G composites under Ar (a) and air (b) atmosphere are plotted in Fig. 4 (since the test temperature did not reach the degradation temperature of the GFC, this discussion focuses solely on the thermal degradation performance of the TPU flame-retardant coating), and the related thermal data are shown in Table 2. As displayed in Fig. 4a, the thermal degradation of all samples under the Ar atmosphere presents two typical weight loss stages. The first stage involves the degradation of the hard segments of the TPU main chain to diols and diisocyanates, while the second stage is attributed to the further breakdown of isocyanates and polyols in the soft segments of TPU chains [38]. However, the thermal oxidative degradation processes of TPU/G-X under the air atmosphere occur in three different stages (Fig. 4c). In addition to the two thermal degradation stages mentioned above, the final stage can be lied to the further thermal oxidative degradation of the char residues produced in the first stage [39]. As observed from Table 2, the initial decomposition temperature ($T_{5\%}$) of TPU/G-X decreases significantly, compared to that of TPU/G. This may be due to SPM flame retardant can catalyze the decomposition of polyurethane bonds into isocyanates, alcohols, and carbon dioxide at lower temperatures, which can delay heat transfer and decrease the fire hazard of TPU/G-X [40, 41]. After the thermal degradation stages, the char yields of TPU/G under the air and Ar atmospheres are 69.20% and 70.82%, respectively. Notably, the char residues of TPU/G-X at 800 °C are significantly higher than TPU/G, indicating that SPM flame retardant effectively enhances the thermal stability of the TPU coating. Furthermore, by comparing the char yield of different samples, it is noted that under the same loading conditions, TPU/G-SM-1

exhibits the highest char yield at 800 °C in both air and Ar atmospheres, indicating that SiAPP actually performs better char formation ability than PPNPP. This phenomenon can be attributed to SiAPP acting as a suitable acid source and demonstrating superior flame retardant performance in the condensed phase.

Additionally, from the differential thermal gravity (DTG) curves in Fig. 4b, d, it can be seen that the main thermal degradation peaks of TPU/G-X are significantly lower than TPU/G, and the corresponding maximum decomposition rate temperature (T_{\max}) is also lower than the control one. This is primarily related to the increase in char yield, as SPM flame retardant effectively improves the stability of the char layer formed during combustion, physically hindering heat transfer and enhancing the fire resistance of the composites.

3.4. Thermal conductivity

The thermal conductivity serves as an important index to evaluate the heat transfer performance of materials, which can be tested by thermal conductivity tester (Fig. 5a). As shown in Fig. 5b, GFC exhibits high thermal conductivity ($49.9 \text{ mW m}^{-1} \text{ K}^{-1}$), while TPU/G has a thermal conductivity of $32.0 \text{ mW m}^{-1} \text{ K}^{-1}$. In contrast, the thermal conductivity of TPU/G-X samples is reduced to varying degrees. The comparison of different samples reveals that the thermal conductivity of the TPU/G-SPM composites tends to increase as the amount of SPM flame retardant decreases, indicating that the incorporation of SPM flame retardant effectively enhances the thermal insulation properties of the coating, potentially reducing the rate of heat transfer during combustion, and thereby improving fire safety. It is evident that TPU/G-SM-1 has the lowest thermal conductivity ($16.7 \text{ mW m}^{-1} \text{ K}^{-1}$). This phenomenon can be attributed to the reason that introduction of SiAPP alters the arrangement of TPU molecules, resulting in a denser structure that hinders the establishment of an efficient heat channel

[42]. In addition, this leads to the thermal conductivity of TPU/G-PM-1 higher than that of TPU/G-SM-1.

3.5. Flame retardant performance

To evaluate the flame retardant performance of the materials, the LOI and vertical burning test are usually employed to assess flammability of polymeric materials. The relevant flammability data are presented in Table 3. The LOI value of the pristine TPU/G sample is 23.3%, indicating a high fire risk. In contrast, the LOI value of TPU/G-SPM-3 reaches 27%. This means that the TPU coating transforms from a flammable material into a highly flame-retardant one at a low load of SPM. Meanwhile, the LOI value of the TPU composites increases with increasing content of SPM, which indicate a significant improvement in the flame retardant properties of the coating. Moreover, as shown in the digital photographs in Fig. 6, TPU/G is ignited rapidly after encountering fire, which eventually burns all the TPU coating on the sample within 20 s. In contrast, TPU/G-SPM-1 passes the vertical burning test, and self-extinguishes immediately after 6 s of ignition with the char residues morphology remaining intact with a small damaged length (120 ± 2 mm). In summary, these results indicate that the TPU coating added with SPM improves flame retardancy of the TPU/G composites.

The CCT is an instrument for evaluating the combustion behavior of materials, which collects the combustion parameters of composites by simulating the fire scenario to comprehensively evaluate the flame retardancy and smoke suppression properties of materials [43]. As shown in Fig. 7 and Table 4, the time to ignition (TTI) of TPU/G is 47s. In contrast, the TTI of composites incorporating only two types of flame retardants exhibits varying trends (TPU/G/SP-1, TPU/G-SM-1 increasing and TPU/G-PM-1 decreasing) compared to the control one. After comparing different samples, it can be found that the TTI of the composites gradually increases with the increase of SiAPP flame retardant. This

phenomenon can be attributed to the higher thermal stability of SiAPP than PPNPP, which is well consistent with the trends observed in thermal conductivity tests. Furthermore, the TTI values of the TPU composites containing SPM flame retardant are all less than 47 s, and gradually decrease with the increase of SPM addition, indicating that SPM flame retardant can catalyze the early decomposition of the TPU coating.

The PHRR is an important parameter for assessing the fire hazard of composites after combustion [44]. The HRR and THR curves are shown in Fig. 7a, b. Due to the high flammability of TPU, TPU/G exhibits high PHRR of 260 kW/m² and THR of 16.7 MJ/m². In contrast, the incorporation of the SPM flame retardant significantly reduces the PHRR and THR of the composites. Particularly, the PHRR and THR of TPU/G-SPM-1 are 110 kW/m² and 10.6 MJ/m², respectively, which are 57.7% and 36.8% lower than those of TPU/G. Notably, TPU/G-SM-1 shows the lowest THR of 6.3 MJ/m², which can be attributed to the high flame retardant efficiency of SiAPP, significantly shortening the combustion time of the composites. Combined with the CCT data, it is concluded that SPM significantly reduces the fire hazard of the TPU coating, which is in good agreement with the results of the TGA and LOI tests.

The impact of cable combustion is often severe due to its imperceptible, rapidly spreading and the emission of large quantities of toxic and harmful smoke. Therefore, it is extremely important to improve the smoke suppression performance of cable materials. The SPR and TSR data of different samples are presented in Fig. 7c, d. TPU/G shows high PSPR (0.1222 m²/s) and TSR (664.5 m²/m²). In comparison, the PSPR and TSR values of TPU/G-SPM-1 are 0.0658 m²/s and 404.2 m²/m², respectively, which are 46.2% and 39.2% lower than those of TPU/G. However, the PSPR (0.1169 m²/s) and TSR (633.6 m²/m²) of TPU/G-SP-1 respectively decrease by only 4.3% and 4.7%, compared to those of the control one, indicating that the incorporation of a small amount of MoO₃ can effectively

enhance the smoke suppression performance of the TPU coating. This can be due to the explanation that MoO_3 , as an inorganic nanofiller, has been shown to synergize with phosphorous-nitrogen flame retardants in polymers (such as VERs and rigid polyurethane foam) to promote the formation of carbon layer, which enables the composites to exhibit excellent smoke suppression [35, 45-47].

The toxic and harmful gases suppression curves of the TPU composites are shown in Fig. 7e-h. The peak of the carbon dioxide production rate (PCO_2PR) and total carbon dioxide yield (CO_2TY) of TPU/G-X are significantly lower than those of TPU/G. Notably, TPU/G-SPM-1 demonstrates the lowest PCO_2PR (0.0560 g/s), which is 53.6% lower than that of the control sample. However, TPU/G-SM-1 exhibits a lower CO_2TY (2.94 kg/kg). Additionally, carbon monoxide (CO) is one of the deadliest gases in a fire hazard. When CO level in the air reaches 1%, it can cause loss of consciousness [48]. The pristine TPU/G shows high peak of carbon monoxide production rate (PCOPR) (0.00245 g/s) and total carbon monoxide yield (COTY) (0.1377 kg/kg). In contrast, TPU/G-X with varying proportions of SPM (12 wt%, 16 wt%, and 20 wt%) show a reduction of over 90% in COTY compared to TPU/G. Specially, TPU/G-SPM-1 shows significant reductions in PCOPR (0.00021 g/s) and COTY (0.0014 kg/kg) by 91.43% and 99.0%, respectively, compared with the control one. This excellent toxic and harmful smoke suppression performance can be attributed to the synergistic effect of SPM in both the condensed and gas phases. Other studies on CO suppression of TPU composites are listed in Fig. 7i, further demonstrating the superiority of this work in terms of toxic gas inhibition performance [11, 20, 49-57].

The mass loss after combustion is an important factor affecting the flame retardant and smoke suppression performance of the composites, as shown in Fig. 7j, the residual mass of TPU/G only 63.89%, and with the addition of SPM flame retardant, the mass loss of TPU/G-X showed a significant

reduction trend. Among them, TPU/G/SM-1 exhibits the highest residual mass (77.26%), which can be attributed to the excellent performance of SiAPP in the condensed phase, which is consistent with the previous analysis. The addition of flame retardant can well catalyse the TPU matrix to generate a dense and stable carbon layer in combustion, which can well reduce the heat conduction and smoke emission in combustion, and reduce the fire hazard of composites.

3.6. Smoke density test

Smoke density testing simulates the smoke density and concentration released by burning materials under fire conditions, which is crucial for ensuring people's health and safety [58, 59]. The smoke density curves of the TPU/G composites are portrayed in Fig. 7k and Table 5. The $D_{s,10}$ and $D_{s,max}$ are defined as smoke density at 10 min and the maximum smoke density, respectively. For TPU/G, $D_{s,10}$ and $D_{s,max}$ are 74.8 and 75.1, indicating that the pure TPU coating emits large amounts of smoke during combustion. In contrast, with the increase of SPM flame retardant addition, the $D_{s,max}$ values of TPU/G-SPM-3, TPU/G-SPM-2 and TPU/G-SPM-1 are 53.5, 37.6 and 30.4, respectively, which are 28.8%, 49.9% and 59.5% less than that of the control sample, demonstrating that SPM flame retardant effectively reduces the concentration of smoke. Notably, the $D_{s,10}$ and $D_{s,max}$ of TPU/G-X show a similar decreasing pattern when the flame retardants are added in equal amounts, suggesting that either SiAPP or PPNPP in combination with MoO_3 can effectively reduce the smoke density of the TPU coatings during combustion. This phenomenon may be attributed to the quenching effects generated during combustion by the phosphorus-nitrogen flame retardant and MoO_3 , as well as the formation of a dense char layer.

3.7. Flame retardant mechanism

To further investigate the flame-retardant mechanism of TPU/G-X, the microstructure of the char

residues was analyzed by SEM. Digital photos and SEM images of the char residues of the TPU/G composites are presented in Fig. 8. It is observed that, for TPU/G, the TPU coating applied to the GFC burns out, and the samples show a clear fiber structure. In contrast, the surfaces of TPU/G-X displayed distinct char structures. Notably, for TPU/G-X containing SiAPP (Fig. 8b-f), the expanded char layer tightly covers the surface of the GFC, which is critical in the heat insulation and oxygen barrier during combustion. This phenomenon can be attributed to the formation of polyphosphoric acids in the decomposition process of APP, which can catalyze the decomposition of the TPU matrix and form an expanded carbon layer. Notably, the char residues of TPU/G-SPM-1 exhibit a highly continuous and dense structure. This intense and solid char layer effectively reduces smoke emissions during combustion, which explains the excellent smoke suppression performance of TPU/G-SPM-1.

The degree of graphitization of the TPU composites is typically analyzed by Raman spectroscopy (Fig. 9a-g). The smaller the I_D/I_G ratio, the greater the degree of graphitization is [60]. TPU/G has the I_D/I_G ratio of 2.49. In contrast, TPU/G-X with the addition of SPM (Fig. 9b-d) have the decreased I_D/I_G ratios (2.34, 2.46 and 2.37, respectively for TPU/G-SPM-1, TPU/G-SPM-2 and TPU/G-SPM-3), indicating that the graphitization degree of the TPU composites is improved by the addition of SPM. Furthermore, comparing the I_D/I_G ratios between TPU/G-SPM-1 and TPU/G-SP-1 indicates that the addition of 5 wt% MoO_3 significantly enhances the graphitization degree of the composites, which is consistent with the CCT and TGA results. It is obvious that TPU/G-PM-1 exhibits the lowest I_D/I_G ratio (1.6) among all TPU samples. However, the flame retardant and smoke suppression performances reported in the CCT data is not ideal. This can be attributed to the char residues generated by TPU/G-PM-1, which shows high density of char residues (as shown in Fig. 8g) but lacks the expansion capability. As a result, it is unable to form a continuous and dense char layer during combustion,

leading to relatively poor smoke suppression performance.

FTIR is adopted to study the chemical composition and molecular structure of char residues of the TPU coating. As plotted in Fig. 9h, the characteristic peak at 1601 cm^{-1} for all the samples corresponds to the unsaturated C=C bonds formed by aromatic compounds after TPU combustion [61]. It is observed that after adding SPM retardant into the TPU coating, the new characteristic peaks at 1221 and 970 cm^{-1} are assigned to the stretching vibrations of P=O and P-O-C, respectively [62, 63]. In addition, the characteristic peak at 1071 cm^{-1} corresponds to the Si-O-Si stretching vibration [64]. Combined with the SEM images of char residue, it can be analyzed that the TPU samples containing silica gel decompose at high temperatures to generate phosphoric acid-containing components, which can accelerate the decomposition of the main chain of the TPU and enhance the char formation properties of the TPU composites.

In order to reveal the flame retardant mechanism of the flame retardant TPU coatings, the relationship between the reduction in PHRR and char residue was investigated under the same amount of flame retardant added, as shown in Fig. 9i. It is noted that the correlation coefficient (R_1^2) between values of char residues and PHRR reduction of TPU/G-X is 0.730, indicating the poor linear correlation. In order to further investigate the mechanism of PHRR reduction, the relationship between the PHRR reduction and the contribution value (defined as the sum of the absolute value of char residue and the gas phase index Y) is presented in Fig. 9j [49]. The introduction of the gas phase index shows a clear linear relationship between the PHRR reduction and contribution values ($R_2^2 = 0.999$), indicating the existence of gas phase flame retardant mechanism for TPU/G-X. As shown in Table 6, it can be observed that the gas phase index of TPU/G-PM-1 is 10.62, which is 3 times as that of TPU/G-SPM-1. Notably, this result is very consistent with the proportion of PPNPP flame retardant added. In

addition, TPU/G-SM-1 has a relatively low gas phase index of 0.57. From comparing different samples, it can be seen that the gas phase index of the TPU composites increases linearly and significantly with the increase of PPNPP addition. It can be speculated that PPNPP flame retardant plays a very important role in the gas phase flame mechanism, while the flame retardant mechanism of SiAPP is mainly reflected in the condensed phase.

Based on the results and discussions presented above, the possible mechanism for enhancing the flame retardant and smoke suppression performance of TPU/G-X is proposed (Fig. 9k). After burning, SiAPP and PPNPP rapidly dehydrate and decompose into components, such as phosphoric acid, metaphosphoric acid and polyphosphoric acid, which can accelerate the char formation of the TPU matrix and promote cross-linking of carbonization [65]. Meanwhile, SiO₂ and MoO₃ form a dense oxide film on the surface, preventing O₂ from entering the interior and thus inhibiting the combustion of TPU coating. On the other hand, SiAPP and PPNPP release non-flammable products, such as H₂O and NH₃ upon combustion, which dilute the concentration of flammable gases. Moreover, SiAPP and PPNPP can degrade to generate free radicals i.e. PO• and HPO• at high temperatures, which can capture active radicals such as H• and OH•, thereby reducing the combustion rate and suppressing the emission of toxic and harmful smoke. Overall, the synergistic effect of SPM in the condensed phase and the gas phase can effectively enhance the flame retardant and smoke suppression abilities of flame retardant TPU coatings.

3.8. Mechanical property

To meet the demands of daily applications, it is crucial to overcome the inherent defects of GFC, such as poor abrasion resistance and brittleness. The mechanical properties of the GFC and TPU/G composites are presented in Fig. 10a. The tensile strength and elongation at break of GFC are 64.7

MPa and 3.4%, respectively. After coating with TPU, TPU/G exhibits a tensile strength of 126.9 MPa, representing a 96.1% increase compared to that of pure fabric. However, the elongation at break decreases to 2.6%, which may be due to the higher strength conferred by the TPU coating at the expense of some toughness. It is noted that the mechanical properties of TPU/G-X are generally improved compared to that of the control sample. In order to investigate the effect of different coating ratios on mechanical properties, the fracture surfaces of all samples were observed by SEM (Fig. 10b-h). Notably, the values of tensile strength of TPU/G-X are higher than that of TPU/G, indicating that the addition of SiAPP and PPNPP can enhance the interfacial compatibility of the TPU coating with GFC.

The mechanical strengthening mechanism of TPU coatings is analysed as shown in Fig. 10i-m. The GFC is unable to maintain its original neatly woven structure after being damaged by external forces (Fig. 10i), and the fibres appear to be dispersed. In contrast, TPU/G-SPM-1 (Fig. 10j, k) has dense and compact structure. Moreover, the fracture region of TPU/G-SPM-1 (Fig. 10l) displays that though the external TPU coating is pulled off, the internal GFC still maintains its original structure, indicating that the TPU coating protects the GFC well from damage in the early stage of tensile. Based on the above analysis, the mechanical enhancement mechanism of the TPU coatings is proposed and illustrated in Fig. 10m. Multiple hydrogen bonding interactions are formed between SPM flame retardant and TPU chains before stretching, which makes the composites present 3D morphology. After the tensile force is applied, the TPU chains are straightened, and the hydrogen bonding of the internal connection is broken and slipped. With the continuous application of the external force, the external TPU coating firstly deforms and break down. Subsequently, after the TPU coating is broken, the tensile force is transferred to the GFC, ultimately causing the breakage of GFC.

4. Conclusions

In this work, the novel phosphoramidate flame retardant PPNPP was synthesized by esterification and compounded with SiAPP and MoO₃ added into TPU to prepare TPU flame-retardant coatings, and finally the flame-retardant TPU/G composites were obtained by double-sided coating on the surface of GFC and heat curing. The results indicate that the SPM flame retardant provides the TPU coating with excellent flame-retardant performance. For TPU/G-SPM-1, the PHRR and THR decreased by 57.7% and 36.8%, respectively, compared to TPU/G. Meanwhile, the incorporation of the SPM flame retardant effectively reduces the emission of toxic and harmful smoke during the combustion of the TPU composites. Notably, this coating demonstrated remarkable suppression of CO emissions. For TPU/G-SPM-1, the PCOPR and CO yield decreased by 91.4% and 98.9%, respectively, compared to the pure sample. Furthermore, the TPU/SPM flame-retardant coating also imparts excellent mechanical properties to the GFC. Compared to pure GFC (64.7 MPa), the tensile strength of TPU/G-SPM-1 is improved by 101%, reaching 130.3 MPa. In summary, this work provides a novel approach for the preparation of fire-resistant TPU composites, demonstrating promising applications in the field of cable wrapping materials.

CRedit authorship contribution statement

Yongqian Shi: Writing - Original Draft, Supervision, Funding acquisition; **Songqiong Jiang:** Writing-Review & Editing, Data Curation, Investigation, Formal analysis; **Jinke Wu:** Conceptualization, Data Curation, Visualization; **Zhendong Chen:** Validation, Visualization; **Cancan Zhang:** Writing-Review & Editing, Validation, Visualization, Supervision; **Yun Zhang:** Methodology, Investigation; **Pingan Song:** Methodology, Investigation; **Yan Zhang:** Validation, Visualization.

Declaration of competing interest

The authors declare that they have no known competing financial interests or personal relationships that could have appeared to influence the work reported in this paper.

Acknowledgement

This work was financially supported by the Key research and development projects of Baoying County (Grant No. BY202205) and International Scientific and Technological Cooperation Program of Ningbo (No. 2024H020).

References

- [1] Y. Li, L. Qi, Y. Liu, J. Qiao, M. Wang, X. Liu, S. Li, Recent Advances in Halogen-Free Flame Retardants for Polyolefin Cable Sheath Materials, *Polymers* 14 (2022) 2876.
- [2] W. An, T. Wang, K. Liang, Y. Tang, Z. Wang, Effects of interlayer distance and cable spacing on flame characteristics and fire hazard of multilayer cables in utility tunnel, *Case Stud. Therm. Eng.* 22 (2020) 100784.
- [3] P. Jia, X. Yu, J. Lu, X. Zhou, Z. Yin, G. Tang, T. Lu, L. Guo, L. Song, B. Wang, Y. Hu, The $\text{Re}_2\text{Sn}_2\text{O}_7$ (Re = Nd, Sm, Gd) on the enhancement of fire safety and physical performance of Polyolefin/IFR cable materials, *J. Colloid Interf. Sci.* 608 (2022) 1652-1661.
- [4] A. Vishwakarma, M. Singh, B. Weclawski, V. J. Reddy, B. K. Kandola, G. Manik, A. Dasari, S. Chattopadhyay, Construction of hydrophobic fire retardant coating on cotton fabric using a layer-by-layer spray coating method, *Int. J. Biol. Macromol.* 223 (2022) 1653-1666.
- [5] W. Al-Shatty, D. A. Hill, S. Kiani, A. Stanulis, S. Winston, I. Powner, S. Alexander, A. R. Barron, Superhydrophilic surface modification of fabric via coating with cysteic acid mineral oxide, *Appl. Surf. Sci.* 580 (2022) 152306.
- [6] J.-C. Yang, W. Liao, S.-B. Deng, Z.-J. Cao, Y.-Z. Wang, Flame retardation of cellulose-rich fabrics via a simplified layer-by-layer assembly, *Carbohydr. Polym.* 151 (2016) 434-440.
- [7] L. Lu, C. Hu, Y. Zhu, H. Zhang, R. Li, Y. Xing, Multi-functional finishing of cotton fabrics by water-based layer-by-layer assembly of metal-organic framework, *Cellulose* 25 (2018) 4223-4238.

- [8] D. Ding, Q. Wu, J. Wang, Y. Chen, Q. Li, L. Hou, L. Zhao, Y.-y. Xu, Superhydrophobic encapsulation of flexible Bi₂Te₃/CNT coated thermoelectric fabric via layer-by-layer assembly, *Compos. Commun.* 38 (2023) 101509.
- [9] M. Ayesb, A. R. Horrocks, B. K. Kandola, The effect of combined atmospheric plasma/UV treatments on improving the durability of organophosphorus flame retardants applied to polyester fabrics, *Polym. Degrad. Stab.* 225 (2024) 8737.
- [10] L. Qi, B. Wang, W. Zhang, B. Yu, M. Zhou, Y. Hu, W. Xing, Durable flame retardant and dip-resistant coating of polyester fabrics by plasma surface treatment and UV-curing, *Prog. Org. Coat.* 172 (2022) 107066.
- [11] W. Wu, W. Huang, Y. Tong, J. Huang, J. Wu, X. Cao, Q. Zhang, B. Yu, R. K. Y. Li, Self-assembled double core-shell structured zeolitic imidazole framework-8 as an effective flame retardant and smoke suppression agent for thermoplastic polyurethane, *Appl. Surf. Sci.* 610 (2023) 155540.
- [12] K. Liu, Y. Lu, Y. Cheng, J. Li, G. Zhang, F. Zhang, Flame retardancy and mechanism of polymer flame retardant containing P-N bonds for cotton fabrics modified by chemical surface grafting, *Cellulose* 31 (2024) 3243-3258.
- [13] Y. Ma, Y. Wang, L. Ma, Z. Zhu, Fabrication of hydrophobic and flame-retardant cotton fabric via sol-gel method, *Cellulose* 30 (2023) 11829-11843.
- [14] D. Zhang, B. L. Williams, S. B. Shrestha, Z. Nasir, E. M. Becher, B. J. Lofink, V. H. Santos, H. Patel, X. Peng, L. Sun, Flame retardant and hydrophobic coatings on cotton fabrics via sol-gel and self-assembly techniques, *J. Colloid Interf. Sci.* 505 (2017) 892-899.
- [15] Y. Huang, S. Jiang, R. Liang, P. Sun, Y. Hai, L. Zhang, Thermal-triggered insulating fireproof layers: A novel fire-extinguishing MXene composites coating, *Chem. Eng. J.* 391 (2020) 123621.

- [16] T.-T. Li, S. Chu, X. Hu, H.-T. Ren, C.-W. Lou, J.-H. Lin, Silica Nanoparticle/TPU Coating Imparts Aramid with Puncture Resistance and Anti-corrosion for Personal Protection, *ACS Appl. Nano Mater.* 6 (2023) 16986-16999.
- [17] A. Moiz, R. Padhye, X. Wang, Coating of TPU-PDMS-TMS on Polycotton Fabrics for Versatile Protection, *Polymers* 9 (2017) 660.
- [18] Y. Liu, X. Cao, J. Shi, B. Shen, J. Huang, J. Hu, Z. Chen, Y. Lai, A superhydrophobic TPU/CNTs@SiO₂ coating with excellent mechanical durability and chemical stability for sustainable anti-fouling and anti-corrosion, *Chem. Eng. J.* 434 (2022) 134605.
- [19] Q. He, W. Wu, H. Hu, Z. Rui, J. Ye, Y. Wang, Z. Wang, Achieving superior fire safety for TPU 3D-printed workpiece with EP/PBz/PDMS coating, *J. Appl. Polym. Sci.* 140 (2023) 53858.
- [20] W. Huang, J. Huang, B. Yu, Y. Meng, X. Cao, Q. Zhang, W. Wu, D. Shi, T. Jiang, R. K. Y. Li, Facile preparation of phosphorus containing hyperbranched polysiloxane grafted graphene oxide hybrid toward simultaneously enhanced flame retardancy and smoke suppression of thermoplastic polyurethane nanocomposites, *Compos. Part A Appl. Sci.* 150 (2021), 106614.
- [21] M. Steinmann, M. Wagner, F. R. Wurm, Poly(phosphorodiamidate)s by Olefin Metathesis Polymerization with Precise Degradation, *Chem. Eur. J.* 22 (2016) 17329-17338.
- [22] Y. Xue, Z. Ma, X. Xu, M. Shen, G. Huang, S. Bourbigot, X. Liu, P. Song, Mechanically robust and flame-retardant polylactide composites based on molecularly-engineered polyphosphoramides, *Compos. Part A Appl. Sci.* 144 (2021) 106317.
- [23] Q. Tai, R. K. K. Yuen, L. Song, Y. Hu, A novel polymeric flame retardant and exfoliated clay nanocomposites: Preparation and properties, *Chem. Eng. J.* 183 (2012) 542-549.

- [24] Y. Xue, M. Shen, Y. Zheng, W. Tao, Y. Han, W. Li, P. Song, H. Wang, One-pot scalable fabrication of an oligomeric phosphoramidate towards high-performance flame retardant polylactic acid with a submicron-grained structure, *Compos. B Eng.* 183 (2020) 107695.
- [25] C. Liu, D. Yang, M. Sun, G. Deng, B. Jing, K. Wang, Y. Shi, L. Fu, Y. Feng, Y. Lv, M. Liu, Phosphorous-Nitrogen flame retardants engineering MXene towards highly fire safe thermoplastic polyurethane, *Compos. Commun.* 29 (2022) 101055.
- [26] Y.-R. Li, Y.-M. Li, W.-J. Hu, D.-Y. Wang, Cobalt ions loaded polydopamine nanospheres to construct ammonium polyphosphate for the improvement of flame retardancy of thermoplastic polyurethane elastomer, *Polym. Degrad. Stab.* 202 (2022) 110035.
- [27] M. Wan, C. Shi, X. Qian, Y. Qin, J. Jing, H. Che, F. Ren, J. Li, B. Yu, K. Zhou, Design of novel double-layer coated ammonium polyphosphate and its application in flame retardant thermoplastic polyurethanes, *Chem. Eng. J.* 459 (2023) 141448.
- [28] W. Zhao, J. Liu, H. Peng, J. Liao, X. Wang, Synthesis of a novel PEPA-substituted polyphosphoramidate with high char residues and its performance as an intumescent flame retardant for epoxy resins, *Polym. Degrad. Stab.* 118 (2015) 120-129.
- [29] X. Ye, Y. Wang, Z. Zhao, H. Yan, A novel hyperbranched poly(phosphorodiamidate) with high expansion degree and carbonization efficiency used for improving flame retardancy of APP/PP composites, *Polym. Degrad. Stab.* 142 (2017) 29-41.
- [30] X. Dong, Y. Ma, X. Fan, S. Zhao, Y. Xu, S. Liu, D. Jin, Nickel modified two-dimensional bimetallic nanosheets, $M(OH)(OCH_3)$ ($M=Co, Ni$), for improving fire retardancy and smoke suppression of epoxy resin, *Polymer* 235 (2021) 124263.

- [31] Z. H. Wu, Q. Wang, Q. X. Fan, Y. J. Cai, Y. Q. Zhao, Synergistic effect of Nano-ZnO and intumescent flame retardant on flame retardancy of polypropylene/ethylene-propylene-diene monomer composites using elongational flow field, *Polym. Compos.* 40 (2018) 2819-2833.
- [32] M. Zhang, X. Ding, Y. Zhan, Y. Wang, X. Wang, Improving the flame retardancy of poly(lactic acid) using an efficient ternary hybrid flame retardant by dual modification of graphene oxide with phenylphosphinic acid and nano MOFs, *J. Hazard. Mater.* 384 (2020) 121260.
- [33] W.-Z. Xu, C.-C. Li, Y.-X. Hu, L. Liu, Y. Hu, P.-C. Wang, Synthesis of MoO₃ with different morphologies and their effects on flame retardancy and smoke suppression of polyurethane elastomer, *Polym. Adv. Technol.* 27 (2016) 964-972.
- [34] A. Yao, C. Liu, Y. Ye, Y. Yang, Z. Wang, H. Wang, Y. Feng, J. Gao, Y. Shi, Functionalizing MXenes with molybdenum trioxide towards reducing fire hazards of thermoplastic polyurethane, *New J. Chem.* 46 (2022) 14112-14121.
- [35] G. Zeng, W. Zhang, X. Zhang, W. Zhang, J. Du, J. He, R. Yang, Study on flame retardancy of APP/PEPA/MoO₃ synergism in vinyl ester resins, *J. Appl. Polym. Sci.* 137 (2020) 49026.
- [36] L. Liu, Y. Xu, Y. Pan, M. Xu, Y. Di, B. Li, Facile synthesis of an efficient phosphonamide flame retardant for simultaneous enhancement of fire safety and crystallization rate of poly (lactic acid), *Chem. Eng. J.* 421 (2021) 127761.
- [37] Y. Feng, J. Hu, Y. Xue, C. He, X. Zhou, X. Xie, Y. Ye, Y.-W. Mai, Simultaneous improvement in the flame resistance and thermal conductivity of epoxy/Al₂O₃ composites by incorporating polymeric flame retardant-functionalized graphene, *J. Mater. Chem. A* 5 (2017) 13544-13556.

- [38] K. Chen, Y. Feng, Y. Shi, H. Wang, L. Fu, M. Liu, Y. Lv, F. Yang, B. Yu, M. Liu, P. Song, Flexible and fire safe sandwich structured composites with superior electromagnetic interference shielding properties, *Compos. Part A Appl. Sci.* 160 (2022) 107070.
- [39] M. Z. Rahman, X. Wang, L. Song, Y. Hu, A novel green phosphorus-containing flame retardant finishing on polysaccharide-modified polyamide 66 fabric for improving hydrophilicity and durability, *Int. J. Biol. Macromol.* 239 (2023) 124252.
- [40] C. Gao, Y. Shi, Y. Chen, S. Zhu, Y. Feng, Y. Lv, F. Yang, M. Liu, W. Shui, Constructing segregated polystyrene composites for excellent fire resistance and electromagnetic wave shielding, *J. Colloid Interf. Sci.* 606 (2022) 1193-1204.
- [41] S. Zhang, X. Liu, X. Jin, H. Li, J. Sun, X. Gu, The novel application of chitosan: Effects of cross-linked chitosan on the fire performance of thermoplastic polyurethane, *Carbohydr. Polym.* 189 (2018) 313-321.
- [42] P. Sun, H. Zhang, Y. Leng, Z. Wang, J. Zhang, M. Xu, X. Li, B. Li, Construction of flame retardant functionalized carbon dot with insulation, flame retardancy and thermal conductivity in epoxy resin, *Constr. Build. Mater.* 451 (2024) 138853.
- [43] W. Wu, W. Zhao, X. Gong, Q. Sun, X. Cao, Y. Su, B. Yu, R. K. Y. Li, R. A. L. Vellaisamy, Surface decoration of Halloysite nanotubes with POSS for fire-safe thermoplastic polyurethane nanocomposites, *J. Mater. Sci. Technol.* 101 (2022) 107-117.
- [44] B.-h. Kang, X. Lu, J.-p. Qu, T. Yuan, Synergistic effect of hollow glass beads and intumescent flame retardant on improving the fire safety of biodegradable poly(lactic acid), *Polym. Degrad. Stab.* 164 (2019) 167-176.

- [45] X. Lyu, H. Zhang, Y. Yan, Effect of expandable graphite and molybdenum trioxide in nitrogen/phosphorus synergistic system on acoustic performance and fire safety in rigid polyurethane foam, *J. Appl. Polym. Sci.* 139 (2022) 52488.
- [46] T. Tanaka, O. Terakado, M. Hirasawa, Flame retardancy in fabric consisting of cellulosic fiber and modacrylic fiber containing fine-grained MoO_3 particles, *Fire Mater.* 40 (2015) 612-621.
- [47] H. Xu, C. Peng, L. Xia, Z. Miao, S. He, C. Chi, W. Luo, G. Chen, B. Zeng, S. Wang, L. Dai, A Novel Anderson-Type POMs-Based Hybrids Flame Retardant for Reducing Smoke Release and Toxicity of Epoxy Resins, *Macromol. Rapid Commun.* 44 (2023) 2300162.
- [48] B. Yu, Y. Shi, B. Yuan, S. Qiu, W. Xing, W. Hu, L. Song, S. Lo, Y. Hu, Enhanced thermal and flame retardant properties of flame-retardant-wrapped graphene/epoxy resin nanocomposites, *J. Mater. Chem. A* 3 (2015) 8034-8044.
- [49] C. Liu, K. Xu, Y. Shi, J. Wang, S. Ma, Y. Feng, Y. Lv, F. Yang, M. Liu, P. Song, Fire-safe, mechanically strong and tough thermoplastic Polyurethane/MXene nanocomposites with exceptional smoke suppression, *Mater. Today Phys.* 22 (2022) 100607.
- [50] W. Cai, Z. Li, T. Cui, X. Feng, L. Song, Y. Hu, X. Wang, Self-assembly of hierarchical MXene@ SnO_2 nanostructure for enhancing the flame retardancy, solar de-icing, and mechanical property of polyurethane resin, *Compos. B Eng.* 244 (2022) 15.
- [51] Y. Hou, C. Liao, S. Qiu, Z. Xu, X. Mu, Z. Gui, L. Song, Y. Hu, W. Hu, Preparation of soybean root-like CNTs/bimetallic oxides hybrid to enhance fire safety and mechanical performance of thermoplastic polyurethane, *Chem. Eng. J.* 428 (2022) 132338.
- [52] W. Cai, T. Cai, L. He, F. Chu, X. Mu, L. Han, Y. Hu, B. Wang, W. Hu, Natural antioxidant functionalization for fabricating ambient-stable black phosphorus nanosheets toward enhancing

- flame retardancy and toxic gases suppression of polyurethane, *J. Hazard. Mater.* 387 (2020) 121971.
- [53] K. Zhou, Z. Gui, Y. Hu, S. Jiang, G. Tang, The influence of cobalt oxide–graphene hybrids on thermal degradation, fire hazards and mechanical properties of thermoplastic polyurethane composites, *Compos. Part A Appl. Sci.* 88 (2016) 10-18.
- [54] C. Nie, Y. Shi, S. Jiang, H. Wang, M. Liu, R. Huang, Y. Feng, L. Fu, F. Yang, Constructing Fireproof MXene-Based Cotton Fabric/Thermoplastic Polyurethane Hierarchical Composites via Encapsulation Strategy, *ACS Appl. Polym. Mater.* 5 (2023) 7229-7239.
- [55] C. Liu, W. Wu, Y. Shi, F. Yang, M. Liu, Z. Chen, B. Yu, Y. Feng, Creating MXene/reduced graphene oxide hybrid towards highly fire safe thermoplastic polyurethane nanocomposites, *Compos. B Eng.* 203 (2020) 108486.
- [56] J. Wang, Y. Hu, W. Cai, B. Yuan, Y. Zhang, W. Guo, W. Hu, L. Song, Atherton–Todd reaction assisted synthesis of functionalized multicomponent MoSe₂/CNTs nanoarchitecture towards the fire safety enhancement of polymer, *Compos. Part A Appl. Sci.* 112 (2018) 271-282.
- [57] C. Wang, W. Xu, L. Qi, H. Ding, W. Cai, G. Jiang, Y. Hu, W. Xing, B. Yu, Hierarchical NiO/Al₂O₃ nanostructure for highly effective smoke and toxic gases suppression of polymer Materials: Experimental and theoretical investigation, *Compos. Part A Appl. Sci.* 175 (2023) 107807.
- [58] X. Chen, Z. Wei, W. Wang, C. Jiao, Properties of flame-retardant TPU based on para-aramid fiber modified with iron diethyl phosphinate, *Polym. Adv. Technol.* 30 (2018) 170-178.
- [59] H. Ren, K. Qing, Y. Chen, Y. Lin, X. Duan, Smoke suppressant in flame retarded thermoplastic polyurethane composites: Synergistic effect and mechanism study, *Nano Res.* 14 (2021) 3926-3934.

- [60] H. Li, D. Meng, P. Qi, J. Sun, H. Li, X. Gu, S. Zhang, Fabrication of a hybrid from metal organic framework and sepiolite (ZIF-8@SEP) for reducing the fire hazards in thermoplastic polyurethane, *Appl. Clay Sci.* 216 (2022) 106376.
- [61] H. Wang, H. Qiao, J. Guo, J. Sun, H. Li, S. Zhang, X. Gu, Preparation of cobalt-based metal organic framework and its application as synergistic flame retardant in thermoplastic polyurethane (TPU), *Compos. B Eng.* 182 (2020) 2036-2045.
- [62] S. Wang, Q. Fang, C. Liu, J. Zhang, Y. Jiang, Y. Huang, M. Yang, Z. Tan, Y. He, B. Ji, C. Qi, Y. Chen, Biomass tannic acid intermediated surface functionalization of ammonium polyphosphate for enhancing fire safety and smoke suppression of thermoplastic polyurethane, *Eur. Polym. J.* 187 (2023) 111897.
- [63] S.-C. Huang, C. Deng, S.-X. Wang, W.-C. Wei, H. Chen, Y.-Z. Wang, Electrostatic action induced interfacial accumulation of layered double hydroxides towards highly efficient flame retardance and mechanical enhancement of thermoplastic polyurethane/ammonium polyphosphate, *Polym. Degrad. Stab.* 165 (2019) 126-136.
- [64] Y. Zhu, H. Wang, L. Fu, P. Xu, G. Rao, W. Xiao, L. Wang, Y. Shi, Interface engineering of multi-component core-shell flame retardant towards enhancing fire safety of thermoplastic polyurethane and mechanism investigation, *Appl. Mater. Today* 38 (2024) 1106-1114.
- [65] M. Yang, X. Li, W. Qin, Y. Wang, C. Gu, L. Feng, Z. Tian, H. Qiao, J. Chen, J. Chen, S. Yin, Multifunctional thermoplastic polyurethane composites with excellent flame retardancy, strain-sensitivity, water penetration resistance and breathability, *Eur. Polym. J.* 195 (2023) 112227.

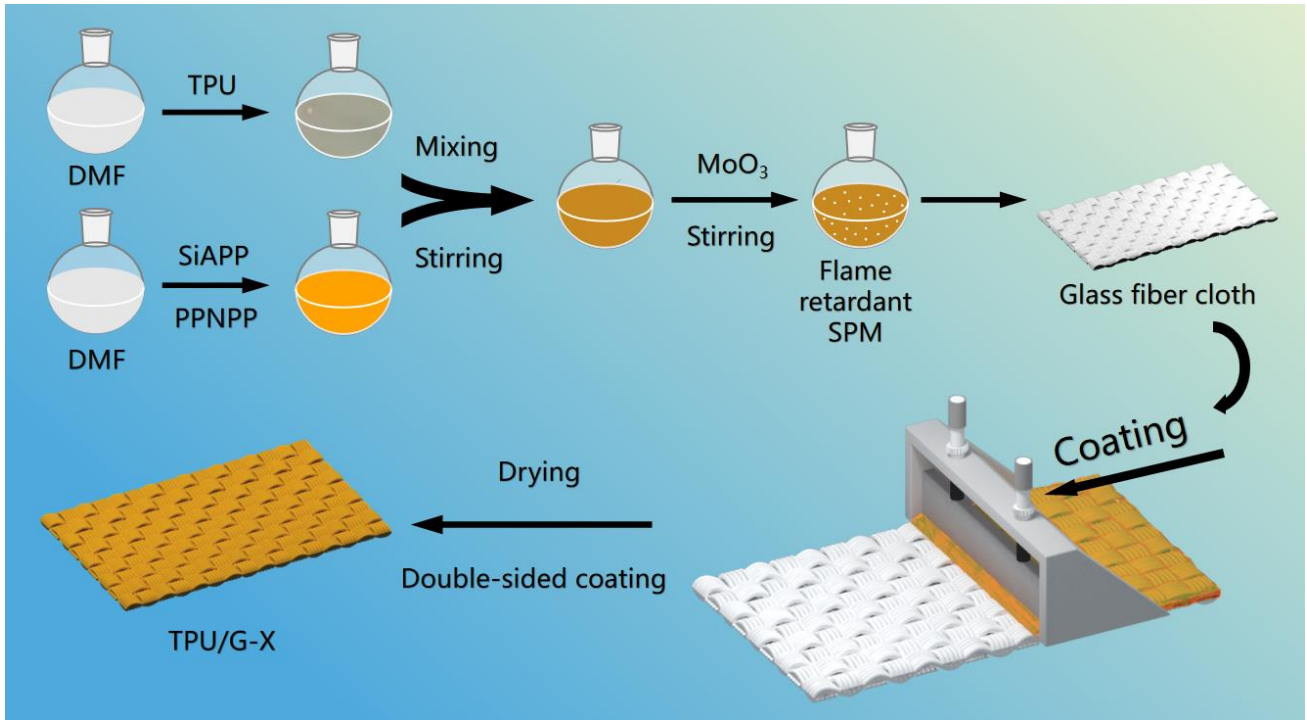


Fig. 1. Schematic diagram for preparation of TPU/G-X.

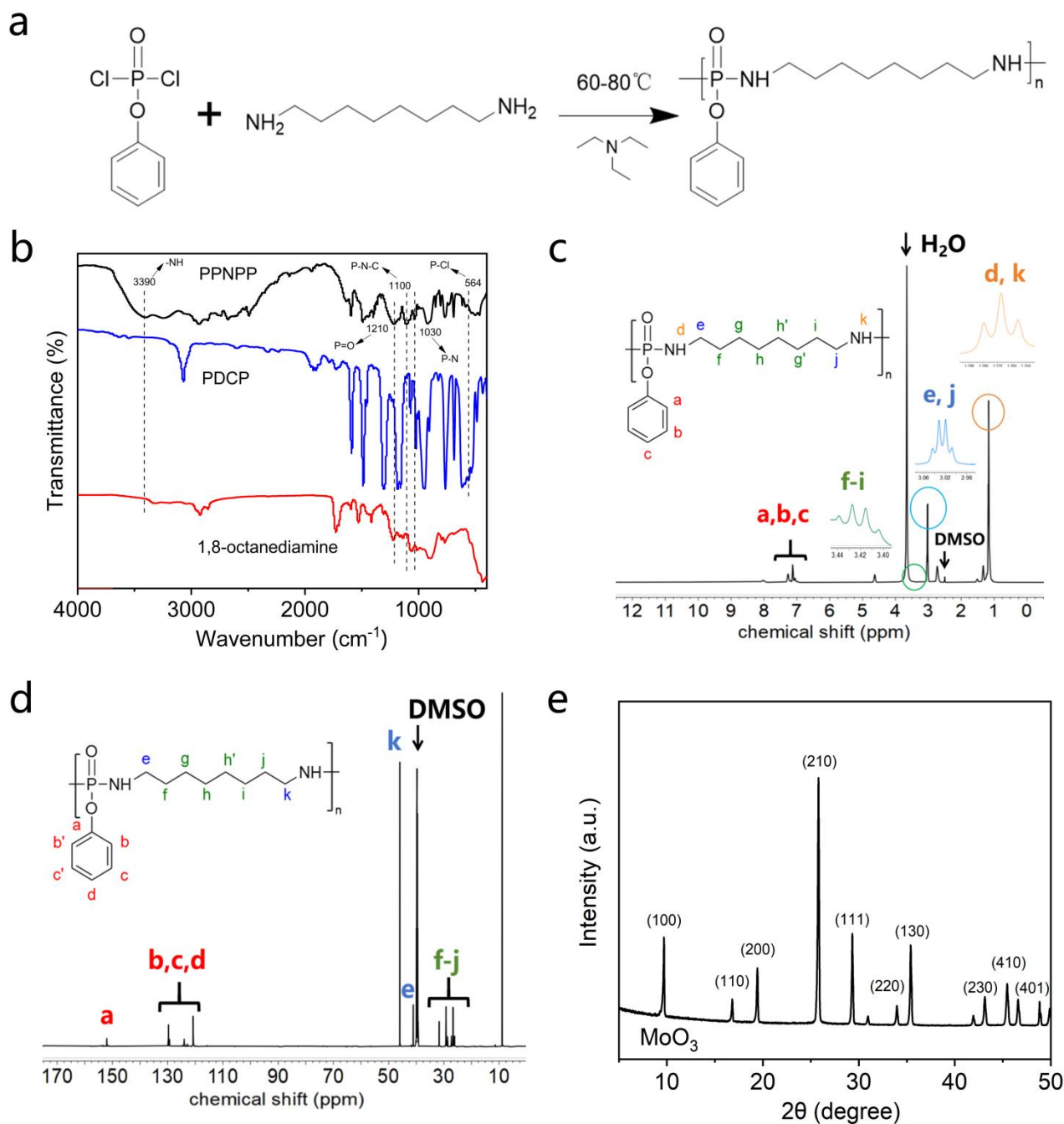


Fig. 2. (a) Preparation route of PPNPP; (b) FTIR spectra of PPNPP and PDCP and 1,8-octanediamine; (c) ^1H NMR and (d) ^{13}C NMR spectra of PPNPP; (e) XRD patterns of MoO_3 .

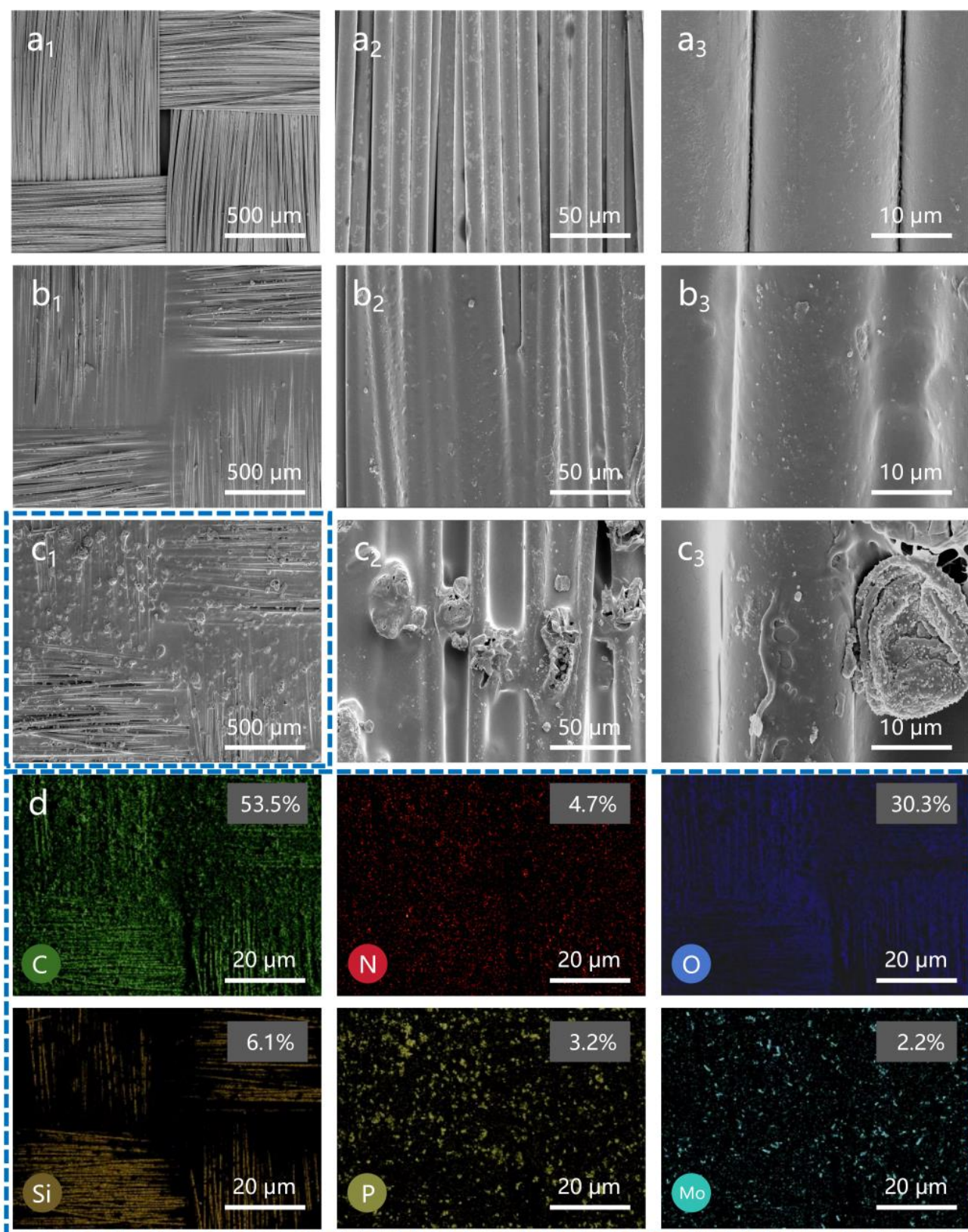


Fig. 3. SEM images of surface of (a) GFC, (b) TPU/G, and (c) TPU/G-SPM-1; (d) Element distribution images of TPU/G-SPM-1(c₁).

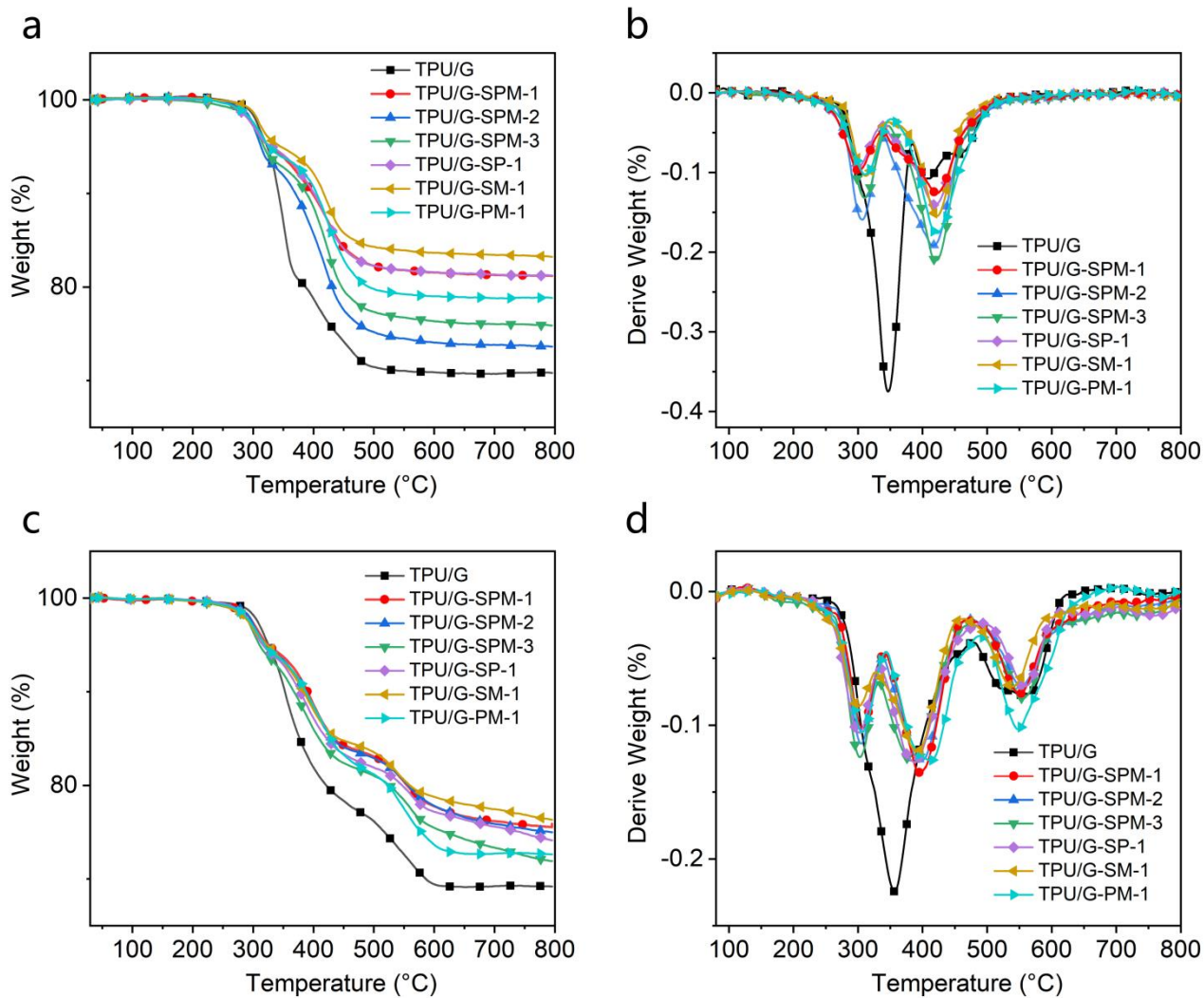


Fig. 4. TGA and DTG curves of the TPU/G composites in (a, b) Ar and (c, d) air atmospheres.

a



b

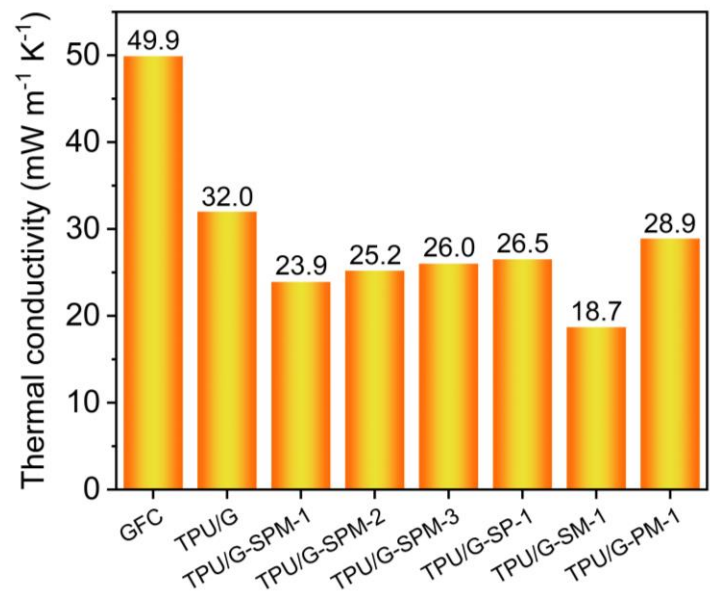


Fig. 5. (a) Photograph of thermal conductivity tester; (b) Thermal conductivity of GFC and the TPU/G composites.

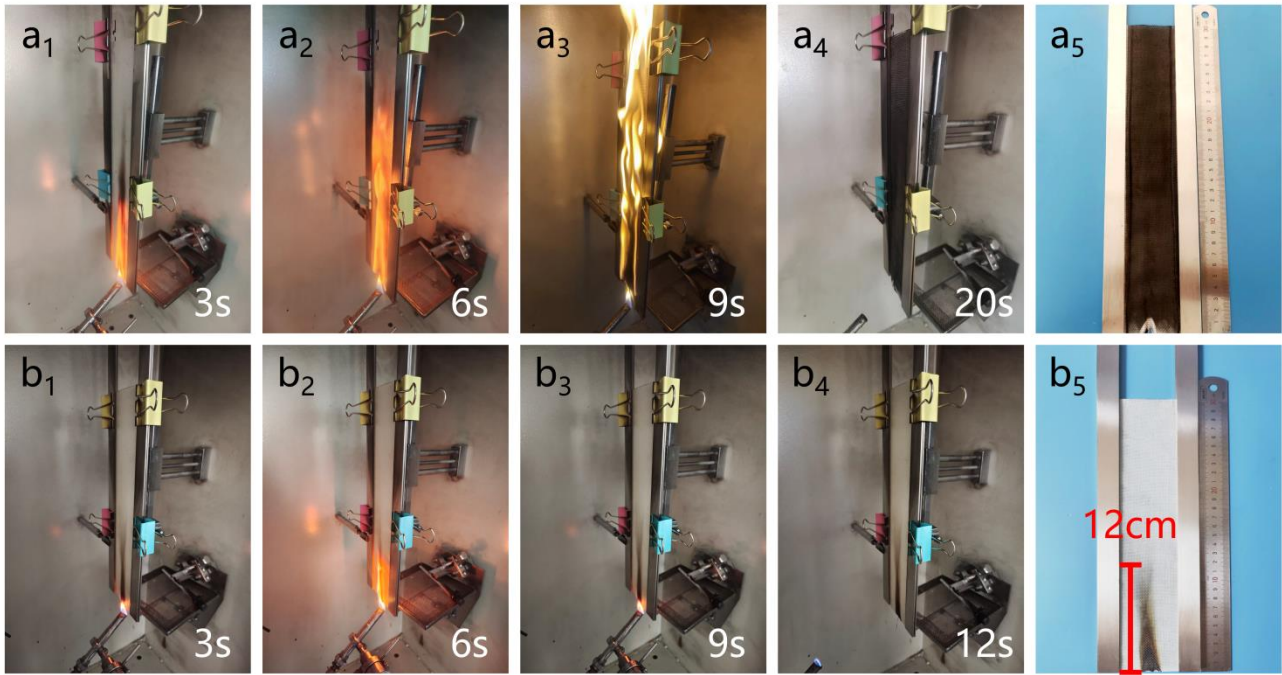


Fig. 6. Photographs of the vertical burning tests for (a) TPU/G and (b) TPU/G-SPM-1.

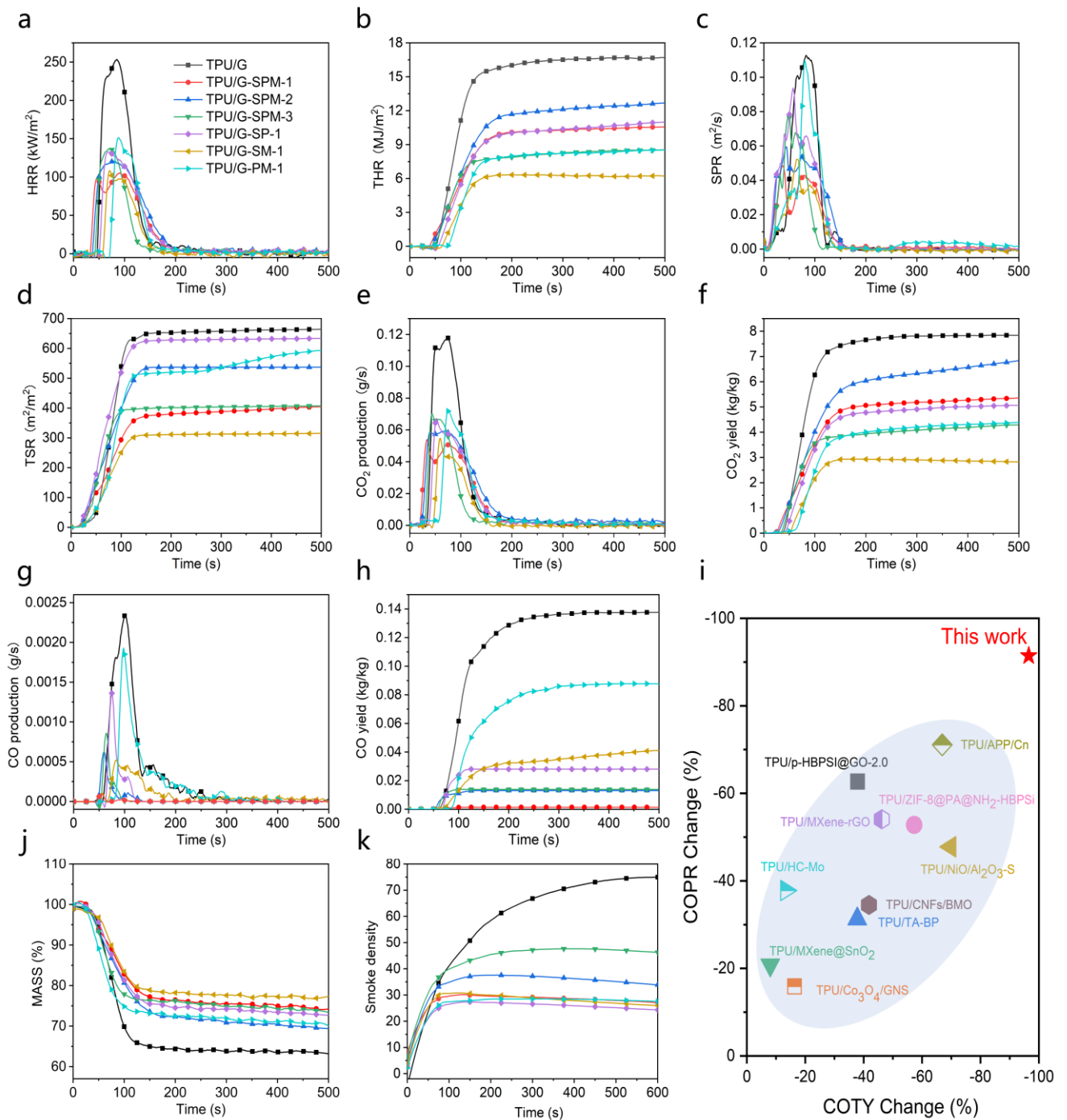


Fig. 7. CCT data: (a) HRR, (b) THR, (c) SPR, (d) TSR, (e) CO₂PR, (f) CO₂TY, (g) COPR, and (h) COTY; (i) Comparison of COPR and COTY reductions with previous works; (j) Weight loss and (k) Smoke density.

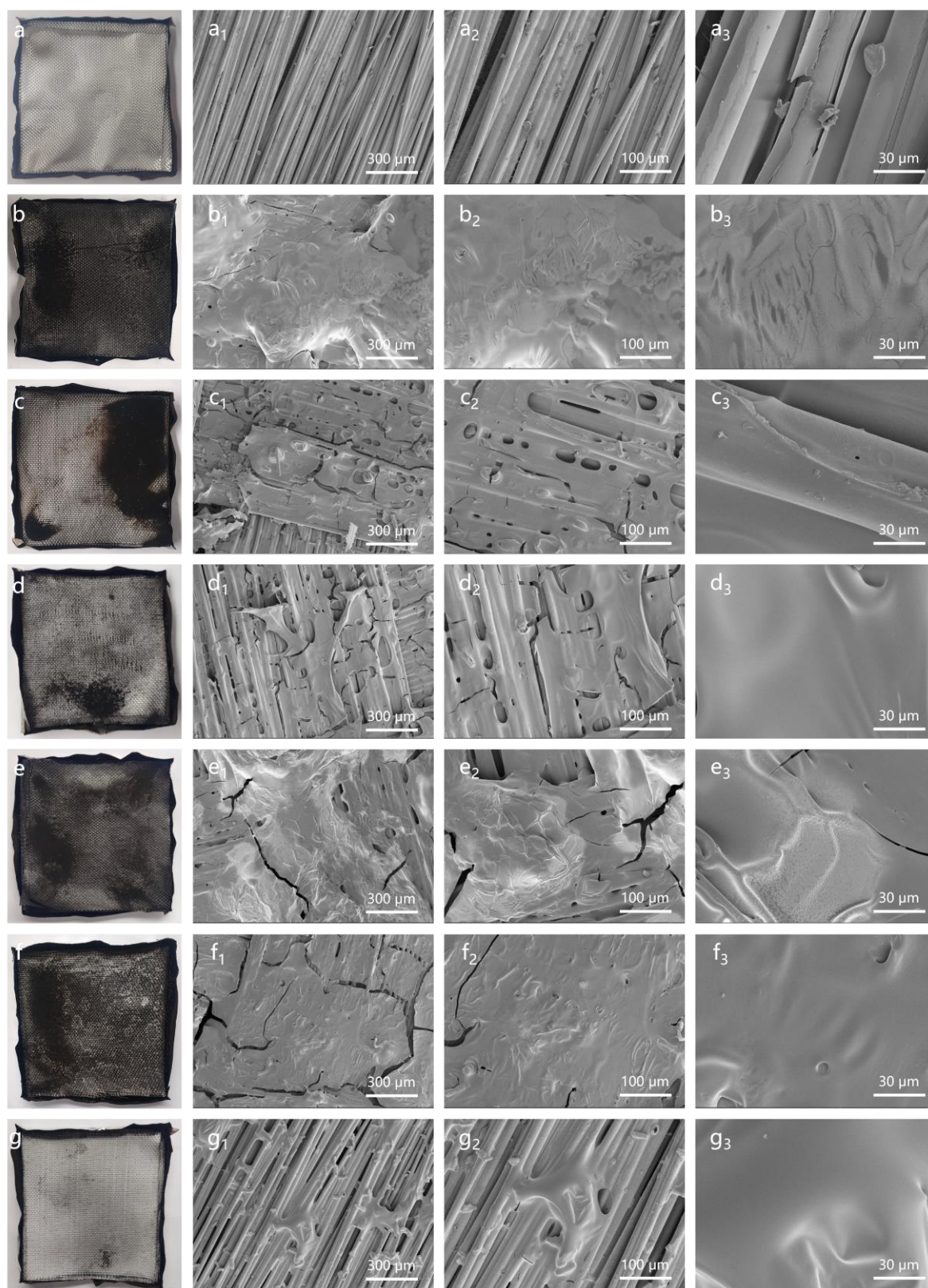


Fig. 8. Digital photos and SEM images of char residues of the TPU/G composites: (a) TPU/G, (b) TPU/G-SPM-1, (c) TPU/G-SPM-2, (d) TPU/G-SPM-3, (e) TPU/G-SP-1, (f) TPU/G-SM-1, and (g) TPU/G-PM-1.

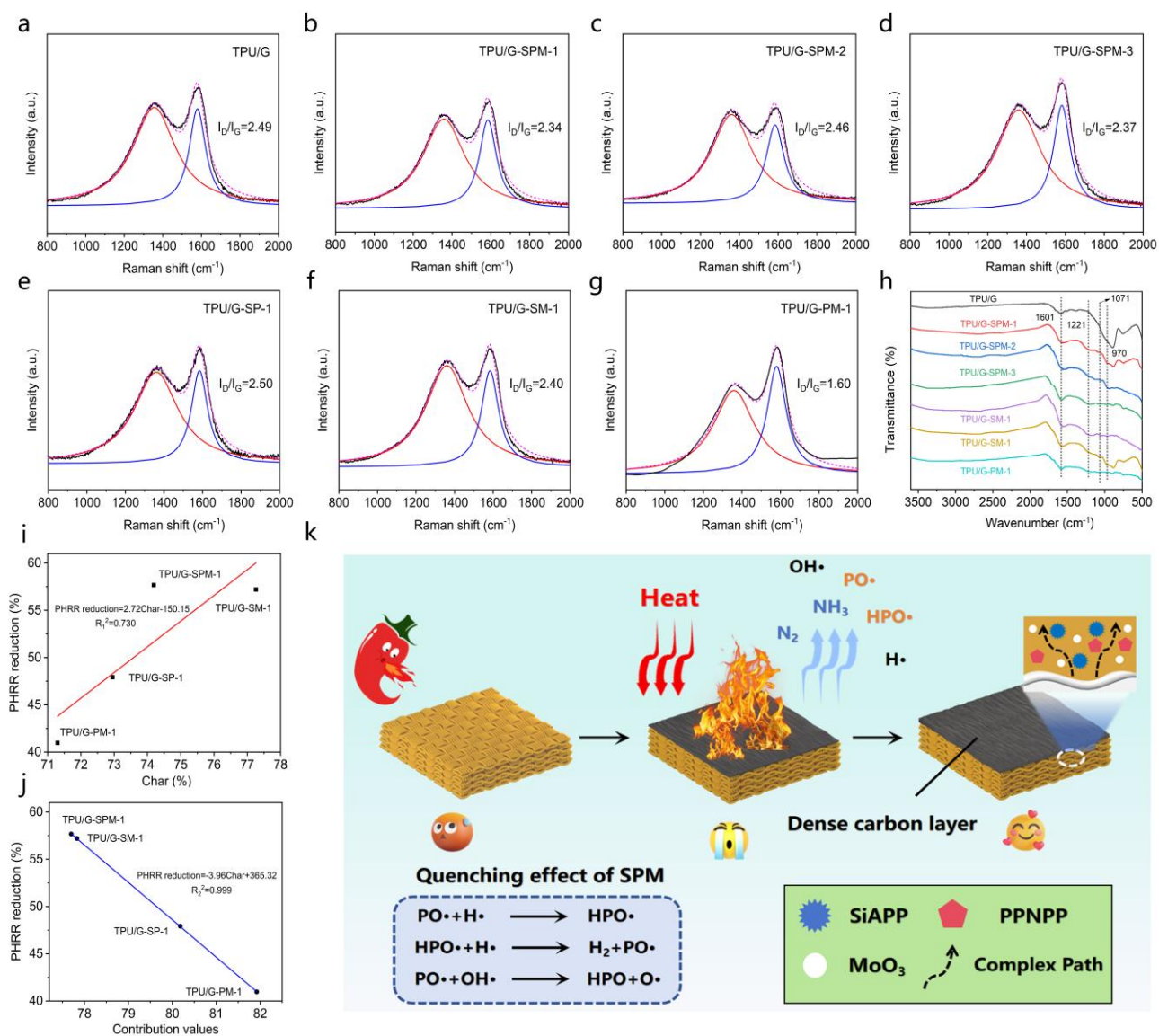


Fig. 9. Raman spectra of char residues of the TPU/G composites: (a) TPU/G, (b) TPU/G-SPM-1, (c) TPU/G-SPM-2, (d) TPU/G-SPM-3, (e) TPU/G-SP-1, (f) TPU/G-SM-1, (g) TPU/G-PM-1, (h) FTIR spectra of char residues of the TPU/G composites; (i) Correlation between the char residues from CCT and PHRR reduction; (j) Correlation between the contributions values and PHRR reduction; (k) Flame retardant mechanism of TPU/G-X.

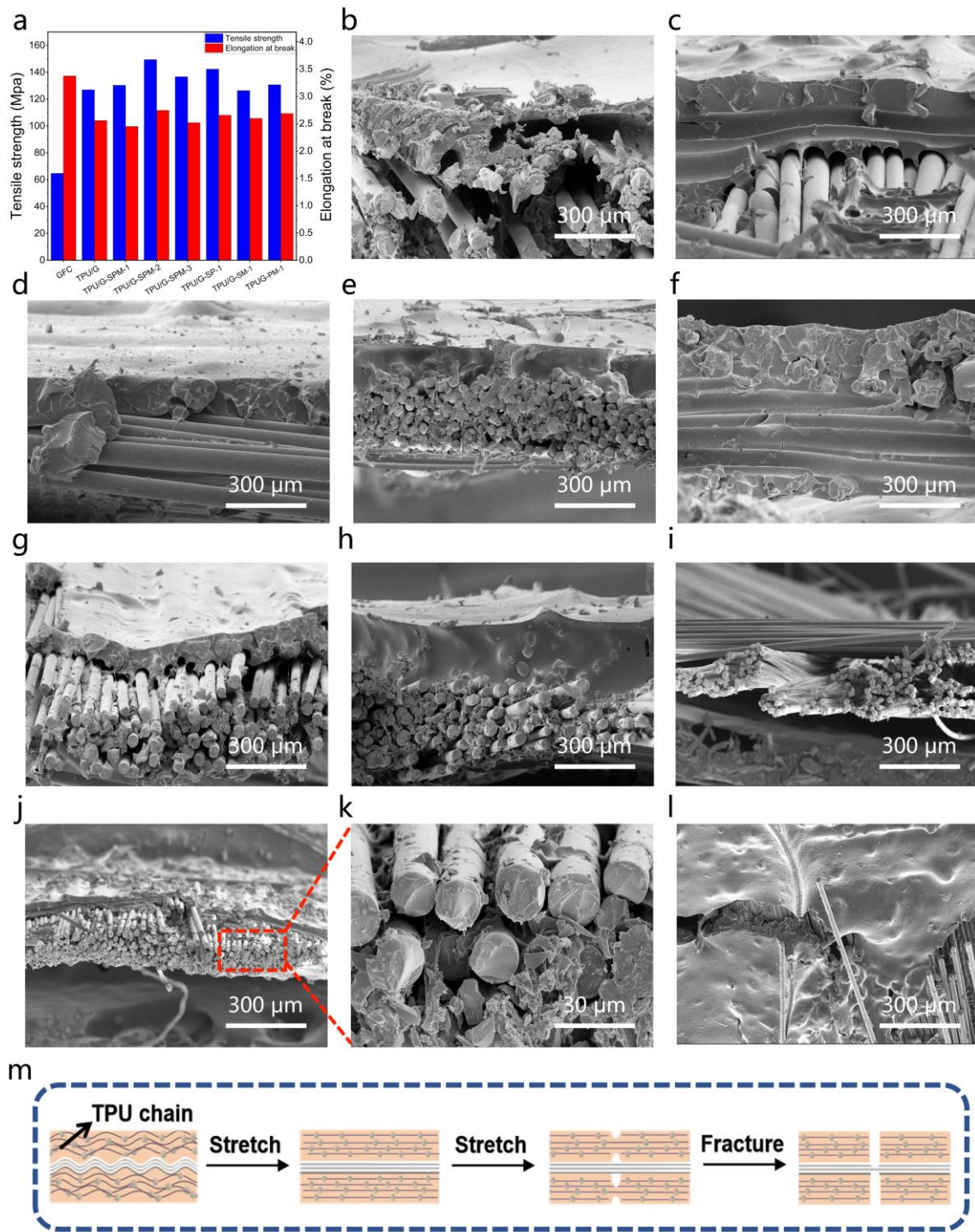


Fig. 10. (a) Tensile strength and elongation of the GFC and TPU/G composites; SEM images of fracture surface of (b) TPU/G, (c) TPU/G-SPM-1, (d) TPU/G-SPM-2, (e) TPU/G-SPM-3, (f) TPU/G-SP-1, (g) TPU/G-SM-1, (h) TPU/G-PM-1, (i) GFC (Flat view), (j, k) TPU/G-SPM-1 (Flat view), and (l) TPU/G-SPM-1 (Top view); (m) Schematic diagram for the mechanical failure process of the TPU/G composites.

Table 1. Formulation of the TPU/G composites.

Samples No.	TPU (g)	SiAPP (g)	PPNPP (g)	MoO ₃ (g)
TPU	100	-	-	-
TPU/SPM-1	80	10	5	5
TPU/SPM-2	84	8	4	4
TPU/SPM-3	88	6	3	3
TPU/SP-1	80	10	10	-
TPU/SM-1	80	15	-	5
TPU/PM-1	80	-	15	5

Table 2. TGA data of the TPU/G composites in air and Ar atmospheres.

Samples No.	$T_{5\%}$ (°C)		T_{max1} (°C)		T_{max2} (°C)		T_{max3} (°C)	Char residue at 800 °C (wt%)	
	Air	Ar	Air	Ar	Air	Ar	Air	Air	Ar
TPU/G	296.5	298.3	355.1	345.7	552.9	408.4		69.20	70.82
TPU/G-SPM-1	277.4	276.7	306.8	299.1	394.4	418.7	550.2	75.54	81.19
TPU/G-SPM-2	281.6	288.7	303.0	304.8	395.7	418.3	554.0	75.00	73.63
TPU/G-SPM-3	273.9	278.1	301.8	308.7	384.1	420.6	554.1	71.91	75.90
TPU/G-SP-1	275.3	273.3	301.8	300.8	387.1	418.7	560.0	74.13	81.23
TPU/G-SM-1	264.7	292.2	305.8	310.2	413.7	422.7	546.8	76.33	83.23
TPU/G-PM-1	277.1	278.6	299.9	308.9	390.4	419.9	539.2	72.64	78.84

Table 3. LOI values and damaged length for the TPU/G composites during vertical burning tests.

Samples No.	LOI (%)	Damaged length (mm)
TPU/G	23.3 ± 0.1	Burn out
TPU/G-SPM-1	28.1 ± 0.2	120 ± 2
TPU/G-SPM-2	27.4 ± 0.2	220 ± 2
TPU/G-SPM-3	27.0 ± 0.2	200 ± 2
TPU/G-SP-1	28.5 ± 0.2	120 ± 5
TPU/G-SM-1	30.8 ± 0.2	110 ± 2
TPU/G-PM-1	26.1 ± 0.2	Burn out

Table 4. Cone calorimetric results for the TPU/G composites.

Samples No.	TTI (s)	PHRR (kW m ⁻²)	THR (MJ m ⁻²)	PSPR (m ² s ⁻¹)	TSR (m ² m ⁻²)	PCOPR (g s ⁻¹)	PCO ₂ PR (g s ⁻¹)	COTY (kg kg ⁻¹)	CO ₂ TY (kg kg ⁻¹)	Char residue (wt%)
TPU/G	47	260	16.7	0.1222	664.5	0.00245	0.1208	0.1377	7.84	63.89
TPU/G-SPM-1	31	110	10.6	0.0658	404.2	0.00021	0.0560	0.0014	5.36	74.19
TPU/G-SPM-2	36	126	12.7	0.0865	537.2	0.00095	0.0629	0.0131	6.83	70.23
TPU/G-SPM-3	41	144	8.5	0.1110	407.4	0.00124	0.0720	0.0138	4.29	73.53
TPU/G-SP-1	50	135	11.0	0.1169	633.6	0.00163	0.0672	0.0280	5.07	72.95
TPU/G-SM-1	59	111	6.3	0.0749	315.0	0.00066	0.0572	0.0411	2.94	77.26
TPU/G-PM-1	41	154	8.5	0.1200	593.8	0.00205	0.0726	0.0878	4.39	71.3

Table 5. Smoke density results for the TPU/G composites.

Samples No.	TPU/G	TPU/G-SPM-1	TPU/G-SPM-2	TPU/G-SPM-3	TPU/G-SP-1	TPU/G-SM-1	TPU/G-PM-1
D,10	74.8	27.1	34.1	51.3	24.5	26	27.6
D,max	75.1	30.4	37.6	53.5	27.5	30.8	28.5

Table 6. The detailed information about contribution values.

Samples No.	Char	Y	Contribution values
TPU/G-SPM-1	74.19	3.51	77.70
TPU/G-SP-1	72.95	7.23	80.18
TPU/G-SM-1	77.26	0.57	77.83
TPU/G-PM-1	71.30	10.62	81.92